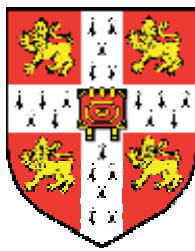


Neural basis of a visuo-motor transformation in the fly

Stephen James Huston
Churchill College



Department of Zoology
University of Cambridge

A dissertation submitted in partial fulfillment of the requirements
for the degree of Doctor of Philosophy, September 2005

Declaration

This dissertation is the result of my own work and includes nothing which is the outcome of work done in collaboration.

Acknowledgements

This dissertation would not have been possible without the support and excellent supervision of Holger Krapp. It was he who first suggested recording from the Neck Motor Neurons and who contributed significant amounts of time and effort to helping me in every possible way.

Simon Laughlin provided guidance and the highly valuable service of forcing me to actually think once in a while. A. Aldo Faisal and Gonzalo Garcia De Polavieja helped with the programming and quantitative analyses. Jeremy Niven and Steve Rogers in particular provided a lot of help when I was trying to get the intracellular experiments working. Tom Matheson also gave me a lot of friendly and useful advice in the first few years of my PhD.

The various people who have passed through the Insect Vision Group have made it an intellectually challenging, fun and supportive place to work. These include in approximate chronological order: Aldo, David, Gonzalo, Jochen, Jeremy, Matthew and Daniel.

Steve Ellis built the CRT meridian without which my experiments would have been impossible. Glenn Harrison built endless electronic gadgets for my experiments and provided advice on all things electrical. Nigel Hall kept the blowfly colony going and Ken Baker provided friendly technical support. Financial support came from the M.R.C, the Cambridge Philosophical Society, the University Access to Learning fund and Churchill college.

Gwyneth Card deserves a special mention for having to compete with flies for my attention over the past four years. Thank you for all the help, fun, proofreading and head wounds.

Finally, thanks to my parents for pretty much everything else. I dedicate this dissertation to them in the hope that it will serve as a faithful doorstep for years to come.

Summary

How the outputs of populations of sensory neurons are used by motor systems to generate appropriate behaviour is a long standing question in neuroscience. I address this problem by studying a comparatively simple model system. In the fly, Neck Motor Neurons control gaze-stabilising head movements that occur during whole-body rotations. These motor neurons receive several sensory inputs including one from well-characterized visual interneurons, Tangential Cells (TCs), which respond to panoramic image shifts induced during self-motion.

In chapter one, I provide a general introduction to sensory-motor circuits and the fly gaze-stabilisation system.

In chapter two, I report that the visual receptive fields of Neck Motor Neurons are similar to those of the TCs. Using this result, I show an alignment between the coordinate systems used by the visual and the neck motor systems to process visual information. Thus, TCs encode visual inputs in a manner already closely matched to the requirements of the neck motor neurons, considerably facilitating the visual-motor transformation

In chapter three, I analyse the gating of neck motor neuron visual responses by convergent mechanosensory inputs from the halteres. Some neck motor neurons do not fire action potentials in response to visual stimuli alone, but they will in response to haltere movements. I show that visual stimuli produce sustained sub-threshold depolarisations in these neurons. These visual depolarisations increase the proportion of haltere-induced action potentials in neck motor neurons. Thus, visual inputs can only affect the spiking output if the halteres are moving. This simple mechanism could explain why flies only make visually induced head movements during walking or flight: behaviours that involve beating the halteres.

By analysing how the outputs of a model sensory system are used, I have shown a novel alignment between sensory and motor neuron populations and a simple mechanism underlying multisensory fusion.

1. Introduction	1
1.1. Properties of sensory-motor circuits.....	2
1.1.1. Temporal processing.....	2
1.1.2. Coordinate transformations.....	3
1.1.3. Multisensory integration	4
1.2. Levels of analysis of sensory-motor circuits.....	5
1.3. The model system: fly gaze stabilisation.....	6
1.3.1. Optic flow and Tangential Cells	7
1.3.2. Neck motor system	8
1.4. Summary	9
2. Receptive fields of Neck Motor Neurons	10
2.1. Abstract	11
2.2. Introduction.....	12
2.2.1. Gaze stabilisation and optic flow.....	12
2.2.2. Coordinate systems in sensory-motor transformations.....	13
2.3. Methods	15
2.3.1. Electrophysiology	15
2.3.2. Visual Stimuli	15
2.3.3. Data analysis	17
2.4. Results.....	21
2.4.1. Neck Motor Neuron receptive fields.....	21
2.4.2. Comparison of NMN and TC coordinate systems.....	23
2.4.3. Estimation of a NMN's TC inputs	25
2.4.4. Comparison of NMN receptive fields to compound eye geometry	27
2.5. Discussion	28
2.5.1. Significance of the alignment between NMNs and Tcs.....	28
2.5.2. Possible Tangential Cell – Neck Motor Neuron connectivity	31
2.5.3. Non-orthogonal sensory motor coordinate systems.....	31
2.5.4. Relationship to other sensory and motor systems.....	32
2.5.5. Relationship between NMN receptive fields and neck muscle pulling planes.....	33

3. Integration of haltere and visual inputs	34
3.1. Abstract	35
3.2. Introduction.....	36
3.3. Methods	39
3.3.1. Electrophysiology	39
3.3.2. Stimulus generation and presentation	40
3.3.3. Data analysis	43
3.4. Results.....	45
3.4.1. Extracellular recordings from Neck Motor Neurons	45
3.4.2. Intracellular recordings from Neck Motor Neurons	48
3.5. Discussion	54
3.5.1. Gating of visual responses by haltere input	54
3.5.2. Sub-threshold response properties	55
3.5.3. Functional gating through a simple mechanism	56
3.5.4. Behavioural correlates of electrophysiological results	57
3.5.5. Visually induced action potentials are phase locked to the haltere beating phase	59
4. Discussion	63
4.1. Visual and motor coordinate systems	64
4.1.1.1.Choice of coordinate systems.....	65
4.2. A qualitative model of the visual contribution to gaze-stabilisation.....	66
4.3. Suggested further experiments.....	67
4.4. Conclusions.....	68
5. Bibliography	69

1. Introduction

Sensory and motor systems are often studied in isolation. During behaviour however, the two systems must interact. How does the necessity of this interaction shape the two systems? This dissertation attempts to address this question through studying how a motor system processes the outputs of a well-characterised sensory system.

1.1 Properties of sensory-motor circuits

As sensory information flows from the sensory system to motor system it is processed in multiple ways. The temporal properties of the sensory signal structure may be altered, the coordinate system used for processing the sensory input may change, and the signal may be integrated with inputs from other senses. The following sections describe each of these processes in more detail.

1.1.1 Temporal processing

Often the temporal properties of a sensory response are not appropriate for the requirements of the motor system. Thus, the sensory signal is often processed to alter its temporal properties before it reaches the motor system. Such temporal processing is seen in the vertebrate vestibulo-ocular system. To keep a level gaze, eye position must compensate for any deviations from a level head position. To do this the eye motor system receives information about head movements from the vestibular sensory system. However, the vestibular system outputs information about head velocity, not position (Jones and Milsum, 1970; Fernandez and Goldberg, 1971). Therefore, when the head moves from a level to a non-level position the vestibular system will only signal during the transition. However, the eyes still need to maintain a compensatory position after the movement has ceased, as the head position will still be non-level. To account for this, the vestibulo-ocular circuit integrates (in the mathematical sense) the transient vestibular sensory output to provide the eye muscles with a sustained head position signal (Skavenski and Robinson, 1973).

1.1.2 Coordinate transformations

Many sensory systems analyse their inputs across a population of neurons. Each neuron within a population encodes a certain subset of the range of possible stimuli. Thus, across the population of neurons, a large number of potential stimuli can be encoded. The way in which responsibility for encoding different portions of the stimulus space is divided up across the population's constituent neurons can be understood by considering neuronal populations as coordinate systems. Each neuron in a population responds to a certain subset of stimuli and can thus be thought of as one axis of a coordinate system for encoding the incoming stimuli. The stronger a neuron's response, the further along its axis the current stimulus is. Thus, by considering the entire population of neurons, an N -dimensional coordinate system can be constructed. In this coordinate system each different stimulus occupies a certain position, dependent on the magnitude of response the stimulus elicits in different neurons. Human colour vision can, for example, be thought of as operating on a three-axis coordinate system. In this coordinate system the wavelength preferences of each of the three cone types defines one axis. Thus, the colour of a stimulus is encoded by the ratio of activity across the three cone types, i.e. the stimulus is placed at a certain point in the three-dimensional coordinate system specified by the cones.

As information passes from the sensory system to the motor system, the coordinate system it is processed through may change. The motor coordinate system is constrained by the requirement for the motor neurons to receive sensory input appropriate for the pulling planes of the muscles. Conversely, the sensory coordinate system is often related to the physical arrangement of the sensory structures, such as the arrangement of photoreceptors. Therefore, there is often the requirement for sensory information to be transformed from a sensory coordinate system to a motor coordinate system by the sensory-motor circuit. Such a sensory-motor coordinate transformation is thought to occur between the owl's optic tectum and the motor system controlling head movements. Masino and Knudsen (1990) studied the head movements produced by electrical stimulation of the optic tectum. The head movements produced by stimulation at different points were identified, and then experiments were performed where stimulation at one point was rapidly followed by stimulation at another point. If the two points stimulated produced head movements that did not share a horizontal or vertical orthogonal component, rapidly following

stimulation at one site with stimulation at another had no effect; the two head movements were produced as normal. If, however, the two head movements shared an orthogonal component, a different result was obtained. Rapidly following the stimulation at one site with stimulation at another site resulted in the second head movement being different to that normally produced during single stimulation. The head movement lacked the orthogonal component that it shared with the movement that preceded it. Thus, there is a 'refractory period' of unknown origin that prevents an orthogonal component of head movement from being used twice in rapid succession. From these results it was inferred that there exists an orthogonal coordinate system between the optic tectum and the motor system whose axes were subject to the refractory period effect observed. In this case, visual information passes from a sensory coordinate system to an orthogonal intermediate system and then to a motor coordinate system defined by the pulling planes of the neck muscles. Masino and Knudsen (1990) suggested that such an orthogonal intermediate coordinate system was a general feature of sensory-motor circuits.

1.1.3 Multi-sensory integration

As the sensory signal passes through a sensory-motor circuit, it is often combined with inputs from other sensory systems. Combining different sensory inputs has multiple advantages for a motor system. Each sensory system responds to a certain set of parameters. By combining complementary sensory inputs, a motor system can extend the parameter range to which it responds. For example, slower visual and faster vestibular inputs are combined to extend the dynamic range of the eye motor system. Combining sensory inputs also provides repeated samples of external events, increasing the confidence with which they can be estimated in the presence of noise.

Many examples of sensory convergence exist; one example is seen in the vertebrate superior colliculus where information from auditory, visual and somatosensory systems converges (Meredith and Stein, 1983). By monitoring the auditory receptive fields of colliculus neurons, Jay and Sparks (1984) showed that colliculus auditory receptive fields shift during eye movements in such a way as to always be aligned with the point in space from which the visual receptive field is receiving its input. Thus, by aligning the way in which the different sensory inputs

are encoded across the superior colliculus, multi-sensory integration is significantly facilitated.

The way in which a sensory input is processed by a motor system can also change according to the behavioural state of the animal. Such context dependent effects are seen in the locust flight system where pre-motor interneurons will only spike in response to sensory inputs if the flight central pattern generator is active (Reichert and Rowell, 1985; Reichert, 1985).

1.2 Levels of analysis of sensory-motor circuits

Generally, studies of sensory-motor circuits have treated the circuits in one of two ways. Those studies of comparatively simple reflex arcs have investigated the sense organ and motor unit in parallel. Conversely, those studies of more complex sensory-motor circuits have, by necessity of the complexity, had to study the sensory and motor systems in isolation.

Unsurprisingly, studies of comparatively simple reflex arcs have shown that the sensory input detected by a reflex's sensors is appropriate for the motor output produced. The classic example of this is the vertebrate stretch reflex where a muscle spindle detects stretching along its muscle's pulling plane and, via a one synapse reflex arc, provides drive to the muscle's motor neurons (Lloyd, 1943; Eccles et al., 1954). As the muscle spindle sits within the muscle it provides feedback to, the direction of stretch it detects is by its very nature aligned with the pulling plane of the muscle. Such an alignment between what is detected by the sensory apparatus and the requirements of the motor system significantly reduces the complexity of neural processing required and allows for the simple circuitry and short latency of spinal reflexes.

Studies of more complex sensory-motor circuits have usually focused on one or the other end of the circuit: either the sensory or the motor system. These more complex circuits tend to encode sensory information over populations of neurons as discussed in section 1.1.2. The study of such sensory systems has been particularly inspired by Barlow's (1961) hypothesis that a major role of a sensory system is to reduce the redundancy with which sensory information is encoded. In this view,

sensory systems optimise information coding efficiency without consideration to how that information is ‘read-out’ by downstream motor neurons. This hypothesis is supported by studies of wind direction-encoding in the cricket cercal system. Jacobs and Theuissen (2000) characterized the coordinate system used by a population of cercal sensory interneurons to encode wind direction and found that each of these interneurons had a cosine shaped tuning curve and responded to one of four orthogonal directions. This orthogonal system provides the optimal way to reduce redundancy between what is encoded by each neuron type and thus increases the coding efficiency.

The consideration of sensory systems in isolation has yielded many important insights. However, studying the sensory and motor systems as separate entities runs the risk of losing any additional understanding that may be obtained through the more integrative approach used to study simpler circuits. Are sensory systems purely optimised for encoding information efficiently or are they also adapted to use a code that is easy for the motor system to ‘read out’? Are those principles of alignment between sensory input and the requirements of the motor system seen in simple reflexes also seen in more complex systems? To answer these questions requires that one sensory system or more be studied in conjunction with the motor system(s) they contribute to. However, the complexity of many sensory-motor circuits prohibits fine-scale comparisons of sensory and motor circuits. A model system is required that is complex enough to encode sensory inputs across populations of sensory interneurons, but simple enough to be tractable.

1.3 The model system: fly gaze stabilisation

A promising model system for investigating sensory-motor circuits is found in the fly gaze-stabilisation system. The neural circuitry in this system is comparatively simple and at least one sensory input is encoded over a population of sensory interneurons. Thus, this circuit is simple enough to study its sensory and motor systems in parallel, yet not just a simple reflex arc.

Flies exhibit impressive flight behaviour, performing fast turns in turbulent air, yet they still manage to maintain a level gaze by moving their head against any body rotation (Hengstenberg, 1993; Schilstra and Hateren, 1999; van Hateren and Schilstra,

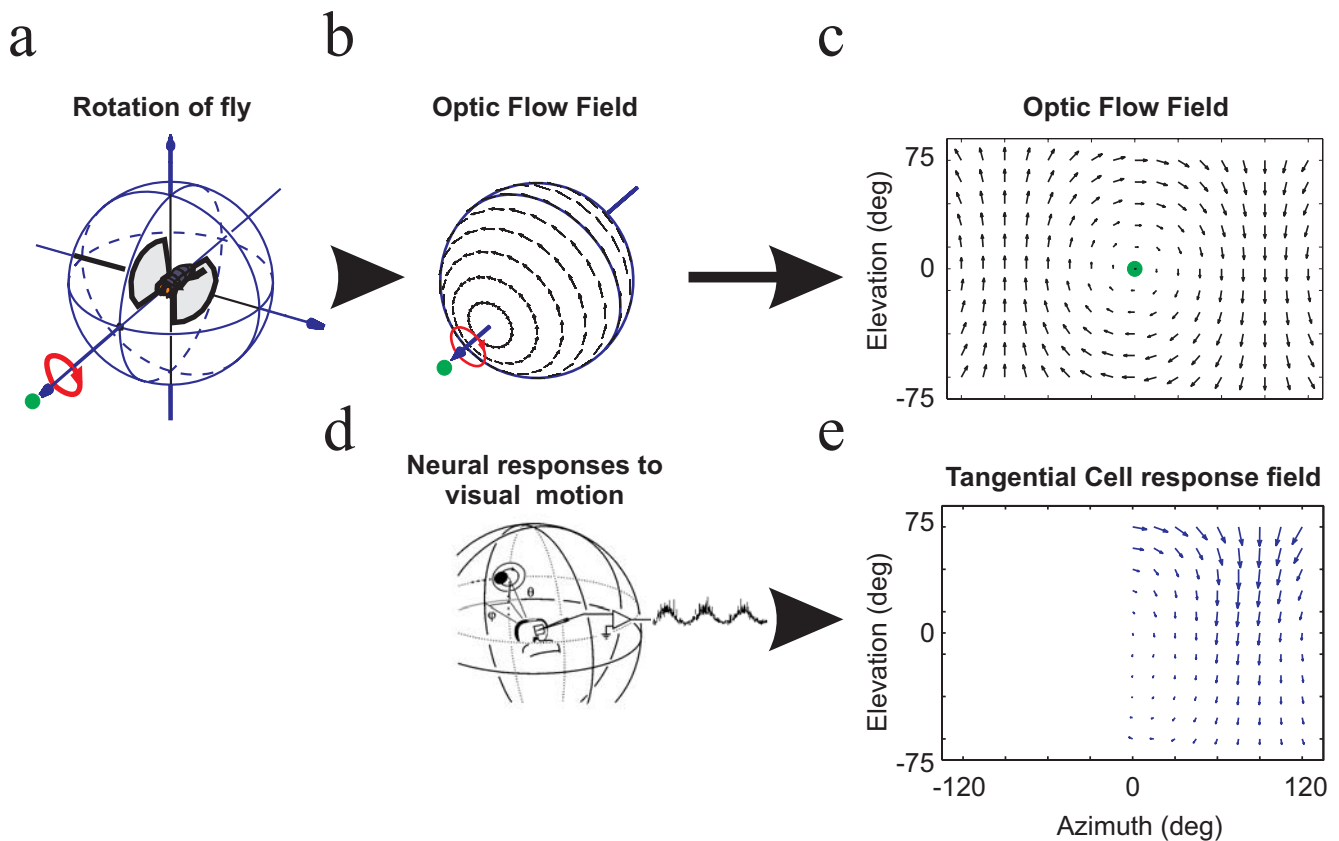


Figure 1.1 Relationship between an optic flow field and the receptive field structure of a Tangential Cell. (a) shows a fly rotating counter-clockwise about its longitudinal body axis, (b) shows the pattern of visual motion, or optic flow field, resulting from such a roll rotation. The optic flow field is plotted on the sphere of visual space surrounding the fly. Orientation and length of each arrow indicate the direction and magnitude of motion at each location. (c) is the same optic flow field as in (b) but plotted in 2-D. The green dot marks the axis of rotation; note that the optic flow field forms a singularity around this axis. (d) is a cartoon of the experimental procedure used by Krapp et al. (1998); local motion stimuli were presented at different points in visual space (defined by azimuth and elevation) to determine the pattern of Tangential Cell local directional tunings across visual space. (e) plots the receptive field structure of one Tangential cell as obtained in the experimental procedure described in (d). The orientation of each arrow indicates the Tangential Cell's preferred direction of local motion at that point in visual space. The length of each arrow gives a relative measure of local motion sensitivity. By comparing (c) to (e) it can be seen that the receptive field structure of the Tangential Cell closely matches the structure of a rotational optic flow field. From this finding it was inferred that each Tangential Cell is tuned to a certain axis of rotation (Krapp et al., 1998). Figure adapted from (Krapp, 2000)

1999). In doing so, flies facilitate visual processing by minimising motion blur and by reducing the visual consequences of self-rotations that interfere with other visual cues (Land, 1999). This gaze stabilisation behaviour is guided by multiple sensory inputs that detect rotations of the fly (Hengstenberg, 1991; Hengstenberg, 1993).

1.3.1 Optic flow and Tangential Cells

One sensory cue used to guide gaze-stabilisation consists of visual inputs from the compound eye. When the fly rotates or translates, the image of its environment moves in the opposite direction across the fly's retina. This characteristic pattern of panoramic visual motion is termed optic flow. Each rotation about different axis results in a characteristic pattern of optic flow. The relationship between a rotation of the fly and the resulting optic flow is shown in figure 1.1.a-c. Note that in the flow field a singularity can be seen where no relative motion occurs. This singularity indicates the axis of the fly's rotation. Flies analyse the optic flow field to estimate and guide their own movements. In the gaze-stabilisation system, optic flow is used to estimate the axis of self-rotation so the fly can produce an appropriate compensatory head movement to keep its eyes level.

Visual motion is detected on a local level (Reichardt, 1961), but to disambiguate the optic flow arising from different rotations requires information about the pattern of visual motion across a wide area (Koenderink, 1987; Dahmen et al., 2001). Therefore, to extract self-motion information, the fly nervous system must at some point integrate local motion signals from over the visual field. This wide-field integration occurs at the level of the Tangential Cells (TCs), sensory interneurons of the fly's lobula plate. These TCs have been the subject of extensive study. The TCs consist of a circumscribed set, each member of which has identifiable anatomical and physiological features (Hausen, 1984). They have been shown to be involved in motor control (Geiger and Nassel, 1981; Hausen and Wehrhahn, 1983) and the horizontal interactions between them have also been studied (Egelhaaf et al., 2002; Haag and Borst, 2004). Krapp et al. (1996; 1998; 2001) performed experiments where the local motion preference of each TC was measured at different points in the visual field. When the local motion preferences of a TC were compared across visual space (figure 1.1.e), it was seen that the pattern of local motion preferences across the TC's receptive field were remarkably similar to the patterns of optic flow experienced

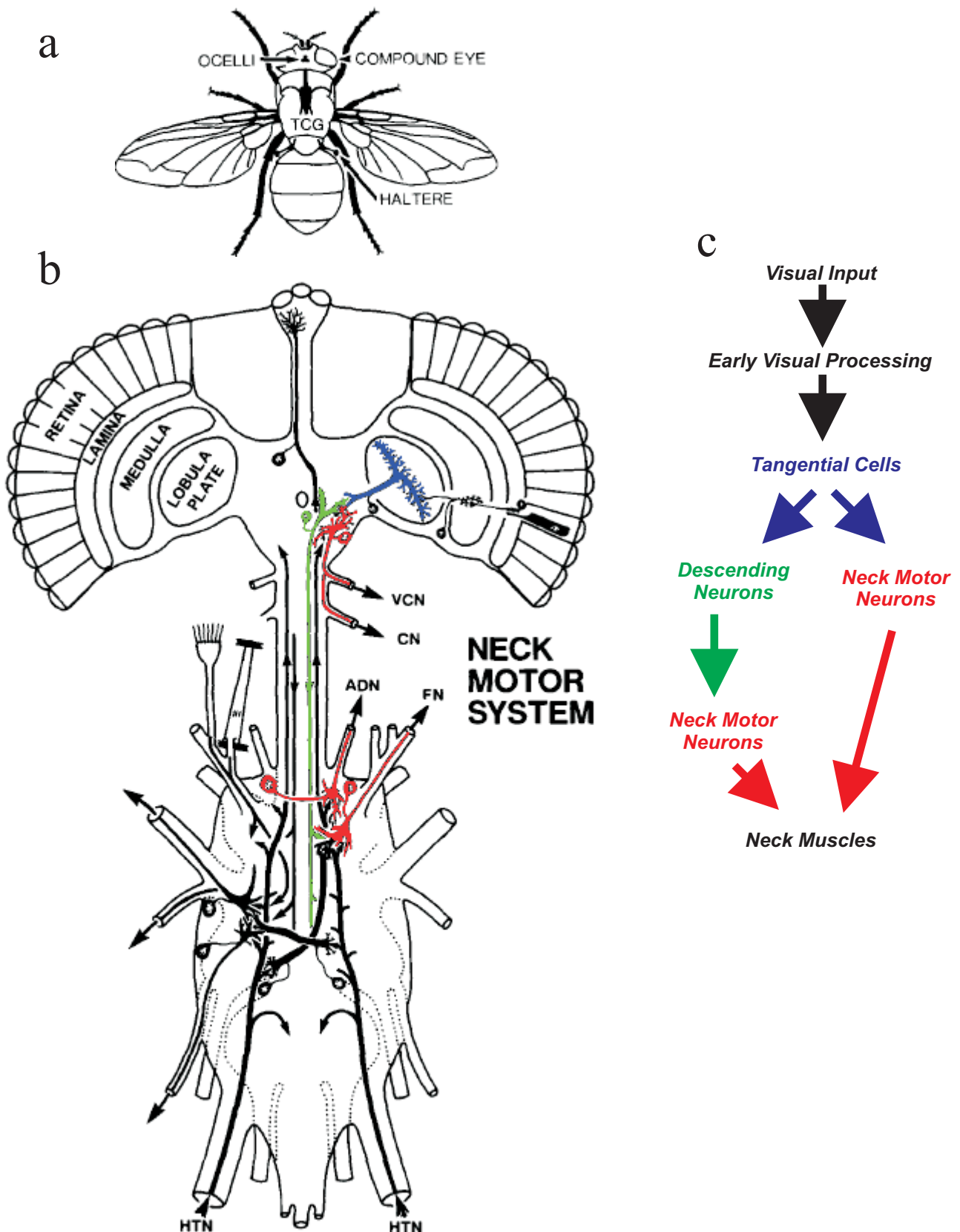


Figure 1.2 Circuit diagram for the gaze-stabilisation system.

(a) is a cartoon of a fly, note the halteres and compound eyes.

(b) is a cartoon of the fly nervous system; a tangential cell is shown in blue; this connects directly to Neck Motor Neurons in the head (shown in red) and, via a descending neuron (shown in green), to Neck Motor Neurons in the thoracic ganglion.

(c) summarises those connections shown in (b), colours of arrows correspond to the colours of neurons shown in (b). Figure adapted from (Hengstenberg, 1991). Abbreviations: VCN: Ventral Cervical Nerve, CN: Cervical Nerve, ADN: Anterior Dorsal Nerve, FN: Frontal Nerve, HTN: Haltere Nerve.

during rotation (compare panel e to c in figure 1.1). Each of the 13 different output TCs had a receptive field structure that appeared to be tuned to the optic flow resulting from rotation about a different axis. Thus, rotational optic flow is encoded over a defined population of sensory interneurons (Karmeier et al., 2005). TCs output to multiple motor systems, one of which is the neck motor system.

1.3.2 Neck motor system

The neck motor system produces the head movements seen during gaze-stabilisation. It consists of 21-22 muscles on either side of the neck which can move the head either by pulling on it directly or by moving the cervical sclerites, which in turn moves the head (Strausfeld et al., 1987). The majority of the neck muscles receive input from only one Neck Motor Neuron (NMN) (Strausfeld et al., 1987). These NMNs can be divided into two groups: those with their cell bodies in the brain and those with their cell bodies in the thoracic ganglion (Strausfeld et al., 1987). Each group gives rise to two neck motor nerves. The NMNs with cell bodies in the brain receive direct synaptic inputs from the TCs, whereas the NMNs with cell bodies in the ganglion receive TC inputs via descending neurons (Milde et al., 1987; Strausfeld et al., 1987; Gronenberg and Strausfeld, 1990; Strausfeld and Gronenberg, 1990; Gronenberg et al., 1995); see figure 1.2 for a simplified wiring diagram.

The extracellular visual responses of NMNs have been investigated to some degree by Milde et al. (1987). They found that NMNs in different neck nerves responded maximally to different directions of visual motion. The directional preferences of NMNs within a given nerve were in rough agreement with the estimated pulling planes of the neck muscles innervated by NMNs of that nerve. This agreement was further supported by whole nerve stimulation experiments, in which stimulating a neck nerve resulted in a head movement approximately aligned with the visual directional tunings of the nerve's constituent NMNs (Gilbert et al., 1995).

Milde et al. (1987) described the directional preferences of the NMNs in terms of their responses to planar motion. The NMN directional tunings were interpreted to mean that each of the NMNs responds to one of the Cartesian components of rotation: roll, pitch or yaw. This interpretation was arrived at because, at the time of the study, TCs were broadly classified into two groups in terms of directional motion selectivity: the Vertical System (VS) TCs sensitive to vertical motion encoding roll and pitch and

the Horizontal System (HS) TCs sensitive for horizontal motion encoding yaw. It was not until Krapp and co-workers (1996; 1998; 2001) mapped the fine structure of TC receptive fields that it became clear that TCs were tuned to many different non-orthogonal axes of rotation. Armed with this new knowledge, the experiments in chapter two use the methods of Krapp and Hengstenberg (1997) to estimate the axes of rotation to which NMNs respond, and thus the coordinate system used by the NMNs.

Another sensory input to the fly gaze-stabilisation circuit comes from the halteres. Halteres are vestigial hind wings that beat anti-phase to the wings and detect fast rotations of the fly through the resulting Coriolis forces (Pringle, 1948; Nalbach, 1993). Studies have also shown that NMNs receive haltere inputs (Strausfeld and Seyan, 1985; Milde et al., 1987).

1.4 Summary

The gaze-stabilisation system of the fly provides a model sensory-motor system with a well-characterised visual input and a comparatively simple neural circuitry. This dissertation aims to take advantage of this model system to investigate the relationship between the visual system and the neck motor system. In chapter two, the visual responses of NMNs are studied to elucidate how visual information encoded in the TC population is utilised by the neck motor system. In chapter three, the responses of NMNs to combined visual and haltere stimulation are studied to investigate how the motor system integrates visual inputs with those from other senses.

2. Receptive fields of Neck Motor Neurons

2.1 Abstract

Much progress has been made in describing sensory and motor systems in isolation. However, to understand the control of behaviour we must know how the two systems interact. To address this gap in our knowledge, this study investigates how visual information is passed to the fly motor system that controls gaze-stabilising head movements. Neck Motor Neurons that drive head movements are probed with visual stimuli to define their receptive fields. This study shows that Neck Motor Neurons have very similar visual receptive fields to those of Tangential Cell interneurons of the third visual neuropile. From each neuron's receptive field, the axis of rotational optic flow field that would generate the greatest response is estimated. By comparing these axes, it is seen that the Tangential Cell and Neck Motor Neuron populations use similar coordinate systems for processing optic flow. In other words, the visual and neck motor systems are aligned with each other. This alignment considerably simplifies the visuo-motor transformation. It is suggested that the fly visual system uses a strategy of extracting visual information in a manner as close to the requirements of the motor system as possible.

2.2 Introduction

Sensory and motor systems have been extensively studied in isolation, however relatively little is known about how the two interact. How are the outputs of sensory systems used by motor systems to generate behaviour? Here this issue is addressed by investigating the visual control of fly head movements. This system provides a tractable circuit in which the outputs of a well-characterised sensory system contribute to guide a known motor output.

2.2.1 Gaze stabilisation and optic flow

Animals need to keep their eyes as steady as possible. This reduces motion blur and allows any pattern matching done by the visual system to operate on the assumption of a level retina (Land, 1999). To maintain a stable gaze, flies and other animals make head/eye movements to counter rotations of the body and keep the eyes level. In flies, many sensory cues contribute to this gaze-stabilisation behaviour, the most well studied of which is vision (Hengstenberg, 1991; Hengstenberg, 1993). When the fly moves, an image of its environment travels across the fly's retina. This visual motion induced by relative movement between the fly and its environment is termed optic flow. Optic flow has a distinctive pattern that is dependent on the nature of the animal's movement. For example, when the fly rotates clockwise about its longitudinal body axis, it will experience downwards motion across its left eye and upwards motion across its right eye. Thus, an animal can estimate its own movements from the optic flow impinging on its retina. The fly uses the self-motion information present in optic flow to guide its gaze-stabilising head movements (Hengstenberg, 1993). In the example of clockwise roll about the longitudinal body axis, the fly would rotate its head counter-clockwise relative to the body, keeping its retina aligned with the external horizon.

A large body of evidence strongly suggests that the visual interneurons of the lobula plate called Tangential Cells (TCs) extract wide field optic flow information from local motion detectors (Borst and Haag, 2002). TCs connect directly and indirectly via descending neurons to Neck Motor Neurons (NMNs) that drive the

muscles responsible for head movements (Strausfeld et al., 1987). In pioneering work, Milde et al (1987) obtained preliminary results about the visual responses of NMNs. However, this work was done at a time when TCs were thought to respond to one of the three Cartesian components of rotation: roll, pitch and yaw. Thus Milde et al. (1987) classified NMNs as either responding to roll, pitch or yaw. The results of Krapp and co-workers (Krapp et al., 1998; Krapp et al., 2001; Karmeier et al., 2005) have since shown that the TC population contains neurons tuned to many different, non-orthogonal axes of rotation. Thus, the NMNs may also be tuned to non-orthogonal axes.

2.2.2 Coordinate systems in sensory-motor transformations

Neuronal populations representing some sensory input space are often regarded as employing a coordinate system defined by the response preferences of their constituent neurons. Each sensory neuron responds to a certain subset of the stimulus parameter space. Thus, each neuron can be thought of as one axis of a N -dimensional coordinate system, the neuronal activity in that neuron giving the magnitude of the current stimulus along the neuron's particular axis. Similarly, a motor system can be thought of as forming a coordinate system with axes defined by the pulling planes of the muscles. Therefore, for the motor system to make use of a sensory input, it must first be transformed from a sensory coordinate system to a form appropriate for the motor coordinate system. How this transformation between the sensory and motor coordinate systems occurs is not well understood.

To try and elucidate the principles underlying sensory-motor transformations, this study investigates the transformation occurring between the Tangential Cells (TCs) and Neck Motor Neurons (NMNs) of the fly gaze-stabilisation system. The receptive fields of TCs have been well characterised and suggest that each TC responds to the optic flow resulting from rotations of the fly about a certain body axis (Krapp and Hengstenberg, 1996; Krapp et al., 1998; Franz and Krapp, 2000; Krapp et al., 2001), although TCs will also respond to translatory optic flow (Kern et al., 2005)). The preferred axis of rotation varies systematically across the population of 26 output TCs (Krapp et al., 1998; Krapp, 2000; Karmeier et al., 2005). Thus, the 26 output TCs of the fly visual system can be thought of as a coordinate system encoding

rotational optic flow. How does the neck motor system extract information from this TC coordinate system? This study obtains, for the first time, detailed descriptions of NMN visual receptive fields and uses them to estimate the axes of rotation to which NMNs would respond if presented with wide-field optic flow stimuli. Using this information it is possible to compare the coordinate systems used by TC and NMN populations for processing rotational optic flow, providing a description of the visuo-motor transformation.

2.3 Methods

2.3.1 Electrophysiology

Female 1-3 day old blowflies (*Calliphora vicina*) from the Department of Zoology, University of Cambridge colony were mounted either dorsal or ventral side up on custom-made holders. The wing bases were waxed and the legs and wings removed. The resulting wounds were sealed with beeswax to reduce fluid loss. The eyes were aligned with the visual stimulus according to the deep pseudopupil (Franceschini, 1975), and the head fixed in position with beeswax. The ocelli were obscured with black paint.

In those experiments where the fly was mounted ventral side up, a small window was cut in the neck or thorax cuticle exposing the neck nerve to be studied. Two hook electrodes constructed from 0.025 mm diameter silver wire were placed under the nerve of interest. Hemolymph was temporarily removed from the recording site and replaced with a petroleum jelly, paraffin oil mixture. The tissue was then kept moist with fly saline, see Hausen (1982) for the saline recipe. In those experiments where the fly was mounted dorsal side up, the methods used were the same except that the hook electrodes were placed under neck muscles instead of a nerve, allowing recordings to be taken from NMN axons at the point of their muscle arborisations. In all, 47 units were recorded from that responded to visual motion over a wide area.

Signals from the hook electrodes were amplified 3000 times by a Brownlee (Santa Clara, CA) Precision amplifier Model 440 operating in differential AC mode. The amplifier output was sampled at 10 KHz by a National Instruments PCI-6025E data acquisition board on a computer running Matlab (Mathworks, Natick, MA). The acquired waveform was spike-sorted using self-written template matching software written in Matlab (figure 2.1).

2.3.2 Visual Stimuli

Visual stimuli were presented on a green Cathode Ray Tube (CRT, P31 phosphor) driven by an Innisfree Picasso Image generator at a refresh rate of 182 Hz.

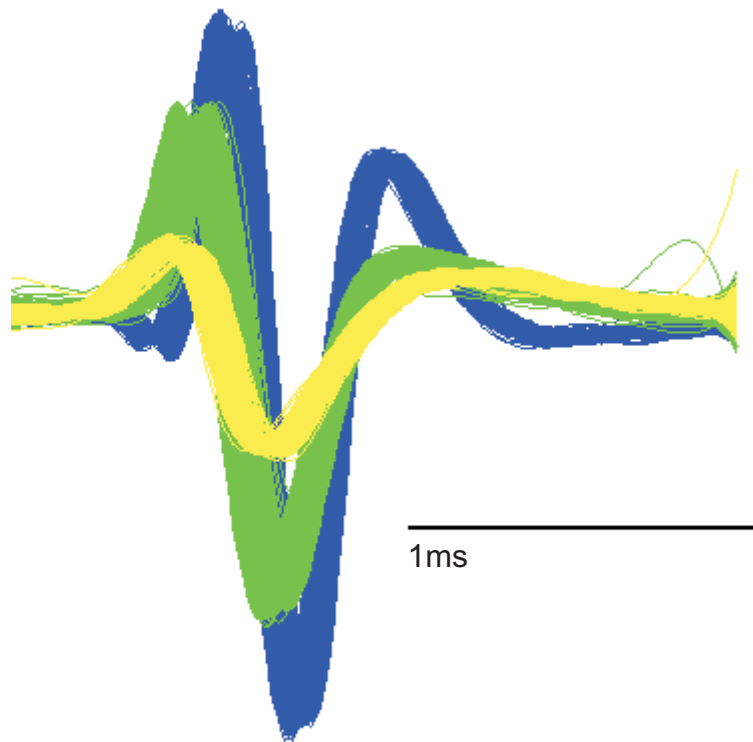


Figure 2.1 Output of the spike sorting program as applied to 32 seconds of a multi-unit recording. All spike waveforms occurring in the 32 second recording are overlaid. The waveforms were sorted into three groups using the spike sorting program. The colour of each waveform indicates the group into which it was sorted.

The CRT was placed 7.4 cm from the fly so that the circular screen aperture subtended a visual angle of 62.6° . Depending on the visual responsiveness of the unit being studied, one of two different types of visual stimulus was used. For those units that were highly sensitive to visual motion, a black dot moving on a circular path was used, similar to Krapp and Hengstenberg (1997). This stimulus consisted of a black dot 7.6° in diameter travelling on circular path of diameter 10.4° across a green background (96% contrast) at two cycles per second. By travelling on a circular path, this stimulus covered all possible directions of visual motion. By correlating a unit's change in spike rate with the direction of dot movement, the directional tuning curve could be rapidly acquired. Both clockwise and counter-clockwise dot rotations were used, allowing the directional tuning of a neuron to be corrected for neural delay. The dot travelled round its circular path six times in each direction, onset transients were excluded from the data analysis by only analysing the responses to the last five stimulus cycles. See Krapp and Hengstenberg (1997) for more details of this method.

If the unit recorded from did not produce a robust response to the dot stimulus, a stronger visual stimulus was used, which took longer to map the receptive field. Squarewave visual gratings of 96% contrast and spatial period 10° were moved, perpendicular to their orientation, with a temporal frequency of 5 Hz across the full extent of the 62.6° diameter screen. 16 different directions of moving grating were used at a spacing of 22.5° . The order of grating presentation was generated in a pseudo-random manner. Before each grating, a blank screen of the same mean luminance as the grating (18 cd/m^2) was shown for five seconds. The spike rate during the blank screen was taken as a baseline; the response to a grating was defined as the mean change in spike rate from this baseline occurring during the one second stimulus. Plotting the responses to visual motion against the 16 different directions revealed the neuron's directional tuning curve for the area of visual space subtended by the stimulus.

The CRT was mounted upon a meridian that allowed it to be moved around the fly's eyes. The CRT could be placed so the screen centre was anywhere between -120° to 120° in azimuth and -70° to 75° in elevation with respect to the centre of the fly's head, $[0^\circ, 0^\circ]$ being directly in front of the fly. By placing the CRT at a variety of locations, directional tunings were obtained at different points in the fly's visual field. During the course of an experiment the CRT was moved to different positions

in a pseudo-random manner. For elevations 15° and -15° , visual stimuli were presented at positions from -120° to 120° with a 15° spacing along the azimuth. For elevations 45° and -45° visual stimuli were presented at 30° azimuth spacing and at elevations 75° and -70° a 45° azimuth spacing was used.

2.3.3 Data analysis

All data analysis was performed using Matlab programs custom written for the purpose of this PhD.

2.3.3.1 Construction of receptive field maps

The neuronal responses obtained at different stimulus positions were analysed to obtain the unit's preferred direction of motion and sensitivity to motion at each point in visual space tested. For the experiments where the dot stimulus was used, the analysis was performed as described in Krapp and Hengstenberg (1997). The direction of dot motion where spikes were most likely to occur was found and defined as the unit's preferred direction of motion at that point in visual space. The unit's sensitivity to motion at one point in visual space was defined as the difference between the number of spikes fired during motion in the unit's preferred direction $\pm 45^\circ$ and the number of spikes fired during motion in the opposite direction $\pm 45^\circ$. For the experiments where the grating visual stimulus was used, a tuning curve was obtained by comparing the unit's response to 16 different directions of visual motion, an example is seen in Figure 2.2c. The peak and relative amplitude of this tuning curve was estimated by finding the phase and amplitude of the fundamental harmonic in a fast Fourier transform of the tuning curve. The preferred direction was defined as the peak of the tuning curve (vertical grey line in figure 2.2.c) and the sensitivity was defined as the amplitude of the tuning curve.

Once the preferred direction and sensitivity to motion for a unit had been obtained at locations across the visual field, they were plotted to give a receptive field map for the unit. An example of one such map is seen in figure 2.2.d. The direction of each arrow gives the direction of visual motion that elicited the largest response when presented in that part of visual space. The length of each arrow gives the

relative sensitivity of the unit to visual motion in that part of visual space. In figure 2.2.d the boxed arrow is derived from the tuning curve in figure 2.2.c. Arrows resulting from the raw data are plotted in black and arrows resulting from interpolated data are plotted in grey. The interpolation method used is that described in Sandwell (1987), it makes no assumptions about receptive field structure other than that the transitions from one data point to another are smooth. The lowest position the CRT could be held at was -70° in elevation, whereas the highest position was 75° . This means that in the experiments where the fly was mounted dorsal side up, the elevation range tested ran from -70° to 75° , whereas in the experiments where the fly was mounted upside down, the elevation range covered was -75° to 70° . To allow the comparison of receptive fields obtained in different experiments, this mismatch was overcome by performing a 5° extrapolation (Sandwell, 1987) on the data taken at an elevation of 70° . Thus the data obtained at an elevation of 70° is not plotted but the data extrapolated to 75° is.

2.3.3.2 Estimation of the rotation that most strongly stimulates a neuron

The receptive field plots allow comparison of the visual responses of individual units. The aim of these experiments, however, is to compare the coordinate systems used by the TC and NMN populations for processing a biologically relevant parameter. Thus, it is necessary to define what axis of rotation each unit responds to. This axis was estimated from a unit's receptive field.

The optic flow that would result from rotation about a certain axis was computed using the algorithm described in Koenderink and van Doorn (1987) and expressed as an array of local motion vectors. The dot products of the local velocity vectors in the optic flow field and the local preferred directions plotted in the receptive field maps were computed. The results of the dot products were summed across the receptive field with appropriate weighting to compensate for the over-sampling of high and low elevations. The resulting number gives a measure of the similarity between the unit's receptive field and the rotational optic flow field. This procedure was repeated for axes of rotational optic flow across the entire sphere with a spacing of 1° between axes tested. In this way, the axis of rotation that generates the optic flow field most similar to the unit's receptive field can be identified. This

axis was defined as the unit's 'preferred axis of rotation'. This definition is based upon the assumption that the more similar an optic flow field is to a unit's receptive field, the stronger the unit's response to the optic flow field will be. Using this method a preferred axis was obtained for all Tangential Cells (TCs)¹ and Neck Motor Neurons (NMNs). The preferred axis can be described by just two numbers, its azimuth and elevation, thus a large number of unit's can be compared simultaneously through the comparison of their preferred axes.

A cluster analysis was used to describe the distribution of TC preferred axes. The Euclidian distance between the TC preferred axes was used to perform a hierarchical cluster analysis based upon the Ward method (Matlab Statistics Toolbox).

2.3.3.3 Estimation of Tangential Cell inputs to a Neck Motor Neuron from its receptive field

To estimate which TCs provide excitatory inputs to NMNs, an optimisation procedure was performed. This optimisation attempted to find the weighted combination of TC receptive fields that would most closely match each NMN receptive field. The binocular receptive fields of the 26 output TC types obtained by Holger Krapp (Krapp, 1995; Krapp et al., 2001) were used for this analysis. A random weight was generated for each of the 26 TCs. The receptive field of each TC was multiplied by its respective weight and the resulting weighted TCs were then summed, giving an output receptive field. This output receptive field was subtracted from the receptive field of the NMN being studied; the result was then squared giving an error term. The smaller this error term is, the closer the output receptive field is to that of the NMN receptive field. The error term was minimised by gradient descent using the delta rule (Widrow, 1960) to alter the weights assigned to each TC. To ensure that the gradient descent algorithm did not become stuck in local minima, noise was added to the output of the delta rule. The amount of noise added was reduced slowly over time (magnitude of noise at iteration $t = 100 * 0.99^t$, 70000 iterations used per optimisation) so at some point the noise present would be large enough to allow escape from a local minimum but not large enough to allow escape

¹ Binocular TC receptive fields were obtained from Krapp (1995), the axis estimation however was done as part of this study.

from a global minimum (method adapted from Kirkpatrick et al. (1983)). To confirm that a global minimum had been reached, each optimisation was repeated ten times from different, randomly chosen starting weights. The TC weights arrived at by the optimisation algorithm specify the combination of TC receptive fields that most closely matches the NMN receptive field. Thus, the weights suggest which TCs provide inputs to the NMN being studied.

2.4 Results

2.4.1 Neck Motor Neuron receptive fields

The relationship between how Tangential Cells (TCs) and Neck Motor Neurons (NMNs) process visual information was investigated by obtaining NMN receptive field maps and comparing them to those of TCs. As noted by Milde et al. (1987) only a sub-population of NMNs fired action potentials in response to visual motion alone, only these units were investigated in this chapter.

The spikes of individual units were easily identifiable from the extracellular recordings; figure 2.1 shows a typical output of the spike sorting program. To create a receptive field map, the directional tuning of NMNs at different points in visual space was measured. Figure 2.2a shows the increase in spike rate in one NMN to local motion in its preferred direction, and figure 2.2b shows the response to local motion in the opposite direction. For the unit shown in figure 2.2, and 45 of the 47 units recorded from, the increase in spike rate during motion in the units preferred direction was larger than the decrease in spike rate during motion in the opposite direction. These responses, along with those to 14 other directions of visual motion are compiled into the visual tuning curve shown in figure 2.2c. This tuning curve, like all others obtained, has one main peak. The direction of motion that causes this peak response is estimated and defined as the preferred direction (grey vertical line in figure 2.2c). The sensitivity to visual motion is defined as the amplitude of the tuning curve. The preferred direction and sensitivity to visual motion were obtained at different locations within the fly's visual field and then plotted as a visual receptive field map as in figure 2.2d. The direction of each vector in figure 2.2d represents the preferred direction of the unit in the portion of visual space denoted by the vector's location. The length of each vector gives the relative motion sensitivity of the unit at that point of visual space. The vector in the box in figure 2.2d is that resulting from the visual tuning curve shown in figure 2.2c.

In those recordings taken near the neck muscles, each action potential was followed by a slower waveform as shown in figure 2.3. The majority of neck muscles only receive one NMN input (Strausfeld et al., 1987), so it is likely that the slower

waveform is generated by the neck muscle innervated by the recorded NMN. As there was a 1:1 relationship between the spike and the muscle waveform, the receptive field of these units can also be considered to be the receptive field of the neck muscle.

As detailed in the methods section, the NMNs were mapped in one of two ways, either with a dot or grating stimulus. Figure 2.4 shows the receptive field maps resulting from a control experiment where two maps were obtained from the same unit, one using the dot (figure 2.4a) and one using the grating stimulus (figure 2.4b). The two maps are very similar, demonstrating that the use of different stimuli in this study does not bias any conclusions made. The only difference in the results obtained from the two methods is that the grating results in a larger number of points having high visual sensitivities (compare figures 2.4a and 2.4b). This is partially due to the grating being a stronger stimulus and partially due to the grating covering a larger area than the dot stimulus, thus ‘blurring’ the receptive field slightly.

Some NMNs responded to visual stimuli over a wide area of visual space whereas others only responded over a small area, typically that in front of the fly. Units were designated as ‘small-field units’ if they did not respond to visual motion over a portion of the visual field greater than 90° in diameter. Examples of wide-field and small-field NMNs are seen in figure 2.5. In the small-field NMN of figure 2.5a, and all small-field NMNs recorded from, the directional sensitivities in the portion of visual space where the unit responded were very similar to the directional sensitivities of wide-field NMNs over the same portion of visual space; compare figure 2.5a to 2.5b. Generally small-field NMNs had larger extracellularly recorded action potentials and lower spontaneous rates than wide-field NMNs.

There is a visual horizon detection input to the gaze-stabilization system (Hengstenberg, 1988; Hengstenberg, 1991). Those small-field cells with vertical sensitivities may be involved in horizon detection. Another possibility is that small-field cells receive wide-field inputs but, with the visual stimulus used, only stimuli in the central region are capable of producing supra-threshold response. The small-field units may only respond in the central region of the visual field as this is the area of binocular overlap. Thus, visual stimuli in this region will excite the NMN via both eyes. The rest of the results section will deal with wide-field NMNs exclusively.

The NMN receptive fields were compared to TC receptive fields obtained in a previous study (Krapp, 1995; Krapp et al., 2001). For each NMN receptive field,

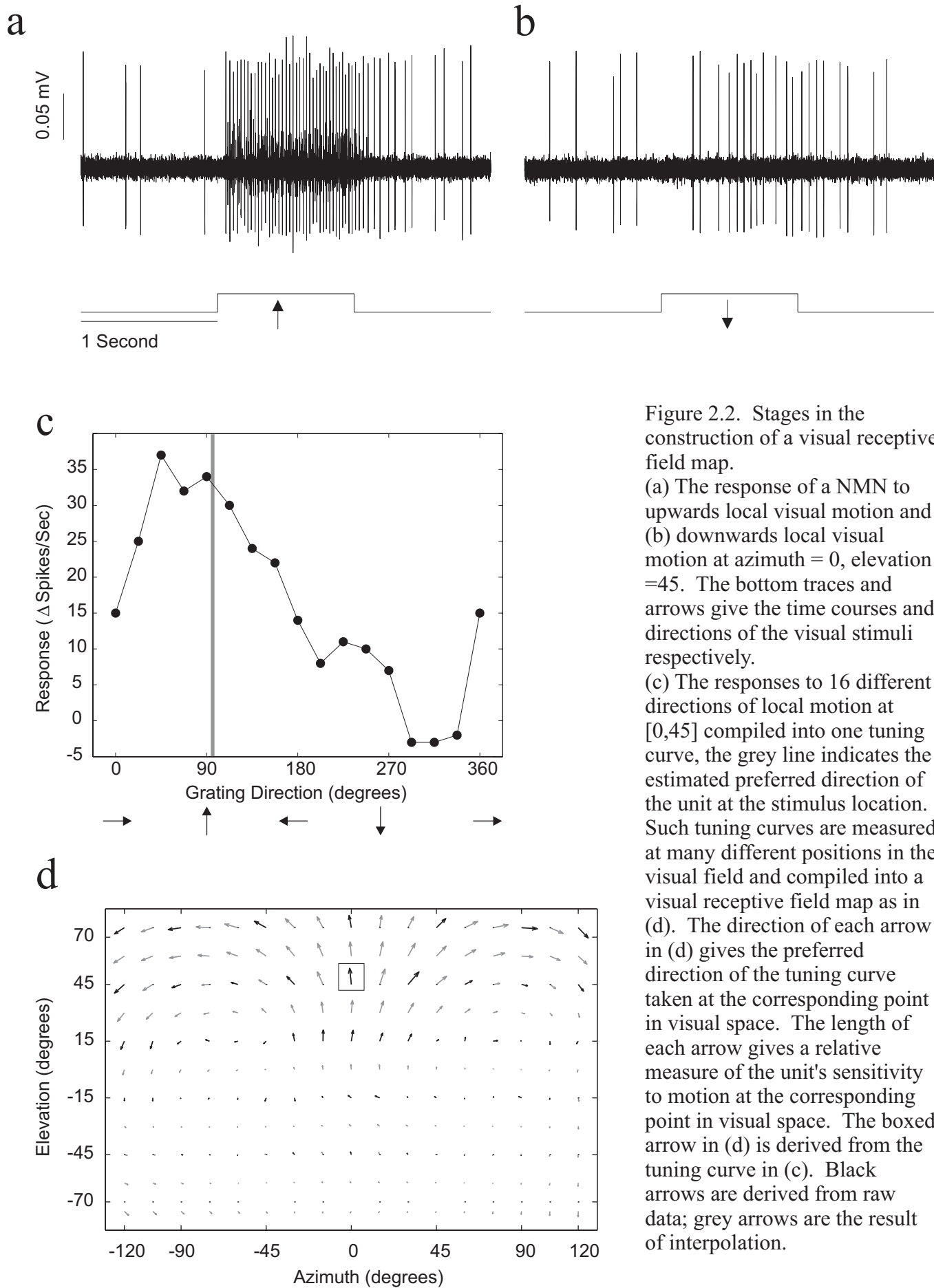


Figure 2.2. Stages in the construction of a visual receptive field map.

(a) The response of a NMN to upwards local visual motion and (b) downwards local visual motion at azimuth = 0, elevation = 45. The bottom traces and arrows give the time courses and directions of the visual stimuli respectively.

(c) The responses to 16 different directions of local motion at [0,45] compiled into one tuning curve, the grey line indicates the estimated preferred direction of the unit at the stimulus location. Such tuning curves are measured at many different positions in the visual field and compiled into a visual receptive field map as in (d). The direction of each arrow in (d) gives the preferred direction of the tuning curve taken at the corresponding point in visual space. The length of each arrow gives a relative measure of the unit's sensitivity to motion at the corresponding point in visual space. The boxed arrow in (d) is derived from the tuning curve in (c). Black arrows are derived from raw data; grey arrows are the result of interpolation.

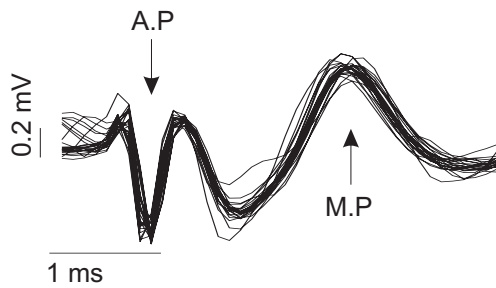


Figure 2.3. Spike waveform of a recording taken at the level of a NMN muscle arborisation. The waveform consists of a fast early component and a late slow component. The fast early component is likely to be the NMN action potential (labelled A.P on figure) whereas the slow component probably reflects the muscle potential (labelled M.P on figure) of the neck muscle innervated by the NMN.

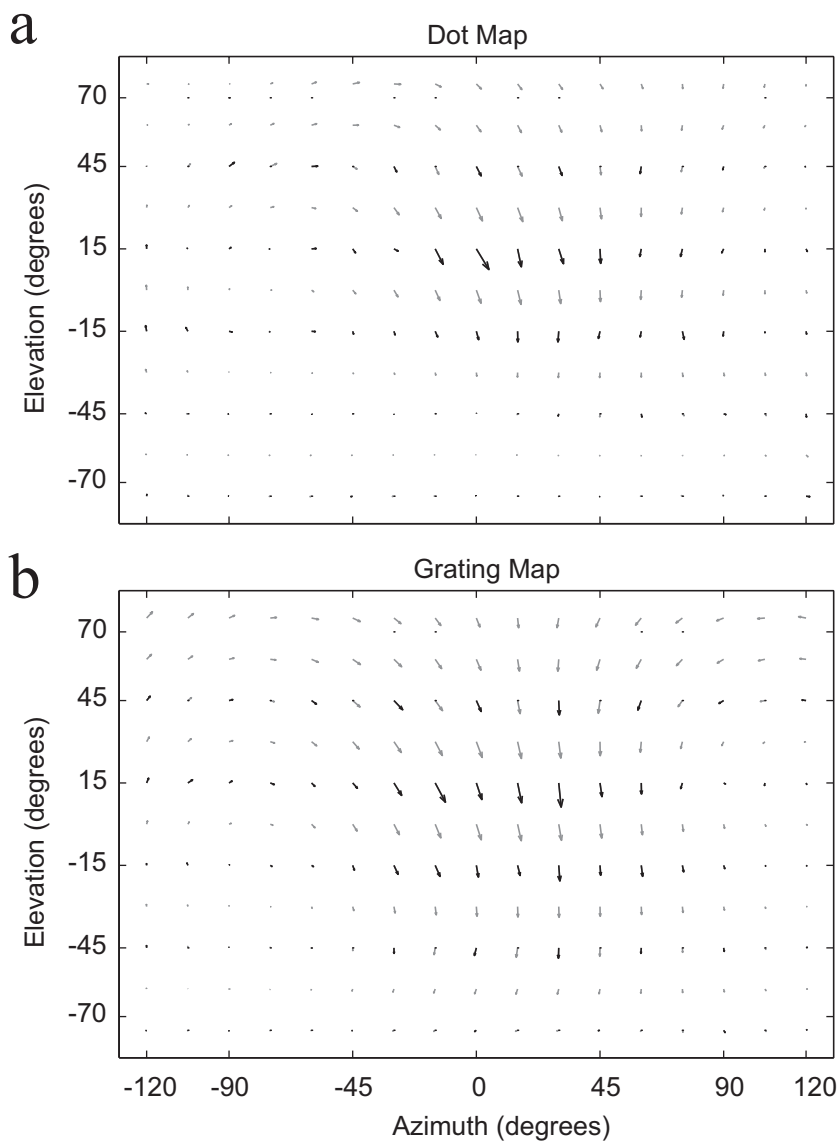


Figure 2.4. Comparison of receptive field maps taken from the same unit using either a dot moving on a circular path (a) or a moving grating (b) stimulus.

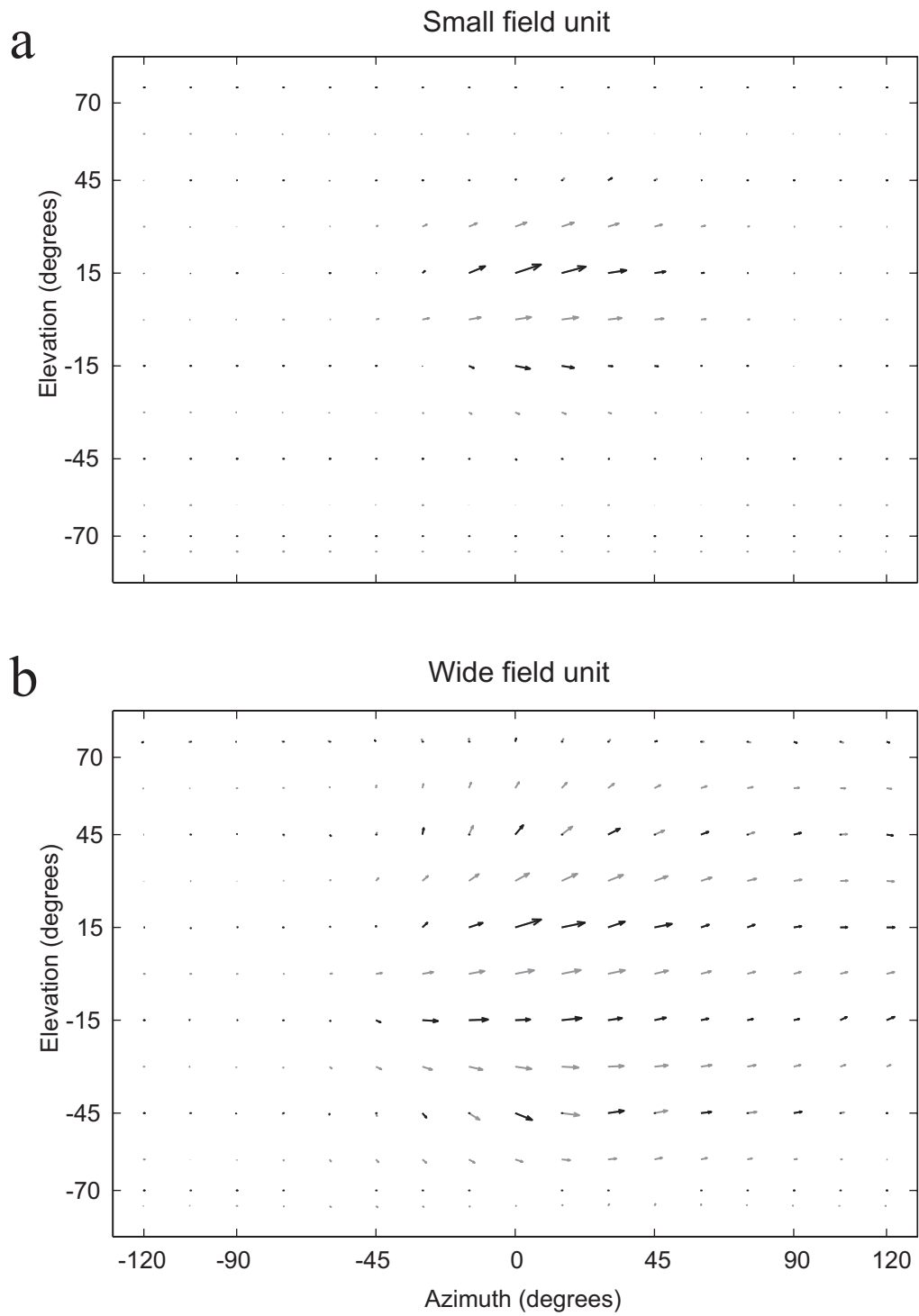


Figure 2.5. Small-field and wide-field NMN receptive fields. Two classes of visually responsive NMNs were observed: small (a) and wide-field (b) units. In small-field units, visual stimuli elicited spikes only over a small area of the visual field. Wide-field units, would respond to visual stimuli over a large area of the visual field.

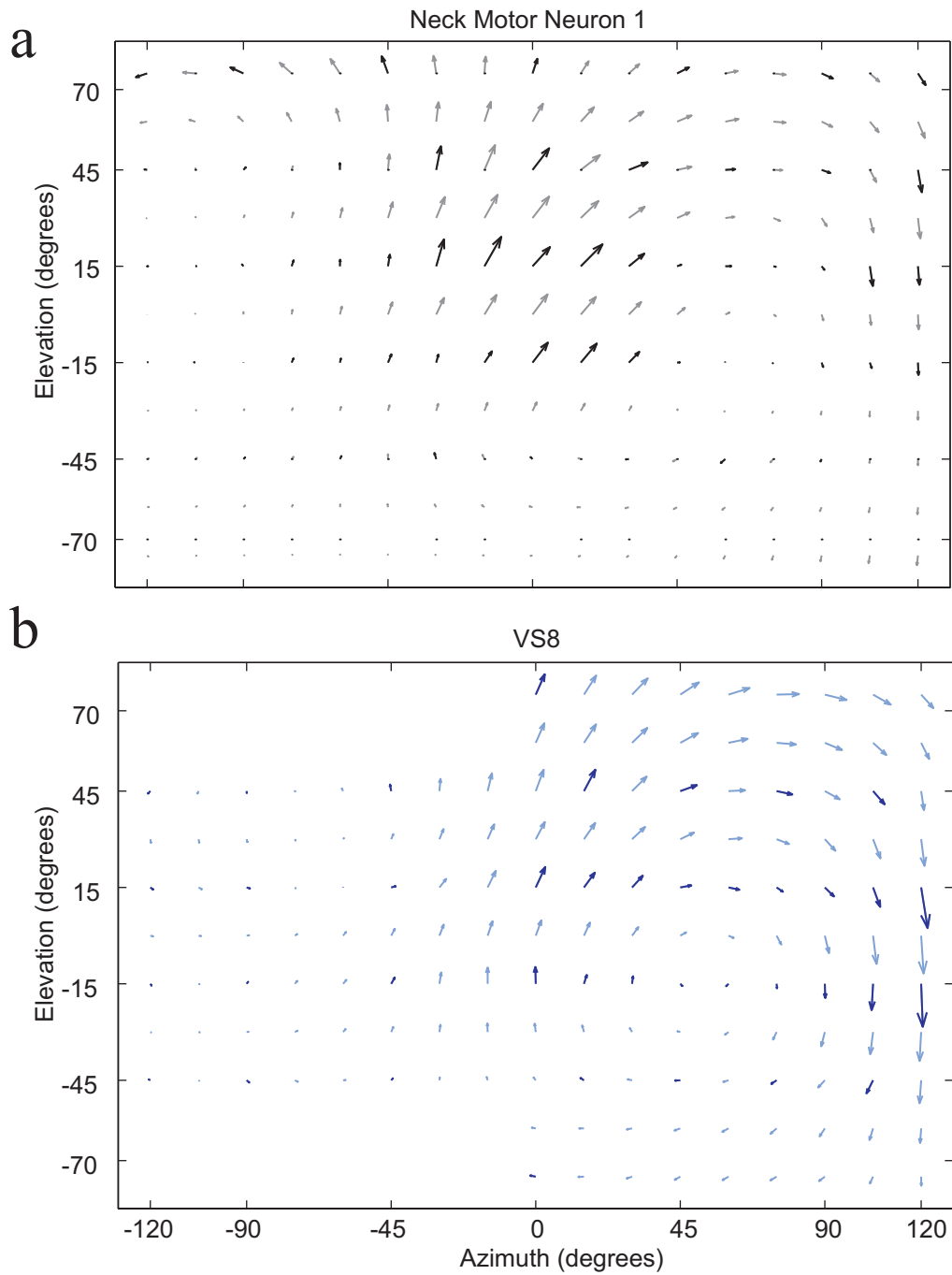


Figure 2.6. Comparison of the receptive fields of an NMN (a) and the VS8 TC (b). The NMN receptive field was obtained with the moving grating stimulus from a recording at the level of NMN neck muscle arborisations. The VS8 receptive field is taken from Krapp (1995).

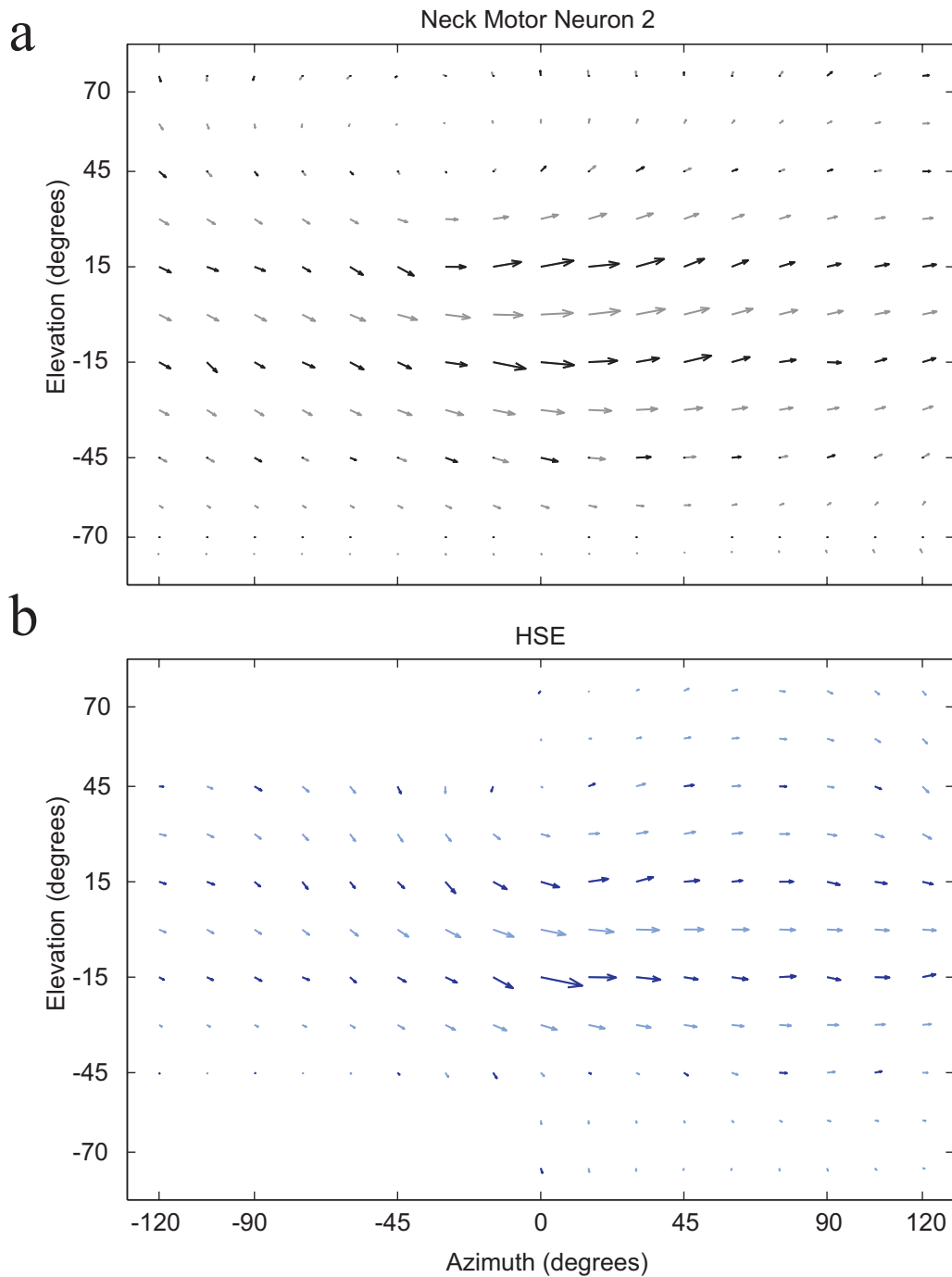


Figure 2.7. Comparison of the receptive fields of an NMN (a) and the HSE TC (b). The NMN receptive field was obtained with the moving grating stimulus from a recording at the level of NMN neck muscle arborisations. The HSE receptive field is taken from Krapp (1995).

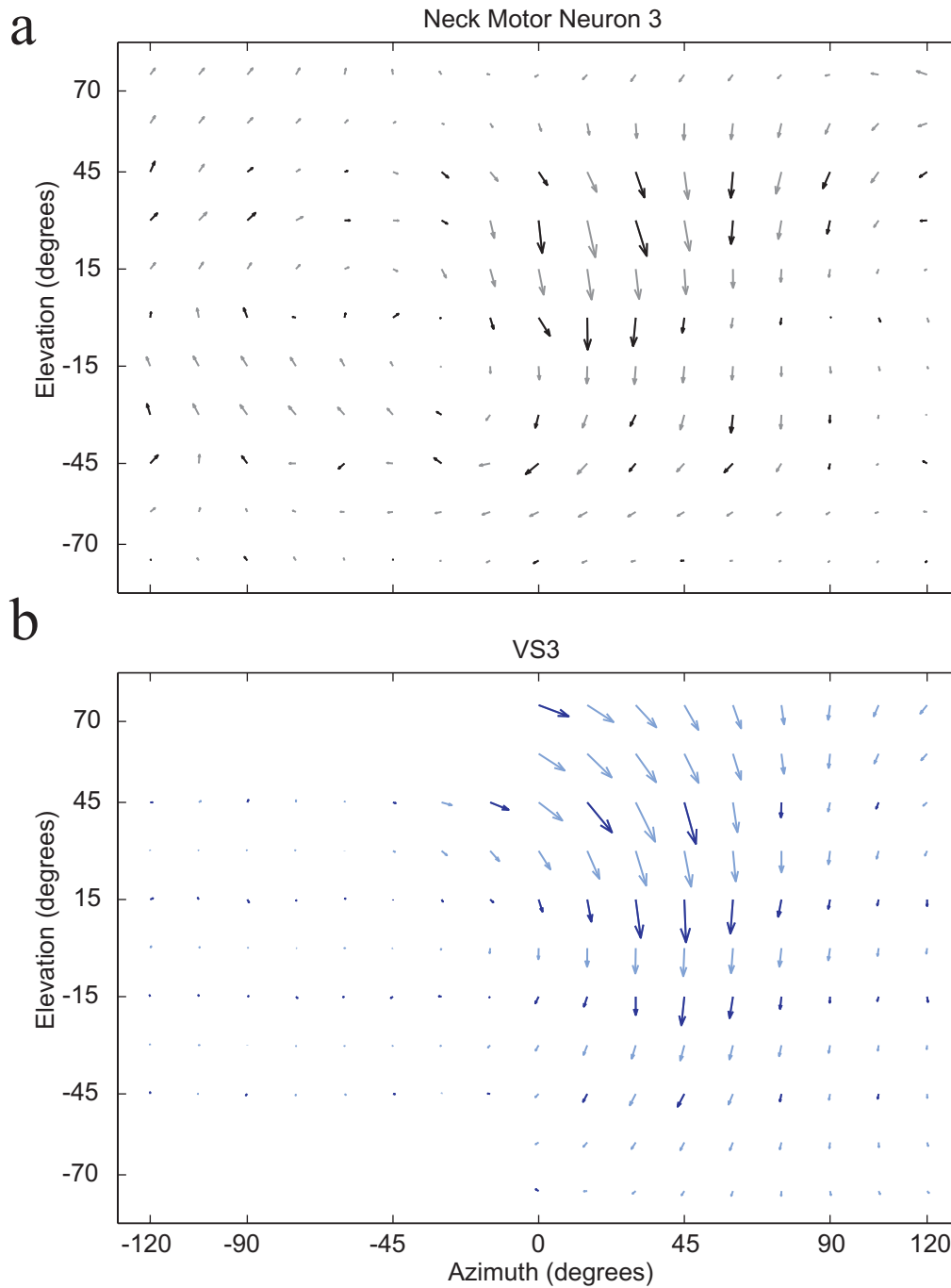


Figure 2.8. Comparison of the receptive fields of an NMN (a) and the VS3 TC (b). The NMN receptive field was obtained with the rotating dot stimulus from a recording at the left cervical nerve. The VS3 receptive field is taken from Krapp (1995).

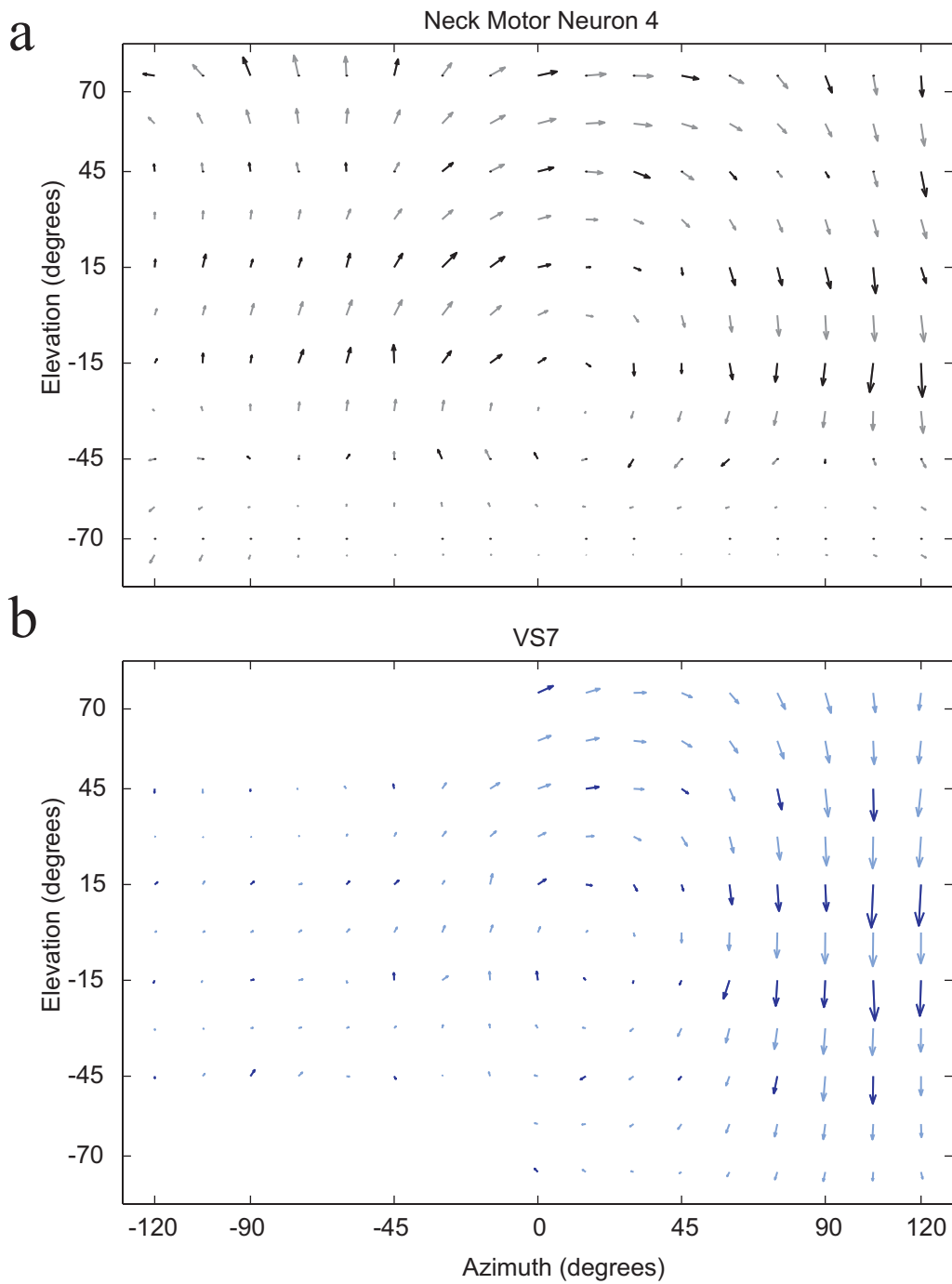


Figure 2.9. Comparison of the receptive fields of an NMN (a) and the VS7 TC (b). The NMN receptive field was obtained with the moving grating stimulus from a recording at the level of NMN neck muscle arborisations. The VS7 receptive field is taken from Krapp (1995).

there was a TC with a receptive field that was strikingly similar. Four examples of NMN receptive fields can be seen in figures 2.6 - 2.9. The NMN receptive fields show similarity to TCs VS8, HSE, VS3 and VS7 respectively. An important feature in the receptive fields is the singularity; this is the point of zero sensitivity, surrounded by rotating directional sensitivities (approximately azimuth = 45, elevation = -15 in figure 2.6b). The singularity is approximately aligned with the axis of rotational optic flow that would maximally stimulate the cell. For each NMN, there is an equivalent TC with a similarly located receptive field singularity, suggesting that the two cells are tuned to similar axes of rotation. The main difference between the NMN and TC receptive fields was that the NMNs displayed stronger binocular responses than the TCs.

2.4.2 Comparison of Neck Motor Neuron and Tangential Cell coordinate systems

The similarity seen between NMN and TC receptive fields suggests that the way in which the TCs integrate local motion to define preferred axes of rotational optic flow already closely matches the requirements of the neck motor system. To understand the nature of this similarity it is necessary to view the relationship between the axes of rotational optic to which NMNs and TCs respond. These axes were estimated from the unit's receptive fields. Figure 2.10a shows the receptive field of a NMN and the axis of rotation that was estimated to most strongly stimulate the neuron (see methods section 2.3.3.2 for details). The preferred axis of rotation provides a biologically relevant way of easily comparing the visual response properties of a large number of neurons and it also allows the neuronal populations to be considered as coordinate systems through which visual information is processed. However, the axis of rotation does not necessarily provide a complete description of the optic-flow that would maximally excite a neuron; for example the neuron in figure 2.5b may respond to translation as well as rotation as has been suggested by Kern et al. (2005) for the Horizontal System TCs.

The preferred axes of TCs and all NMNs recorded from are plotted in figure 2.10b on a two-dimensional plot and also on a sphere to remove the distortions that occur when plotting spherical data in two-dimensions. The NMN data appear to fall

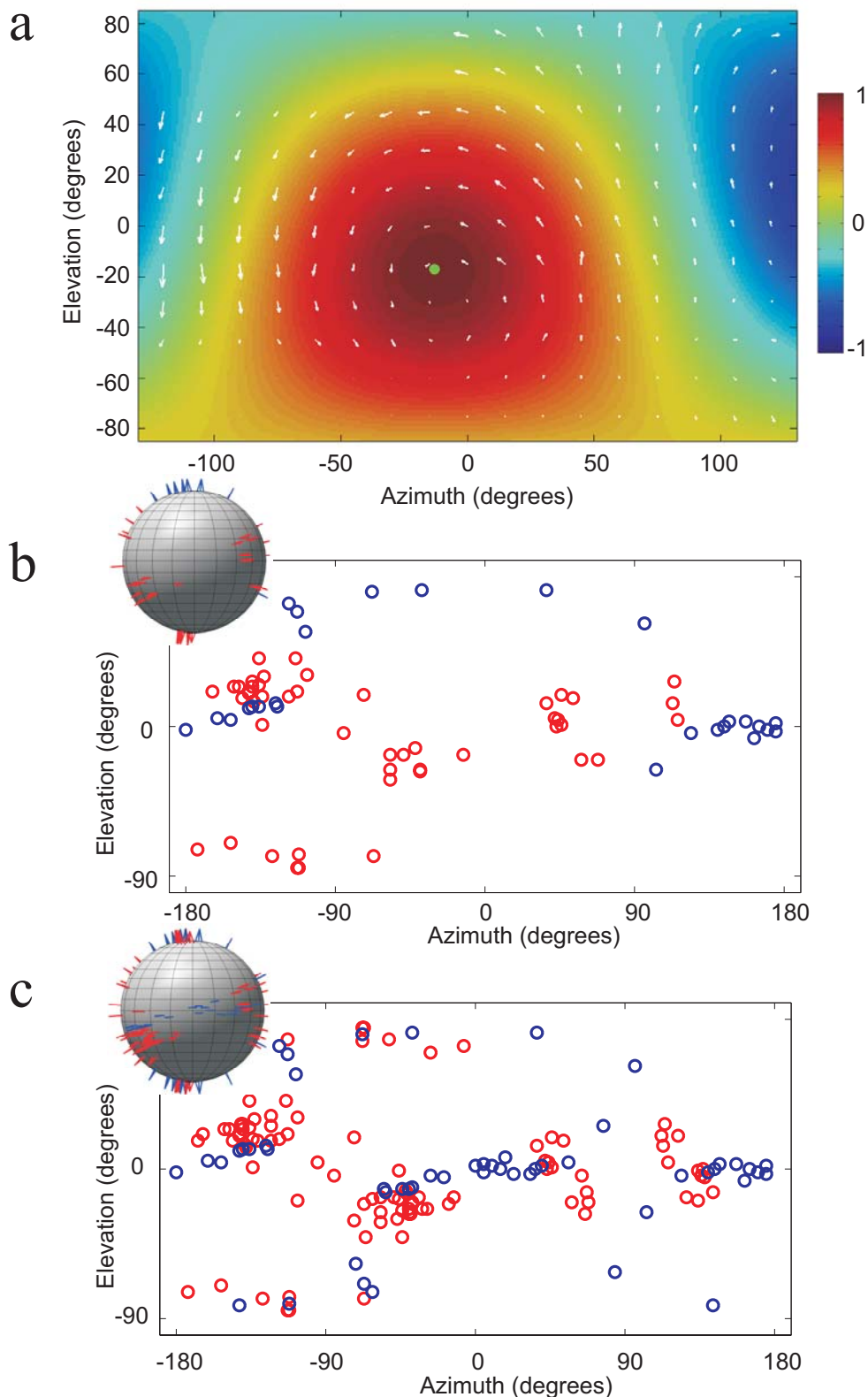


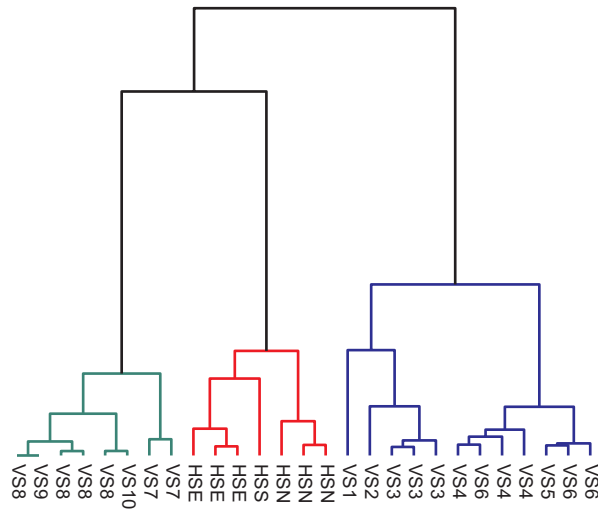
Figure 2.10. Preferred axes of rotation for NMNs and TCs.

(a) An example of how the preferred axis of rotation is estimated from a receptive field. The white arrows describe an NMN receptive field. The background colour at any one point gives the relative similarity between the receptive field and counter-clockwise rotational optic flow about an axis through that point in visual space. The green dot marks the axis of rotational optic flow that was most similar to the receptive field, it is this axis which is defined as the NMN's 'preferred axis of rotation'.

(b) A scatterplot of the preferred axes of all 47 NMNs (red circles) measured and 30 TCs (blue circles) from Krapp (1995). The sphere shows the same data plotted in three dimensions to compensate for the distortion introduced at high and low elevations when plotting spherical data in two dimensions. Thus, it can be seen that the axes at high and low elevations are tightly clustered, even though the distortion in the 2-D plot makes them appear spread out.

(c) The same scatterplot as in (b) but with each preferred axis duplicated and transformed to account for the preferred axis of the equivalent cell on the other side of the fly. Thus for each unit recorded from there are two circles on the scatterplot.

a



b

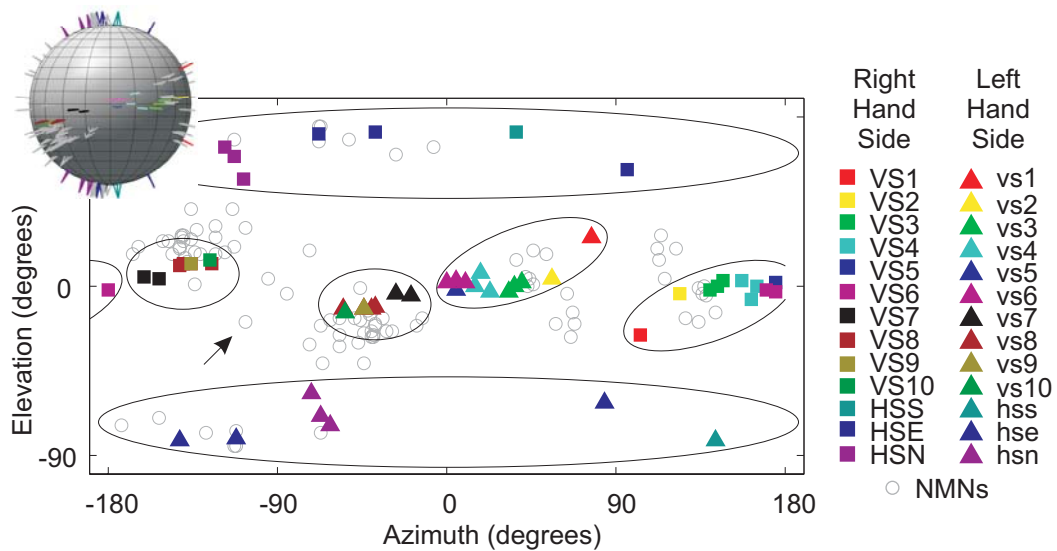


Figure 2.11. Clustering of TC axes.

(a) A dendrogram giving the results of a hierarchical cluster analysis applied to the TC preferred axes. The length of the vertical links indicates the magnitude of dissimilarity between the connected TCs or clusters of TCs. The cluster analysis was performed using the Ward method applied to Euclidian distance between preferred axes.

(b) The same plot as in figure 2.9c but with the individual TCs colour coded for identification of cell type. The three major clusters shown in (a) are shown as six oval boundaries, three clusters for the TCs from each side of the brain.

into clusters, but there is no obvious relationship between the NMN axes and the TC axes. The TC data, however, were taken only from one side of the brain, whereas the NMN data were obtained from NMNs on both sides of the fly. This means that figure 2.10b is comparing monolateral data to bilateral data. To allow a comparison of bilateral to bilateral data, figure 2.10c shows each neuron's preferred axis of rotation twice: once as in figure 2.10b and once transformed to represent the preferred axis of an equivalent neuron on the other side of the fly². This duplication of axes is based upon the assumption that the TCs and NMNs are bilaterally symmetrical, which has been shown for the TCs (Strausfeld, 1976) and the NMNs (Strausfeld et al., 1987). Using figure 2.10c to compare bilateral TC data to bilateral NMN data, it is clear that the TC axes fall into clusters, and the NMN axes are approximately aligned with these clusters, as opposed to being equally distributed about the sphere. In other words, the coordinate systems used by the NMNs and TCs to process rotational optic flow are roughly aligned with each other. This finding confirms on a population level what was seen in the comparison of individual receptive fields (figures 2.6-2.9): the receptive field of each NMN is similar to that of one of the TCs. The variability in the estimated NMN axes of preferred rotation is greater than that seen in the TC axes; this is expected as the visual responses of NMNs were observed to be more variable than those of TCs. This greater variability in NMN visual responses was also observed by Milde et al. (1987).

To quantify the TC clusters, a hierarchical cluster analysis was performed upon the TC preferred axes of rotation. The output of this cluster analysis (cophenetic correlation coefficient = 0.82) is shown as a dendrogram in figure 2.11a. The vertical lines in the dendrogram give a measure of the 'dissimilarity' (Ward method) between TC groups. Three of the vertical lines in figure 2.11a are much longer than any of the rest. Therefore, TCs from one side of the brain are grouped into 3 clusters: VS1-6, VS7-10 and HSS/E/N. This results in six clusters in total when both sides of the brain are considered. It should be noted that the VS1-6 cluster is made up from two smaller clusters VS1-3 and VS4-6. However, as the dissimilarities between the two sub-clusters are smaller than those between the other clusters, the TCs population will be treated as consisting of only three clusters.

² Note that this transformation does not simply mirror transform the axes. Each axis exits the sphere at two points and only the exit point for counter-clockwise visual motion is shown. Therefore a transformed yaw sensitive neuron will have its plotted axis moved from the bottom of the sphere to the top.

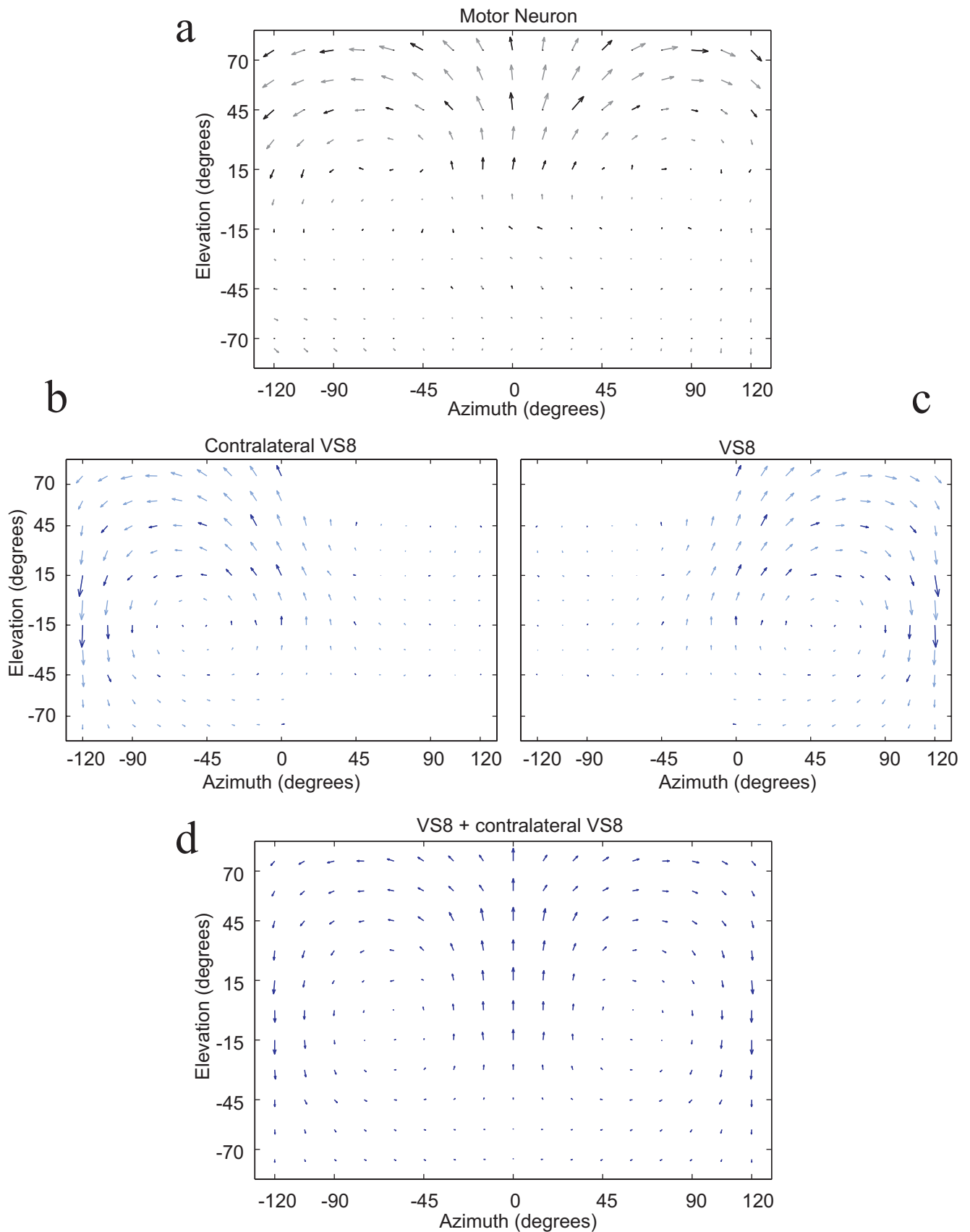


Figure 2.12. Example of a NMN that was not aligned with any TC cluster.
 (a) The receptive field of the NMN. The NMN recording was obtained at the level of NMN arborisations in the neck muscles.
 (b) The receptive field of VS8, taken from Krapp (1995).
 (c) The same receptive field as in (b) but transformed to simulate the receptive field of VS8 on the other side of the brain.
 (d) The two VS8 receptive fields in (b) and (c) combined.

Boundaries are drawn around the TC clusters in figure 2.11b to allow comparison to the NMN data. Again it can be seen that each NMN preferred axis associates with one of the clusters. One set of NMNs is an exception to this alignment. Two NMNs (therefore four circles in figure 2.11.b) do not align with any of the TC axis clusters. The axes of these NMNs (see arrow on figure 2.11.b) fall between the VS7-10 clusters from either side of the fly. The receptive field of one of these NMNs is plotted in figure 2.12a. This receptive field strongly suggests that the NMN responds to the optic flow resulting from nose-downwards pitch. Responding to pitch requires that the NMN's receptive field is bilaterally symmetrical. As all TCs get stronger input from either one or the other eye, there is no equivalent TC to this NMN. However, if the receptive fields of VS8 cells from either side of the brain (figure 2.12b and c) are combined, the resulting receptive field (figure 2.12d) is very similar to that of the NMN. Thus, it appears that this NMN is not aligned with any of the TC clusters because to get the required binocular input it needs to receive equal inputs from TCs on opposite sides of the brain. By definition TCs from different sides of the brain belong to different clusters, in this case those either side of the NMN's preferred axis. Therefore the NMN cannot be aligned with any one TC cluster. Generally, however, an alignment exists between the preferred axes of rotation in the TC population and the equivalent axes for the NMNs recorded from.

2.4.3 Estimation of a Neck Motor Neuron's Tangential Cell inputs

The alignment between the NMNs and TCs should simplify the neural connectivity and processing underlying the visuo-motor transformation. One hypothesis is that the major excitatory input to a NMN comes from the TC cluster with which the NMN is aligned. To test this hypothesis requires information about the neural connections between TCs and NMNs, information which cannot be determined from the preferred axes and requires difficult and lengthy double recording experiments. As data from double recordings are not currently practical, an attempt was made to obtain a first order approximation of the connections between TCs and NMNs by analysing NMN receptive fields. An optimisation was performed to determine which weighted combination of TC receptive fields most closely

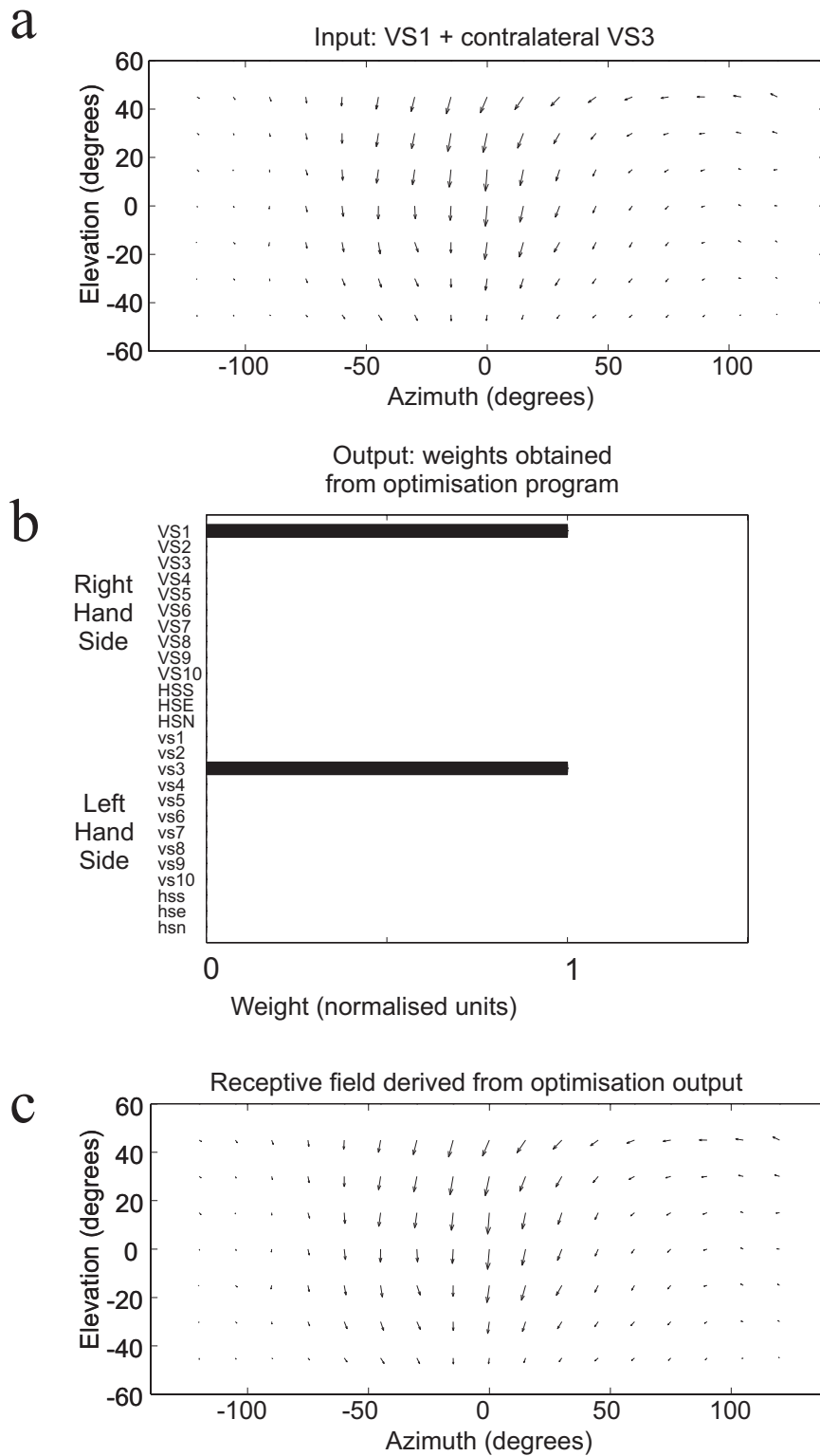


Figure 2.13. Results of a control where the optimisation algorithm was applied to an artificially generated receptive field.

(a) The input to the optimisation algorithm: a receptive field generated by combining the receptive fields of VS1 and the contralateral VS3 together.

(b) The weight set outputted by the optimisation algorithm as applied to the receptive field in panel (a). Error bars are plotted giving the standard deviation of the weight sets arrived at by 10 runs of the algorithm; however the error bars are too small to be visible.

(c) The receptive field generated using the weights outputted by the optimisation.

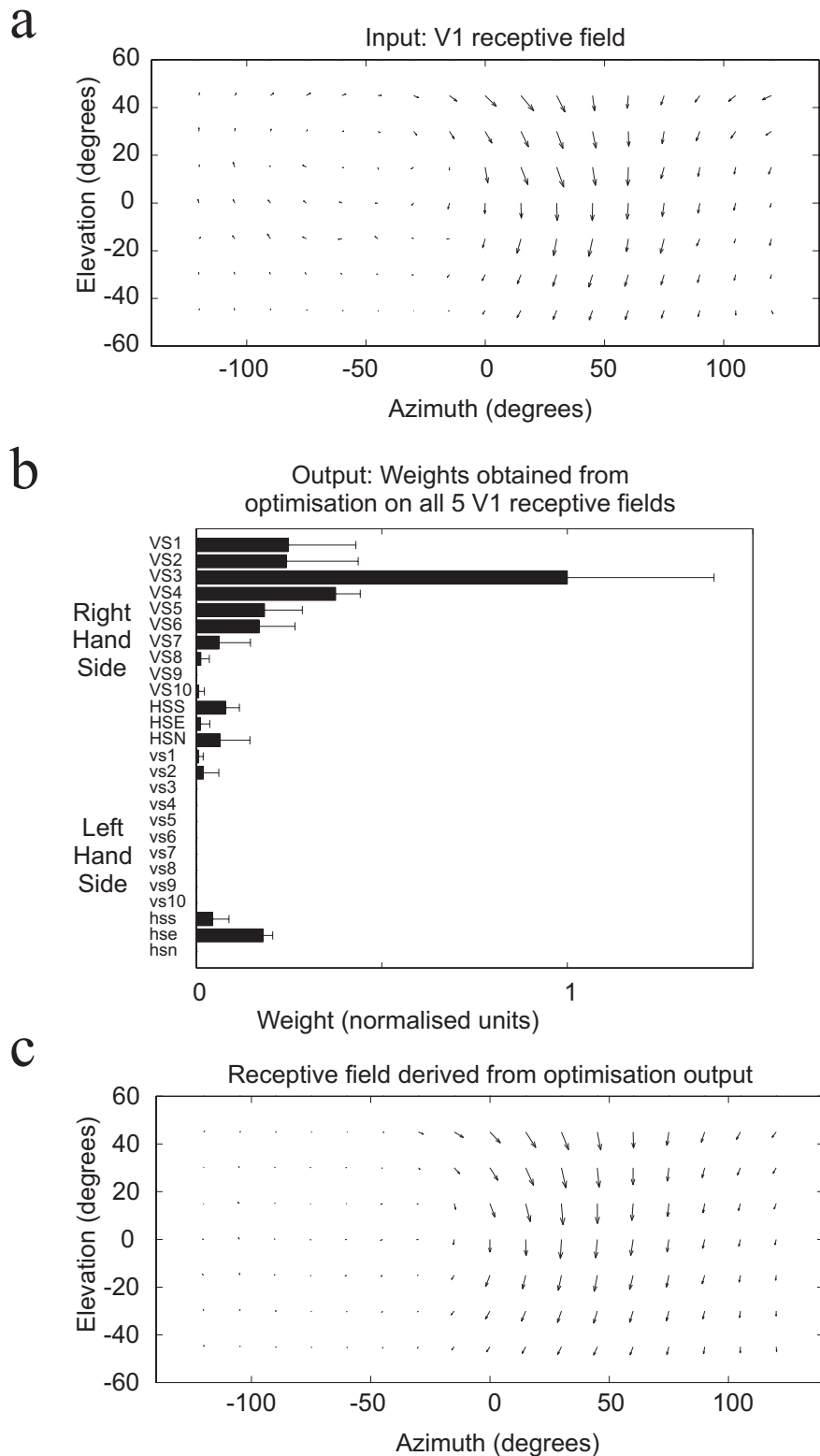


Figure 2.14. Results of a control where the optimisation algorithm was applied to 5 examples of the V1 spiking lobula plate interneuron.

(a) The receptive field of one of the 5 V1 cells used (V1 data obtained from Krapp et al. (1995; 2001)).

(b) The mean weights generated by the optimisation algorithm for all 5 different V1 cells. The error bars give the standard deviation of the weights arrived at for the 5 different V1 cells.

(c) The receptive field generated using the weights outputted by the optimisation algorithm.

matches the NMN receptive fields (see the methods section for details of the optimisation method used). Those TCs whose receptive fields are highly weighted when trying to re-create a NMN receptive field are likely to provide a strong input to the NMN.

To determine the precision of the optimisation algorithm's solutions, control trials were carried out. A test receptive field was generated by combining the VS1 and contralateral VS3 receptive fields (figure 2.13a). When the optimisation algorithm was applied to the test receptive field it arrived at the correct solution, weighting VS1 and the contralateral VS3 equally and giving all other TCs weights of zero (figure 2.13 b and c). As another control, the optimisation was run on the receptive field of the lobula plate spiking V1 cell whose TC inputs are partially known (Kurtz et al., 2001; Warzecha et al., 2003). Five V1 receptive fields from different flies (data provided by Holger Krapp (Krapp, 1995; Krapp et al., 2001; Karneier et al., 2003)) were subjected to the optimisation (figure 2.14). For all five V1 receptive fields, the optimisation consistently weighted the VS1-6 and contralateral HSE receptive fields highly, but the exact weights used varied according to the specific V1 receptive field used (figure 2.14b). The strong weighting of VS1-6 inputs is in approximate agreement with the known inputs to V1. Only VS1-3 are known to input to V1 (Kurtz et al., 2001; Warzecha et al., 2003), however neighbouring TCs have lateral connections (Haag and Borst, 2004). Thus, VS4 may have access to V1 via its lateral connection to VS3. The fact that the optimisation output uses VS4-6 as well as VS1-3 may reflect these lateral connections. The contralateral HSE input, however, is not in agreement with the literature. The results of these controls suggest that the optimisation can provide information about the general trend of connectivity but not precise information about the specific inputs to one cell. Information about the general trend of connectivity however is sufficient to answer the question of whether a NMN takes the majority of its inputs from the TC cluster it is aligned with or whether the NMN integrates inputs from many different TC clusters.

The results of the optimisation as applied to one NMN are shown in figure 2.15. For this NMN the optimisation weighted TCs VS2-5 strongly, implying that this NMN gets the majority of its excitatory inputs from the VS1-6 cluster. VS1-6 is also the cluster with its preferred axes of rotation closest to that of the NMN. Similarly, figure 2.16 shows the output of the optimisation as applied to a different

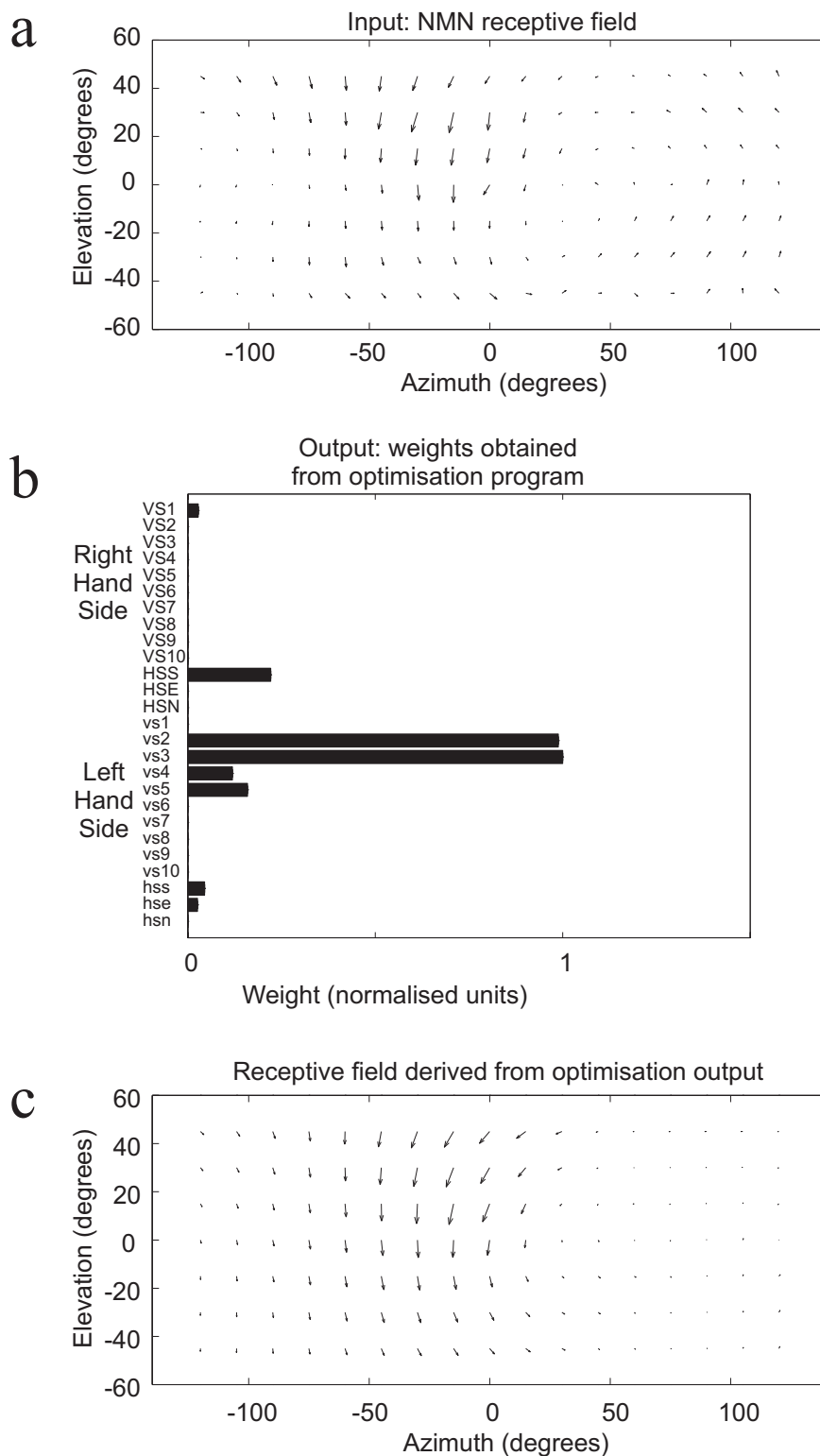


Figure 2.15. Results of the optimisation algorithm as applied to an NMN receptive field.

(a) The receptive field of an NMN obtained from the cervical nerve using the rotating dot stimulus. This served as the input to the optimisation algorithm.

(b) The weight set outputted by the optimisation algorithm as applied to the receptive field in panel (a). Error bars are plotted giving the standard deviation of the outputs of 10 runs of the algorithm, however the error bars are too small to be visible.

(c) The receptive field generated using the weights outputted by the optimisation algorithm.

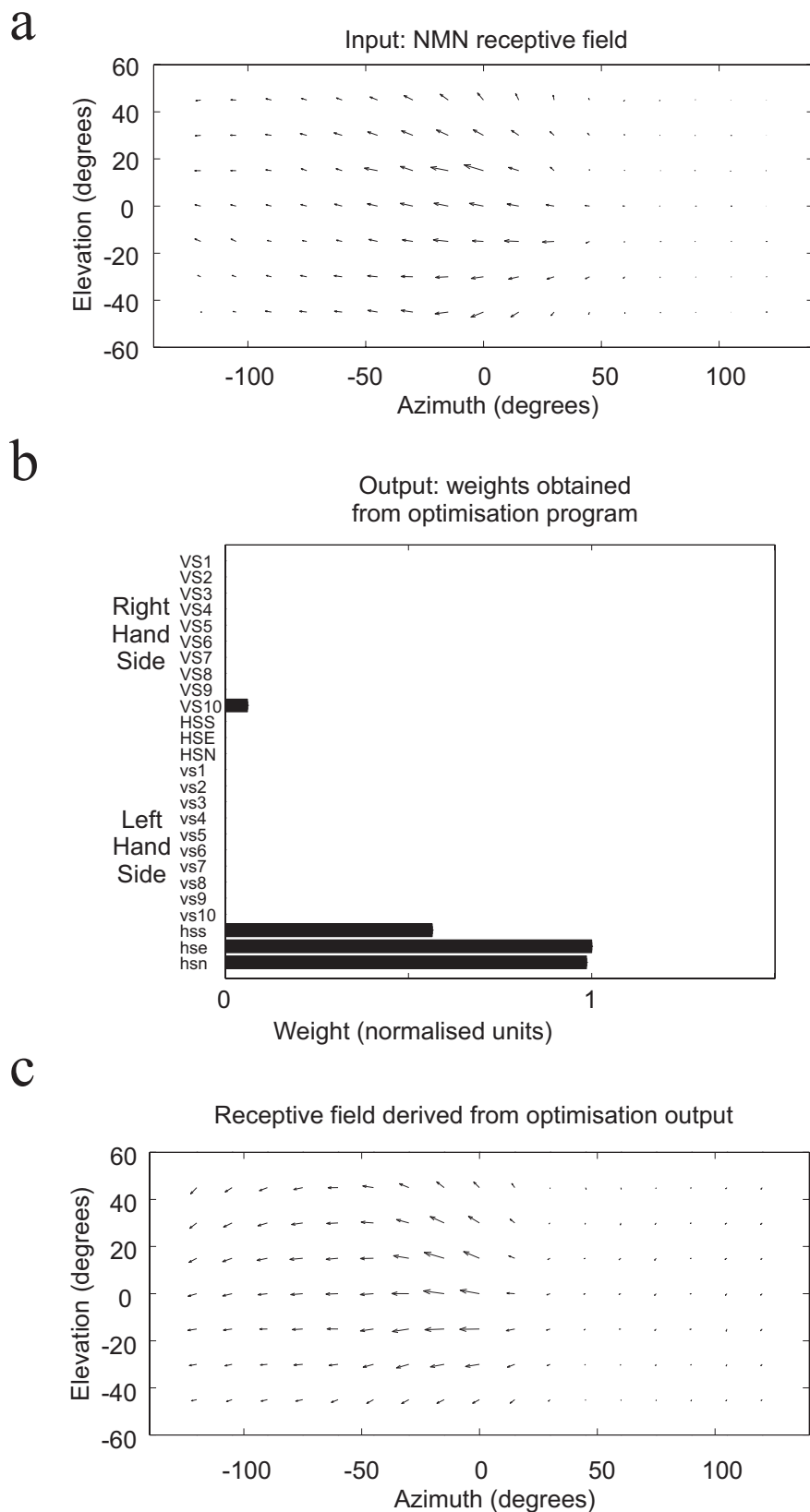


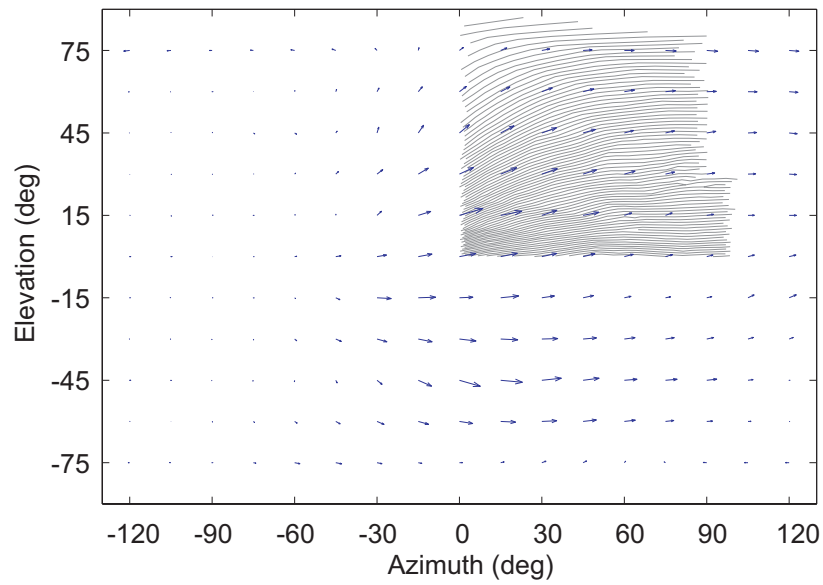
Figure 2.16. Results of the optimisation algorithm as applied to an NMN receptive field. (a) The receptive field of an NMN obtained from a unit recorded at the level of its neck muscle arborisation using the grating stimulus. This receptive field served as the input to the optimisation algorithm. (b) The weight set outputted by the optimisation algorithm as applied to the receptive field in panel (a). Error bars are plotted giving the standard deviation of the outputs of 10 runs of the algorithm, however the error bars are too small to be visible. (c) The receptive field generated using the weights outputted by the optimisation algorithm.

NMN. Again, the optimisation puts the majority of weights on the TC cluster closest to the NMN's preferred axis; Horizontal System TCs in this case. This analysis was applied to all NMNs and it was found that in 40/47 of the NMNs recorded from the TC cluster that the optimisation weighted the most is the same as the TC cluster closest to the NMNs preferred axis of rotation. If the optimisation provides an accurate description of TC-NMN connectivity, then NMNs receive the majority of their excitatory inputs from the TC cluster they are aligned with. Thus, the alignment between the two populations significantly simplifies the visuo-motor transformation.

2.4.4 Comparison of Neck Motor Neuron receptive fields to compound eye geometry

The results presented here show an alignment between the coordinate systems used by TCs and NMNs to process rotational optic flow. Other work (Petrowitz et al., 2000; Egelhaaf et al., 2002) has shown that the receptive field organization of some TCs can be explained by characteristic distortions of the ommatidial rows in the fly's hexagonal compound eye lattice. Therefore, it would be expected that the receptive field organization of the NMNs may also reflect the orientation of certain ommatidial rows within the fly compound eye lattice. An HS like NMN receptive field is plotted in figure 2.17 along with the horizontal ommatidial rows of the compound eye (data from Petrowitz et al. (2000)), it is thought that the majority of horizontal motion is detected over these rows (Buchner, 1976) Similarly a VS like NMN receptive field is plotted in figure 2.18 along with the vertical ommatidial rows of the compound eye over which it is thought the majority of vertical motion is detected. The NMN preferred directions correlate well with the orientation of the ommatidial rows, reflecting an alignment between the visual periphery and the motor system, two points at either end of the visuo-motor circuit.

a



b

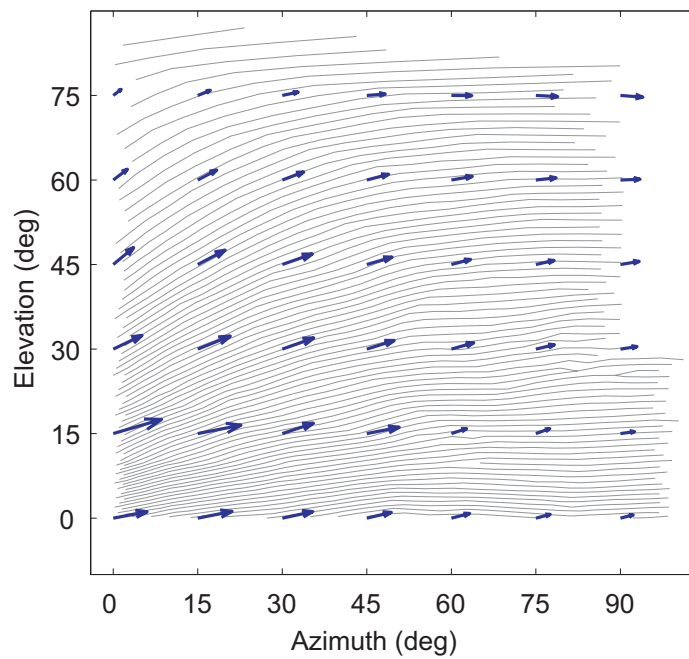


Figure 2.17. The receptive field of an NMN compared to the horizontal ommatidial rows of the compound eye.

(a) The receptive field of an NMN recorded at the level of the NMN's neck muscle arborisations. Also plotted are the horizontal rows of the compound eye (data from Petrowitz et al. (2000)).

(b) The same plot as in (a) but only showing the upper right quadrant of the visual field.

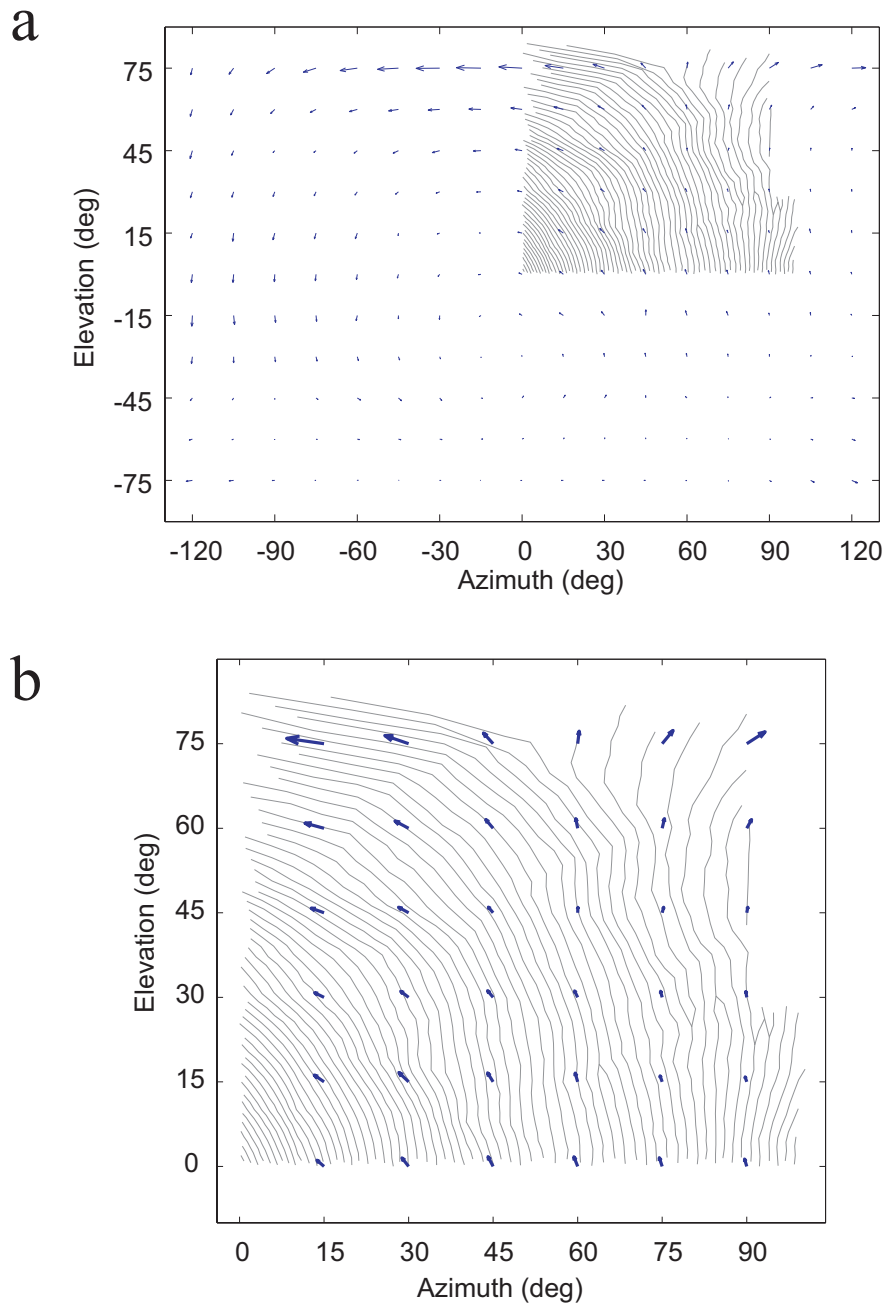


Figure 2.18. The receptive field of an NMN compared to the vertical ommatidial rows of the compound eye.
 (a) The receptive field of an NMN recorded at the level of the NMN's neck muscle arborisations. Also plotted are the vertical rows of the compound eye (data from Petrowitz et al. (2000)).
 (b) The same plot as in (a) but only showing the upper right quadrant of the visual field.

2.5 Discussion

The fly visual system is one of the main model systems used to study sensory processing. However, very little is known about how the outputs of this visual system are utilised by the fly's motor systems. Indeed, up to now only one study has looked at the visual responses of Neck Motor Neurons (Milde et al., 1987). The work presented here is the first study to have examined the visual properties of fly Neck Motor Neurons (NMNs) in detail. By analysing how the visual receptive fields of NMNs relate to those of visual system Tangential Cells (TCs) this study has made the first step in understanding how outputs of a well-characterised sensory system are used by downstream motor systems.

A sub-population of NMNs have large receptive fields like those of the TCs. The fine structure of the directional tunings within these receptive fields follows characteristic patterns. These patterns strongly suggest that each NMN is tuned to the optic flow resulting from rotation about a certain axis. The axes of rotation to which the NMN population is tuned are aligned with the equivalent axes in the TC population. Thus, the coordinate systems used by the visual and motor systems for processing rotational optic flow are aligned.

2.5.1 Significance of the alignment between Neck Motor Neurons and Tangential Cells

Generally sensorimotor circuits are thought to involve transformations between very different sensory and motor coordinate systems, often through intermediate coordinate systems (see for example Masino and Knudsen (1990)). Here it has been shown that the coordinate systems used by sensory TCs and NMNs are very similar. What, if any, advantage does this similarity confer? The similarity means that TCs are extracting optic flow information in a manner already aligned with the requirements of the neck motor system. This strategy means that

significantly less processing of the visual information is required, allowing the use of simpler neural circuitry.

The TCs are the first point in the fly visual system at which local motion inputs are combined to obtain information about rotational optic flow. This means that from the very first point at which it is extracted, optic flow information is encoded in a manner already aligned with the requirements of the neck motor system. Thus, a major portion of the visuo-motor transformation occurs at the level of the visual system. This finding suggests the TCs are very closely integrated with the motor system. What other properties do TCs share with the motor systems; do they, like motor systems, respond to multiple sensory inputs? Preliminary experiments done as part of my thesis work and the results of others (K. Hausen, personal communication; T. Maddess, personal communication) show that TCs respond to non-visual inputs such as antennae stimuli and movement of the abdomen. Thus, the TCs perform part of the visuo-motor transformation and display multi-sensory responses. Given this evidence, the distinction that TCs are visual interneurons as opposed to pre-motor interneurons becomes less clear.

The results presented here can explain a puzzling feature of the TC coordinate system. Given a certain number of sensory neurons with cosine shaped tuning curves such as the TCs, the most efficient arrangement of the neurons' preferred axes would be that with equal spacing between the axes. Equal spacing of the preferred axes reduces the redundancy in what is encoded by different neurons. Such a strategy is seen in other sensory systems (Lewis and Kristan, 1998; Jacobs and Theunissen, 2000), but not in the TCs where the axes are not equally spaced (Krapp et al., 1998; Krapp, 2000). There are 26 output TCs encoding rotational optic flow, many more than the theoretical minimum requirement of three. A modelling study (Karmeier et al., 2005) has shown that because of this over-complete basis set, coding performance is only subtly reduced by the TC axes' deviation from equal spacing. Therefore there is no major disadvantage for the TCs to deviate from equal spacing, but does the particular arrangement used have any advantage? The results presented here suggest that the deviation from equal spacing is the result of the TC-NMN alignment, reducing the complexity of the visuo-motor transformation. This reduction in complexity means that fewer neuronal connections are needed for the visuo-motor circuit, increasing its speed, reducing its metabolic cost and reducing the cumulative effects of synaptic noise.

Alignment between sensory and motor coordinate systems has been found in the visual input to the vertebrate vestibulo-ocular system. On-off type directionally selective ganglion cells of the rabbit retina respond to one of four different directions of motion. These four different directions of motion are aligned with the pulling planes of the four rectus muscles of the eye (Oyster and Barlow, 1967; Oyster, 1968). Downstream neurons integrate signals from these retinal ganglion cells, maintaining the alignment with the eye muscles (Graf et al., 1988; Simpson et al., 1988). It should be noted that rabbit vestibular canals and eye muscles are closely, but not exactly aligned (Soechting and Flanders, 1992), making it difficult to determine which of the two the visual neurons are aligned with. Similar results have been obtained in the pigeon where an alignment was found between the semi-circular canals and neurons that respond to rotational and translational optic flow (Wylie and Frost, 1993).

The NMN and TC coordinate systems were characterised here by estimating each neuron's preferred axis of rotation from its receptive field. One limitation of this method is that it assumes approximately linear integration of local motion inputs over the receptive field, potentially biasing results. A more direct method of estimating the preferred axes utilises wide-field visual stimuli (Karmeier et al., 2003, 2005). However, to generate wide-field visual stimuli requires complex, custom-made equipment (Lindemann et al., 2003) and it has been shown that preferred axes of rotation estimated from TC receptive fields agree with those estimated using wide-field stimuli (Karmeier et al., 2003, 2005). Therefore the preferred axes estimated in this study are likely to be accurate.

The alignment seen between the TC and NMN population is not perfect. Some of the misalignment is due to there being increased scatter in the NMN axes resulting from NMN visual responses being more variable than those of TCs. However, even when the increased NMN variance is taken into account, some misalignment between the TC and NMN population still exists. This may be because some NMNs have not been recorded from. For example, no NMNs were recorded that perfectly aligned with VS4-6 TCs; it is possible that such NMNs exist but were missed in this study. Another factor to take into account when considering the nature of the TC NMN alignment is that the NMNs have strong binocular receptive fields and are therefore probably integrating TC inputs from both sides of the brain. This binocular integration can shift the preferred axis slightly, explaining some of the subtle misalignments seen in figure 2.10c.

2.5.2 Possible Tangential Cell – Neck Motor Neuron connectivity

How exactly does the TC-NMN circuitry take advantage of the alignment between the two neural populations? One simple way to utilise the alignment would be for each NMN to receive inputs from those TCs with receptive fields similar to that required by the NMN. In other words, each NMN takes its main input from the TC cluster with which it is aligned. It is not immediately apparent that this hypothesis is true; it is possible to arrive at a receptive field with the same preferred axis through many different combinations of TC inputs. To test this hypothesis, an optimisation was performed to determine which combination of TC inputs most closely fits the NMN receptive field data. The results of the optimisation were in agreement with the hypothesis. The NMN receptive field data is best explained by a connectivity rule where each NMN gets its main excitatory input from the cluster of TCs aligned with the NMN. This connectivity rule not only provides the best match to the data but also provides an elegant way in which the TC-NMN alignment may be used to simplify the visuo-motor circuit.

The results of the optimisation should be treated with caution however. Control experiments indicated that the optimisation algorithm could not perfectly predict neural inputs. Furthermore, the algorithm assumed only simple weighted summation of TC inputs occurs, discounting many potential neural mechanisms such as inhibition and non-linear integration. However the hypothesis tested with the optimisation only required information about general patterns of connectivity. Also, it is striking that the highly unconstrained optimisation arrived at such a simple solution. This hypothesis deserves to be tested using paired recordings.

2.5.3 Non-orthogonal sensory-motor coordinate systems

It has been suggested that a common principle of sensory-motor transformations is the existence of an intermediate step between sensory and motor coordinates where an orthogonal coordinate system is used (Masino and Knudsen, 1990, 1993). Indeed orthogonal intermediate steps have been found in three of the

most well characterised sensory-motor circuits: the leech local bend reflex (Lewis and Kristan, 1998), barn owl head movements (Masino and Knudsen, 1990, 1993) and the cricket cercal system (Jacobs and Theunissen, 2000). The one previous study of NMN responses to visual motion described the NMNs as responding to roll, pitch or yaw stimuli, implying orthogonality (Milde et al., 1987). Here it has been shown that NMNs have preferred axes of rotation that are non-orthogonal and fall between pure roll, pitch and yaw. The TC preferred axes are also non-orthogonal (Krapp et al., 1998; Krapp, 2000). Thus, for those NMNs that receive direct inputs from TCs there can be no intermediate orthogonal step in the visuo-motor transformation. Therefore the principle of an intermediate orthogonal stage does not apply to the direct TC-NMN circuit. It would be interesting to study the descending neurons that connect TCs to those NMNs with indirect TC inputs. Are these descending neurons operating as an orthogonal intermediate step between TCs and the NMNs receiving indirect TC input?

2.5.4 Relationship to other sensory and motor systems

The NMNs receive many sensory inputs, of which vision is only one. How does the coordinate system used by the NMNs for processing rotational optic flow relate to other senses? The halteres also input to the NMNs (Strausfeld and Seyan, 1985), providing information about rotations in a higher frequency range than that covered by vision. The halteres measure self-rotation over four axes, two redundant vertical axes and two horizontal axes at $60^\circ/-120^\circ$ and $120^\circ/-60^\circ$ (Nalbach, 1994). These four axes are roughly aligned with the NMN preferred axes of rotational optic flow. This introduces the possibility that the entire gaze-stabilisation system shares a common coordinate system. A similar principle of a common pre-motor coordinate system for integrating multiple sensory inputs has been observed in vertebrates (Jay and Sparks, 1984; Graf et al., 1988; Simpson et al., 1988; Wylie and Frost, 1993; Wylie et al., 1998; Frost and Wylie, 2000). Given the close alignment between the haltere system and the TCs it would be interesting to study how the two sensory inputs interact at the NMNs, this is the topic of the next chapter.

The Neck motor system is not the only motor system to receive input from the TCs, flight and walking are also guided by TC outputs. How does the coordinate system used by the TCs relate to the motor coordinate systems of the wings and legs? This issue requires further investigation.

2.5.5 Relationship between Neck Motor Neuron receptive fields and neck muscle pulling planes

This study has measured the visual receptive fields of NMNs. How the visual receptive field of a NMN relates to the pulling plane of the neck muscle it innervates is not known. The pulling plane of a muscle in a non-orthogonal system such as the neck motor system is unlikely to be parallel with the axis of its sensory input. This is due to the fact that muscles usually act in concert and therefore any individual muscle is required to be most active not during a movement parallel with its pulling plane, but during an off axis movement when it is partially pulling against other muscles (Pellionisz and Llinas, 1980; Soechting and Flanders, 1992). Therefore, without knowing the details of how the neck motor system functions, it is difficult to predict a relationship between the visual input to a NMN and the pulling plane of the muscle it innervates. A simple relationship may exist, however, as all but two NMNs innervate a single neck muscle (Strausfeld et al., 1987). If further work is able to elucidate this relationship it will be very interesting to compare the TC coordinate system to the coordinate system defined by neck muscle pulling planes.

In conclusion, this study has shown a novel alignment between the axes used by the visual system and the neck motor system to process rotational optic flow. It is suggested that this alignment reflects a strategy to extract visual inputs in a manner that is as close to the requirements of the motor system as possible. This is illustrated in figures 2.17 and 2.18 where it is seen that the structure of the compound eye matches the preferred directions of motion within NMN receptive fields. Thus at the very sensory periphery, visual motion is already extracted in a form close to the requirements of the motor system.

3. Integration of haltere and visual inputs

3.1 Abstract

Many motor systems receive inputs from more than one sensory organ. The task of integrating multiple sensory inputs is not a trivial one, as different sensory systems often have very different output signal structures. Here the integration of mechanosensory haltere and visual inputs is studied at the level of fly neck motor neurons. Neck motor neurons drive muscles that make gaze-stabilising head movements when the fly is rotated. These motor neurons receive many sensory inputs that monitor rotations of the fly, two of which come from the halteres and the visual system (Strausfeld and Seyan, 1985; Milde et al., 1987).

Extracellular recordings reveal that some neck motor neurons fire action potentials in response to haltere stimulation but not in response to visual stimuli. Visual stimuli, however, can modify the spike rate of these neck motor neurons during simultaneous haltere stimulation. Thus, visual stimuli only alter the spike rate of these neck motor neurons when the halteres are moving. This corresponds to a haltere dependent gating of the visual inputs' influence on the neck motor neurons' output. The gating seen in these experiments correlates well with results from behavioural studies where gaze-stabilising head movements were only made by flies during behaviours that involve beating the halteres (Hengstenberg et al., 1986).

To try and elucidate the nature of the sub-threshold events underlying this gating, intracellular recordings were made from neck motor neurons of the frontal nerve. Visual stimuli moving in a neck motor neuron's preferred direction elicit sustained sub-threshold depolarisations. Haltere stimulation results in compound excitatory postsynaptic potentials (EPSPs) and action potentials that are phase-locked to the haltere stimulus waveform. Combining haltere and visual stimulation results in a higher rate of spiking than haltere stimulation alone. Indirect evidence suggests that this increase in spike rate is due to visually induced depolarisation causing more haltere induced compound EPSPs become suprathreshold. Thus, a comparatively simple mechanism of neural summation combined with the non-linearity of action potential generation could account for the gating observed and may well explain the context dependent effect of visual stimuli seen in behaving flies.

3.2 Introduction

This chapter examines multisensory integration in fly Neck Motor Neurons (NMNs). Nearly all motor systems integrate inputs from multiple sense organs; this provides various advantages. Sampling the same event with multiple senses provides repeated samples of the event that can be averaged to reduce any noise in the sensory inputs. Different sense organs often respond to different parameters of a stimulus, allowing any pattern matching that is required to operate over a larger range of parameters, thus increasing the confidence with which a certain stimulus is resolved. If the different sensory inputs respond to different frequency components of the stimulus then integrating multiple senses increases the frequency range of stimuli to which the motor system can respond. The advantages provided by multiple sense organs come at the cost of the extra neural processing required to integrate diverse inputs. Different sensory systems often have very different output signal structures, so integrating them in a meaningful way is not trivial. Relatively little is known about how nervous systems achieve this task.

Multisensory integration has been studied in a small number of neural systems, where it has been found that inputs from one sense organ significantly affect the neural responses to another sensory input. This interaction between two sensory inputs can take many different forms. For example, inputs from one sense organ can gate the transmission of information from another sense organ to the motor system. In the crab, inputs from the statocysts (the crab's equivalent of our semi-circular canals) can only make the motor neurons spike if they occur at the same time as non-specific mechanosensory stimulation (Silvey and Sandeman, 1976). A second form of multisensory interaction occurs when one type of sensory input modulates a neuron's strength of response to another sensory input. For example, the sensitivity to visual stimuli of some mammalian superior colliculus neurons can be dramatically altered by the presence of an auditory stimulus (Meredith and Stein, 1983). A third kind of multisensory interaction occurs when one sensory input alters a neuron's tuning or receptive field in a different sensory modality. An example of one sensory input shifting the receptive field for another sense is seen in 'space constant' neurons of crayfish where statocyst inputs can move the visual receptive fields of a neuron

across the retina so that the neuron always responds to visual stimuli from the same point in external space regardless of the orientation of the crab (Wiersma, 1966). Finally, many examples exist of sensory processing being modulated, not by other sensory inputs directly, but by a motor pattern dependent signal, such as the output of a central pattern generator (Reichert and Rowell, 1985; Reichert, 1985; Wolf and Burrows, 1995; Staudacher and Schildberger, 1998; Buschges and Wolf, 1999; Staudacher, 2001; Poulet and Hedwig, 2002).

The types of multisensory interaction described above are seen at many different levels of sensory-motor circuits. Descending neurons conveying information from the brain to thoracic ganglia often receive multiple sensory inputs, and these inputs interact in a non-linear manner (locust: Rowell and Reichert (1986) fly: Milde and Strausfeld (1990)). In the thoracic ganglia some pre-motor interneurons are also a site of multisensory interactions (Newland, 1999). Finally, motor neurons themselves can also integrate multisensory information (Silvey and Sandeman, 1976).

As illustrated by the above examples, multisensory integration is a pervasive feature of sensorimotor systems. However we still lack an understanding of how the outputs of different sensory systems are integrated in a meaningful way. Neck Motor Neurons (NMNs) provide an opportunity to study this fundamental problem; they receive many different sensory inputs (Sandeman and Markl, 1980; Strausfeld and Seyan, 1985; Milde et al., 1987), two of which come from well studied systems: the compound eye and the halteres. The fact that two sensory systems that provide input to NMNs have been well described, along with the comparative simplicity of the neural circuit and the defined behavioural output makes fly NMNs a potentially rewarding system in which to study multisensory integration.

This chapter examines the interaction between haltere and visual NMN inputs. The previous chapter was concerned with studying the sub-population of NMNs that fire action potentials in response to visual stimuli, here those NMNs will be referred to as type I units. In the terminology of Milde et al. (1987) type I units are ‘visual’ NMNs. Those NMNs that fail to spike in response to visual stimuli alone are the focus of this chapter, and will be referred to as type II units. In the terminology of Milde et al. (1987), type II units are ‘non-visual’ NMNs. In light of the many examples of one sensory input changing a neuron’s response to another input, this study investigates whether type II NMNs respond to visual stimuli in the presence of another sensory input, that from the halteres.

Halteres are the fly's organ of balance, functionally equivalent to human semi-circular canals. They are small club-shaped appendages located at the meeting point of the thorax and abdomen. The halteres beat in anti-phase to the wings during flight and detect the Coriolis forces induced by rotations of the fly (Nalbach, 1993; Nalbach and Hengstenberg, 1994). Because of the oscillatory nature of the haltere system, its neural outputs are highly rhythmic (Pringle, 1948). The visual system also responds to rotations of the fly, but responds to much slower rotations than the halteres (Hengstenberg, 1993; Sherman and Dickinson, 2003), and its outputs are not rhythmic. NMNs must integrate fast, rhythmic haltere inputs with slower non-rhythmic outputs of the visual system in a way that produces a useful motor output.

3.3 Methods

3.3.1 Electrophysiology

3.3.1.1 Extracellular recordings

All experiments were performed on female, one to three-day-old blowflies (*Calliphora vicina*) from the Cambridge Department of Zoology colony. Each fly was mounted dorsal side up, and a small window was cut in the neck cuticle. Hook electrode recordings were made from Neck Motor Neurons (NMNs) at the level of their neck muscle arborisations. See the previous chapter for details of the dissection and data acquisition.

3.3.1.2 Intracellular recordings

The fly's legs and wings were removed and it was mounted ventral side up upon a custom made holder. The ocelli were obscured using black paint. The head was aligned with the visual stimulus using the pseudopupil (Franceschini, 1975) and fixed with beeswax. The neck sclerites were waxed to reduce movement. A small window was cut in the cuticle and air sacs, exposing the fly's Frontal Nerve (FN) and the extreme anterior portion of the prothoracic ganglion. Large neck muscles not innervated by the FN were cut to reduce movement. A 0.025mm diameter silver wire hook was placed under the FN to add support and act as an indifferent electrode. If further support was necessary, fine cactus spines were used to support the FN root and anterior portion of the prothoracic ganglion. The preparation was kept moist with fly Ringer solution (see Hausen (1982) for the recipe used).

Thick walled Borosilicate glass micropipettes (resistance 70-120 M Ω) filled with 2 M Potassium Acetate were used to record from Frontal Nerve motor neuron axons within either the left or right FN about 0.3mm from the prothoracic ganglion. A recording was only accepted if the recorded resting membrane potential was in the range -55 to -75mV. Stable recordings lasted for 10-60 minutes. Occasionally the NMN would fire a burst of action potentials, these bursts correlated with haltere

beating and contraction of the leg muscles, and have been described elsewhere (Sandeman and Markl, 1980; Milde et al., 1987). Any data taken during these bursts were discarded and the experimental trial repeated.

The neural signals were amplified 10-fold and low-pass filtered at 6 kHz by a NPI SEC-10L amplifier operating in bridge balance mode, then amplified 5 fold by a custom made DC amplifier. Data were acquired at 20 kHz through a National Instruments PCI-6025E board on a computer running Matlab (Mathworks, Natick, MA).

3.3.2 Stimulus generation and presentation

3.3.2.1 Visual stimuli

As in the previous chapter, visual stimuli were presented on green Cathode Ray Tube (CRT, P31 phosphor) driven by an Innisfree Picasso Image generator at a refresh rate of 182 Hz. The CRT was placed directly in front of the fly at a distance of 7.4 cm so that the circular screen aperture subtended a visual angle 62.6° in diameter. Square wave gratings of 96% contrast and spatial period 10° were moved with a temporal frequency of 5 Hz in one of sixteen different directions. Between grating presentations a blank screen was shown with the same mean luminance as the grating (18 cd/m^2). The CRT was mounted on a separate platform to the preparation in an attempt to mechanically isolate the two. A transparent electrical shield was placed in front of the CRT to reduce electrical noise.

3.3.2.2 Haltere stimuli

The calypter of the haltere to be studied was removed. To control haltere movement in the extracellular experiments, a Ling Vibrator (model 101, Ling Dynamic Systems, Royston) was attached directly to the fly's right haltere using solvent-free adhesive (Bostik, Leicester). In the intracellular experiments the fly's left haltere was coated in solvent free adhesive and iron powder ($<212 \mu\text{m}$ particles, Sigma-Aldrich) and then moved magnetically via a 4x3 mm neodymium magnet attached to a Ling Vibrator. The posterior portion of the eye on the same side as the

stimulated haltere was painted black to block any visual input from the moving haltere stimulus. In all experiments the haltere was oscillated through a vertical angle of approximately 50° in a plane approximately equal to the horizontal angle of the resting haltere (30° posterior from the horizontal as viewed from above).

3.3.2.3 Protocols during extracellular recordings

Haltere stimuli: In all cases, only the fly's right haltere was stimulated. The Ling vibrator controlling haltere movement was oscillated in an approximately square wave manner at various frequencies between 10 and 120 Hz. Those units that responded to this stimulus were selected for analysis. At the end of the experiment the stimulus was detached from the haltere and the protocol repeated to check that the stimulus was not stimulating the neuron through non-specific vibration.

Visual stimuli: The fly was shown a series of gratings that moved for one second. At each presentation the direction of grating motion was chosen in a pseudorandom manner from 16 different options spaced at 22.5° . Between grating presentations, the fly was shown a 6-second blank screen with the same mean luminance as the grating to allow for recovery from any possible adaptation. In those experiments where the receptive field was mapped, mapping protocols were the same as in the previous chapter with a screen visual angle of 62.6° .

Combined haltere and visual stimuli: The same sequence of moving visual gratings as in the visual stimuli protocol were shown while the fly's right haltere was oscillated at a fixed frequency (10-120 Hz depending on the experiment). The haltere stimulus was started two seconds before the visual stimulus. This delay ensured that the visual stimulus occurred well after the bursting activity that often accompanied haltere stimulus onset. Six type II and four type I NMNs across ten flies were studied using these protocols. Each protocol was repeated between 1 and 15 times.

3.3.2.4 Protocols during intracellular recordings

Haltere stimuli: Both halteres were touched in succession with a fine plastic tube. In all cases, touching one haltere would elicit many more action potentials than touching the other. This difference was very clear-cut and enabled the unambiguous identification of the ‘preferred haltere’ of the NMN, which was defined as the haltere whose movement would elicit the most action potentials.

The haltere stimulator was aligned with the fly’s left haltere. In the case of recordings from the left FN, the stimulated left haltere was the ipsilateral haltere and in the case of right FN recordings, the contralateral haltere. By recording from different nerves in different experiments, recordings were obtained both where the haltere stimulus was on the ‘preferred haltere’ and where the stimulus was on the ‘non-preferred’ haltere. The haltere stimulus oscillated with a triangular waveform at either 10.5 or 105 Hz. A triangular waveform was used as it is closer to the fly’s natural haltere beating movements than a square or sine-wave (Nalbach, 1993; Fayyazuddin and Dickinson, 1996). The haltere was oscillated at 10.5 Hz, as this was slow enough to not affect the stability of the recording and to see separate responses to different phases of the stimulus oscillation. Female blowflies beat their halteres at 105-120 Hz (Pringle, 1948). To test whether the results obtained at 10.5 Hz also apply at more naturalistic frequencies, experiments were also performed using 105 Hz haltere stimulation.

Non-oscillating ‘ramp and hold’ stimuli were also applied to the haltere. The haltere was held in its lowest position for 200 msec, raised at constant velocity to its highest position (equivalent to half a triangle wave, or ‘ramp’), and then held there for another 200 msec. The speed of movement during the ramp transitions between the low and high positions was such that it was identical to the speed of movement in either the 10.5 Hz or 105 Hz triangle waveform stimuli. In such a manner the response to one direction of movement could be separated out.

At the end of the experiment, the electrode was withdrawn from the axon. At this point the haltere stimulus was presented as a control to check that the stimulus itself was not inducing any electrical or movement artefacts in the recording.

Visual stimuli: Identical to the extracellular recordings visual stimuli protocol.

Combined haltere and visual stimuli: The same sequence of visual stimuli as shown in the visual stimuli protocol were shown while the halteres were oscillated. The haltere stimulus was oscillated along a triangular waveform at either 10.5 Hz or 105 Hz depending on the experiment. As in the extracellular protocol, the visual stimulus was started two seconds after haltere stimulus onset. 27 type II and 10 type I NMNs across 37 flies were studied using these protocols. Each protocol was repeated between 1 and 5 times. Not all flies were subjected to all protocols (see figure legends for N-values specific to each protocol).

3.3.3 Data analysis

Extracellular signals were spike-sorted using a template-matching spike sorting program custom written in Matlab. For both the extracellular and intracellular experiments, the spiking response to visual motion was defined to be the difference between the number of spikes during a one second grating presentation and the number of spikes during the preceding one second of blank screen. The spiking response to visual stimuli during haltere stimulation was similarly defined as the difference between the number of spikes during one second of concurrent visual and haltere stimulation and the number of spikes during the preceding second of just haltere stimulation. By comparing the responses of one unit to sixteen different, equally spaced directions of visual motion, a directional tuning curve was constructed. The tuning curve peak was estimated by finding the phase of the first harmonic in a Fourier transformation of the tuning curve. The peak of the tuning curve gives the direction of visual motion to which the cell responds most strongly, referred to here as the cell's 'preferred direction'.

In those intracellular experiments where there were no spikes in response to visual motion, the sub-threshold response was defined as the difference between the mean membrane potential during one second of grating motion and the mean membrane potential during the preceding second of blank screen. Using this response, a tuning curve and estimate of the preferred direction were produced in the same manner as for the spiking responses.

Some intracellular recordings were taken from the fly's right FN while others were taken from the fly's left FN. To allow the comparison of these results, the directional tuning curves acquired from units in the right FN were mirror transformed horizontally over the vertical axis so as to be the same as those of the equivalent units in the left FN. Circular statistics were performed in custom written Matlab programs, and all non-circular Statistics were performed in SPSS (SPSS Inc, Chicago).

3.4 Results

3.4.1 Extracellular recordings from Neck Motor Neurons

The extracellular responses of NMNs to multimodal stimuli were measured in a series of experiments pairing visual motion stimuli with induced haltere movements. Four type I and six type II NMNs were studied extracellularly across ten flies.

3.4.1.1 Responses to visual stimuli

As was seen in the previous chapter and other studies of blowflies (Milde et al., 1987), only a sub-population of the NMNs, those with small extracellular action potential waveforms and high spontaneous spike rates, fired action potentials in response to visual stimuli. Units with larger extracellular recorded action potentials and low spontaneous rates did not spike in response to visual stimuli. For convenience, those units that spiked in response to visual stimuli are termed type I units and those that did not spike in response to visual stimuli are termed type II units.

3.4.1.2 Responses to haltere stimuli

When the fly's right haltere was oscillated vertically some of both types of unit responded with action potentials that were phase-locked to the haltere stimulus waveform. This phase-locking can be seen in figure 3.1a, where all spikes fired by a representative unit occurred after the downswing, within a 15 millisecond window of the 100 millisecond long stimulus cycle. The phase locking remained at all frequencies tested (10-120 Hz), indicating that the neurons were not just firing at a fixed frequency coincidentally phase-locked to the stimulus. Different units would spike at different phases of the haltere stimulus. If the amplitude of the haltere stimulus was reduced, the percentage of haltere stimulus cycles that resulted in an action potential was reduced.

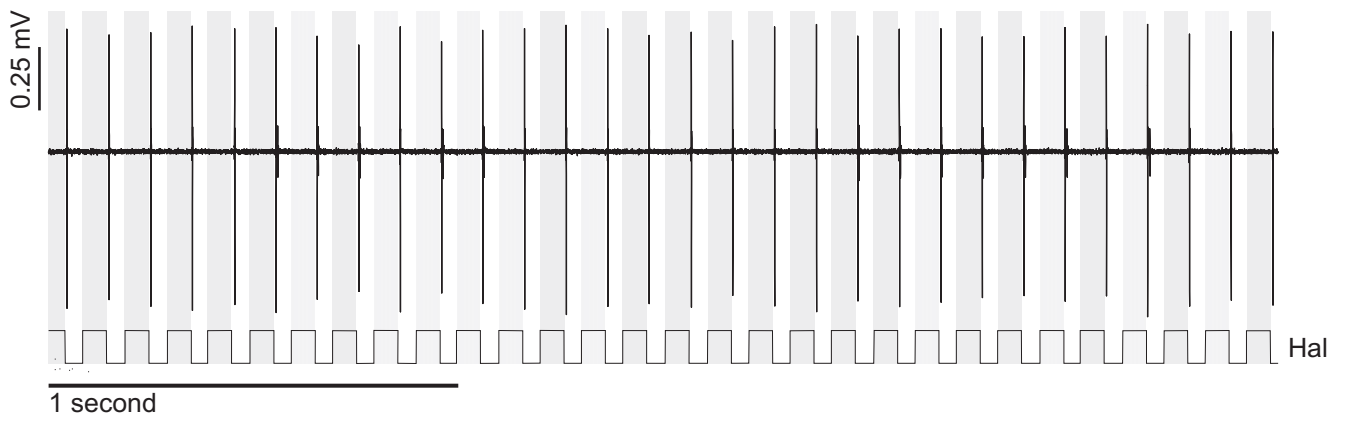
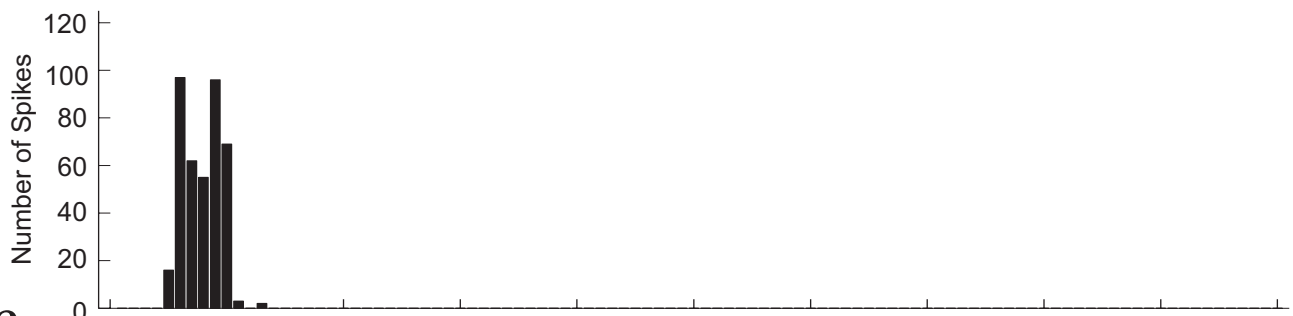
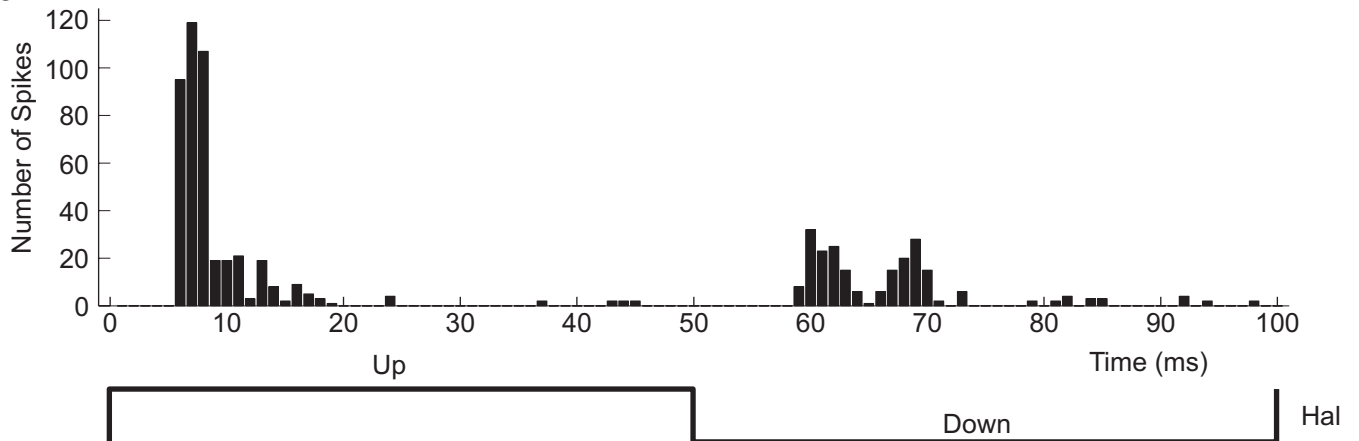
a**b****c**

Figure 3.1 Phase locking of NMN extracellularly recorded spikes to the haltere stimulus:

(a) Response of a typical type II NMN to 10 Hz ~squarewave vertical movements of the fly's right haltere. Bottom trace indicates the haltere stimulus waveform.

(b) Histogram of spike timing relative to haltere stimulus for a different type II NMN during simultaneous squarewave 10Hz haltere and standard visual stimulation in the cell's preferred direction (see methods for details of visual stimulus). 400 spikes were grouped in 1 msec bins. The trace at the bottom of (c) indicates the haltere stimulus waveform.

(c) Histogram of spike timing relative to haltere stimulus for a type I NMN during simultaneous haltere and visual stimulation. 666 spikes were grouped in 1 msec bins. Bottom trace indicates the haltere stimulus waveform.

3.4.1.3 Responses to visual and haltere stimuli combined

Many of type II NMNs that were initially unresponsive to visual stimuli responded to visual motion when the fly's right haltere was oscillated simultaneously. When the haltere was oscillated, a certain baseline spiking activity resulted. If a moving grating was then shown, the response of the neuron increased above that induced by the haltere stimulus alone. Thus, visual stimuli produced a spiking response in type II units only when the haltere stimulus was present. This is a robust effect. Examples are seen in figures 3.2c and 3.3d, where the haltere stimulus amplitude has been fixed just below that required to elicit spikes. When a visual stimulus is presented in addition, the units spike, whereas they do not in response to the visual stimulus alone (figures 3.2a and 3.3b).

The visual responses of type II units seen during haltere stimulation were not just a general up regulation of response due to the presence of any visual input, but were dependent on the direction of the visual grating (figures 3.2.c,d and 3.3.c,d). The extra spikes induced by a visual stimulus were compared across 16 different directions of visual motion. When the responses to different directions of motion are plotted together, they form single peaked tuning curves (figures 3.2f and 3.3f), confirming that the visual response was highly directional. In all six type II units recorded from, the number of extra spikes induced by a visual stimulus during haltere stimulation was significantly dependent on the direction of visual motion (visual tuning curves subjected to a non-linear regression with cosines of amplitude $\neq 0$, $P < 0.05$ for all six units, $P < 0.001$ for 4/6 units).

The extra spikes induced by visual stimulation during haltere oscillation were highly phase locked to the haltere stimulus. This phase locking is seen in the representative example shown in figure 3.1b where all 400 spikes fired during concurrent haltere and visual stimulation occurred within a 9 msec segment of the 100 msec haltere stimulus waveform (32.4° of the stimulus' 360° period). In five of the six type II units studied, the visual stimulus increased spike rate during motion in the preferred direction, and only produced a subtle reduction of spike rate in the anti-preferred direction. This effect can be seen as a vertical asymmetry in the tuning curves of figures 3.2.f and 3.3.f where the tuning curve peaks are due to an increase in spikes per second whereas the troughs result from an approximately zero response. In

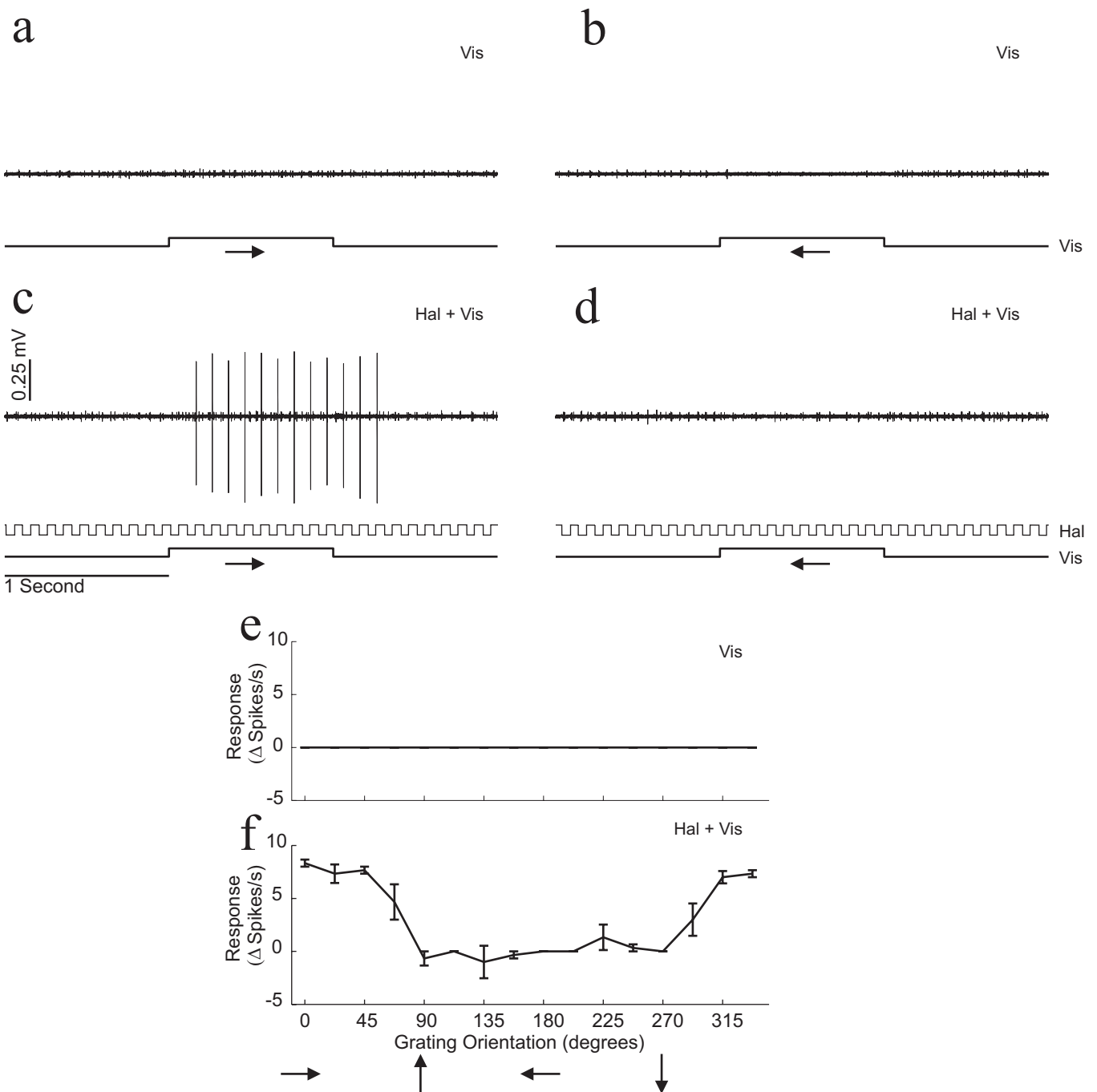


Figure 3.2 Spiking response of a type II NMN to haltere and visual stimuli. Response of the NMN to rightwards (a) and leftwards (b) visual motion. (c) and (d) are responses to rightwards and leftwards visual motion combined with 10 Hz squarewave right haltere stimulation. In panels a-d the traces at the bottom of the panels indicate the waveforms of the visual and haltere stimuli; Also shown are directional visual tuning curves resulting from the NMN's responses to 16 different directions of visual grating without (e, $n=3$ for each grating direction) and with (f, $n=3$, error bars = standard error) 10 Hz right haltere stimulation. All panels share common scale bars.

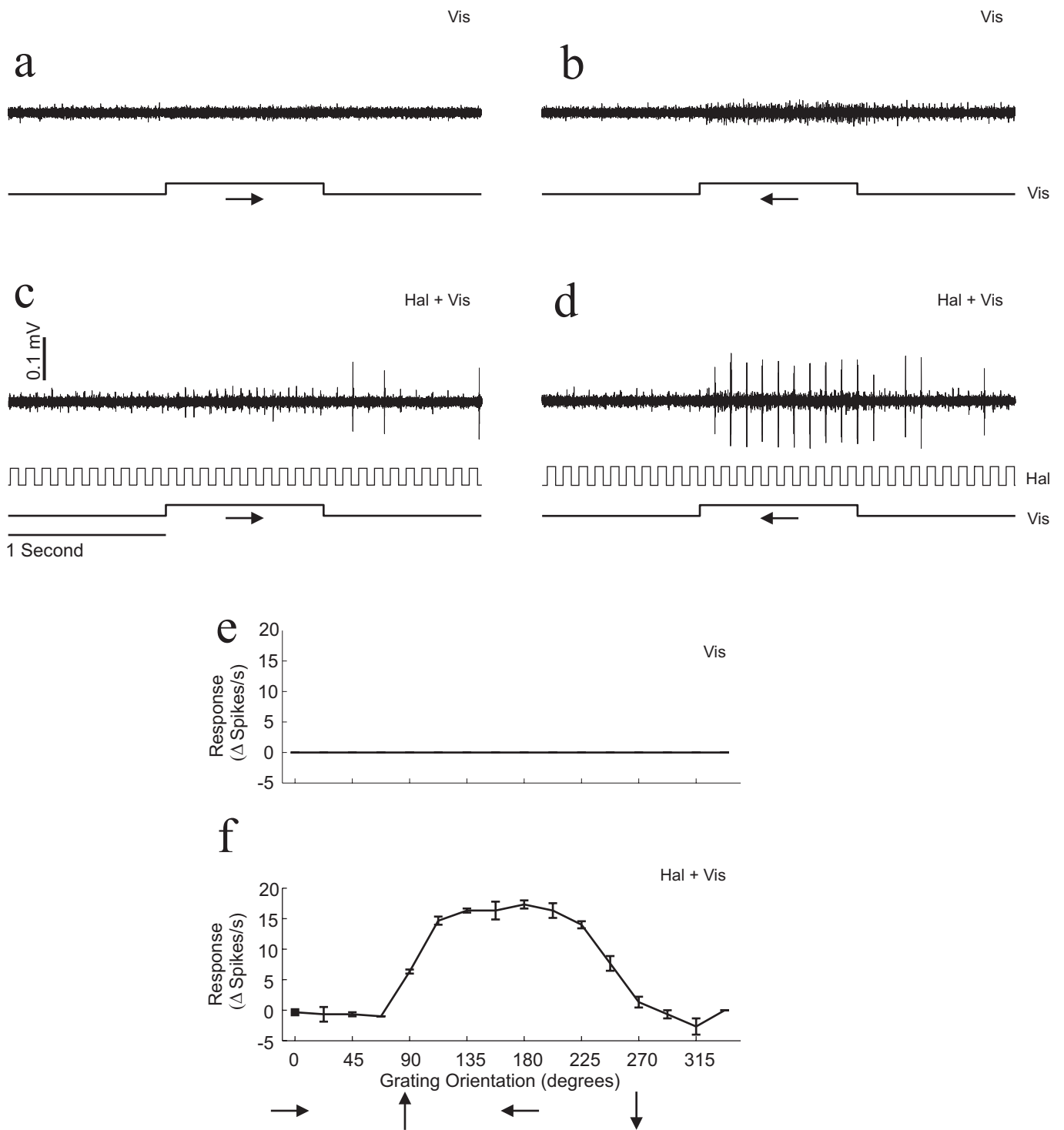


Figure 3.3 Spiking response of a type II NMN, with a different preferred direction to that in figure 3.2, to haltere and visual stimuli. Response of the NMN to rightwards (a) and leftwards (b) visual motion; (c) and (d) are responses to rightwards and leftwards visual motion combined with 10 Hz squarewave right haltere stimulation. In panels a-d the traces at the bottom of the panels indicate the waveforms of the visual and haltere stimuli; Also shown are directional visual tuning curves resulting from the NMN's responses to 16 different directions of visual grating without (e, $n=3$ for each grating direction) and with (f, $n=3$, error bars = standard error) 10 Hz right haltere stimulation. All panels share common scale bars.

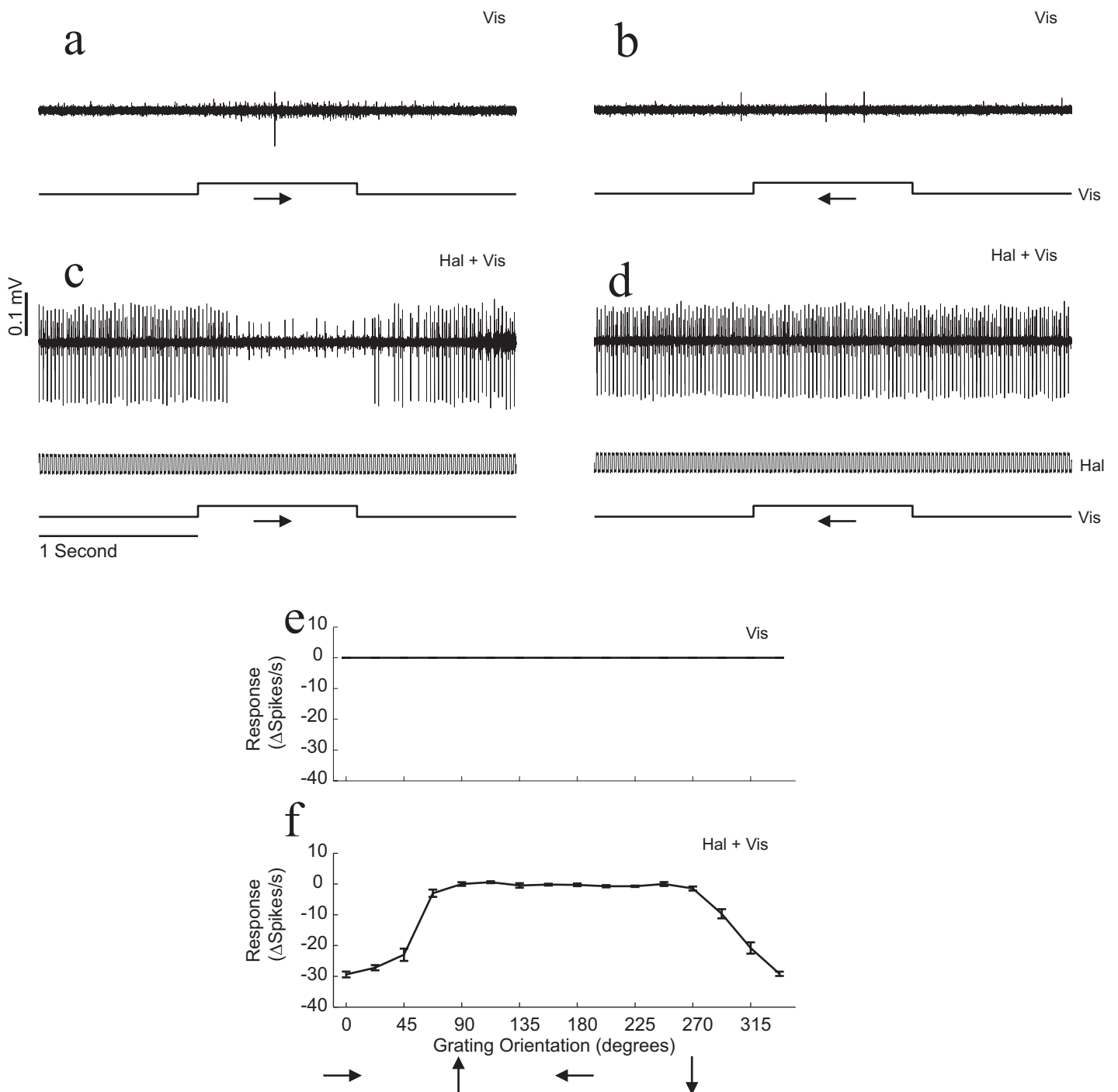


Figure 3.4 Spiking response of a type II NMN to haltere and visual stimuli. Response of the NMN to rightwards (a) and leftwards (b) visual motion; (c) and (d) are responses to rightwards and leftwards visual motion combined with 50 Hz squarewave right haltere stimulation. In panels a-d the traces at the bottom of the panels indicate the waveforms of the visual and haltere stimuli; Also shown are directional visual tuning curves resulting from the NMN's responses to 16 different directions of visual grating without (e, $n=3$ for each grating direction) and with (f, $n=15$, error bars = standard error) 50 Hz right haltere stimulation. All panels share common scale bars.

one unit however, the opposite was true and the effect of the visual stimulus was to reduce spike rate in the anti-preferred direction, but not increase it in the preferred direction. This unit is seen in figure 3.4, where the tuning curve trough results from a decrease in spikes per second and the tuning curve peak results from approximately no change in spike rate.

By using the haltere and visual stimuli together in this way, it was possible to map the visual receptive fields of those neurons that do not respond to visual motion alone. One example of such a visual map from a type II unit is shown in 3.5. This map was obtained in the same manner as those in the previous chapter except that all visual responses were recorded during oscillation of the fly's right haltere. To determine whether the motor neuron responded to different types of visual motion at different phases of the haltere cycle the unit's spikes were split into two, those that occurred during the haltere stimulus upswing and those that occurred during the haltere stimulus downswing. The upswing and downswing spikes from the same motor neuron were then converted into two separate maps. The two maps were qualitatively the same (data not shown), except that the upswing spikes could be elicited by visual stimuli over a wider visual area than the downswing spikes, reflecting that it was easier to evoke spikes during the upswing phase of the haltere stimulus.

3.4.1.4 Responses of units that spike in response to vision alone

Many of the type I cells also responded to the haltere stimulus in a phase locked manner. This can be seen in figure 3.1c, where the vast majority of the unit's spikes occur within a small segment of the haltere stimulus cycle. The presence of the haltere stimulus did not shift the peak of the type I units' directional tuning curve, but did in some cases increase the tuning curve amplitude as seen in figure 3.6. This preservation of the preferred direction of visual motion during haltere stimulation is also seen in figure 3.7 where the visual receptive field of one type I unit is shown as mapped with and without concurrent stimulation of the right (contralateral) haltere. Haltere stimulation did not change the directional structure of the NMNs receptive field, but did increase the neuron's sensitivity to visual motion, widening slightly the visual area over which it will respond to visual stimuli.

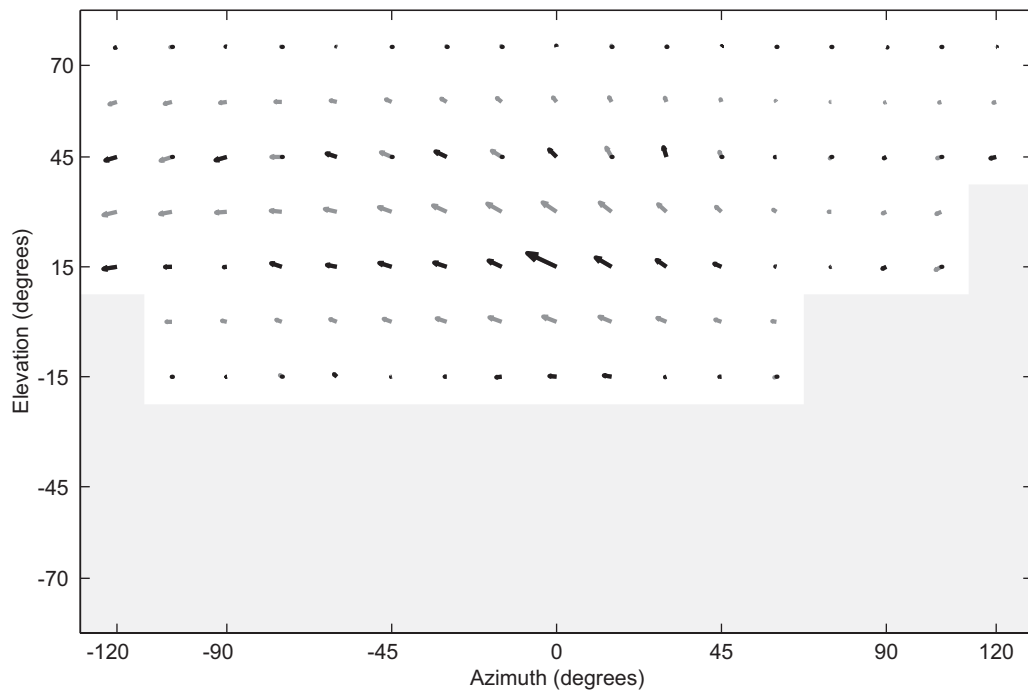


Figure 3.5 Map of a type II NMN's preferred direction and sensitivity over the visual receptive field during 10 Hz squarewave stimulation of the right haltere. Orientation of the arrows gives the NMN's preferred direction of visual motion at that point in visual space; length of arrows gives the normalised motion sensitivity. Black arrows are actual data points, grey arrows are the result of interpolation. The shaded area covers those points where no visual stimulation was possible due to the presence of the haltere stimulation apparatus.

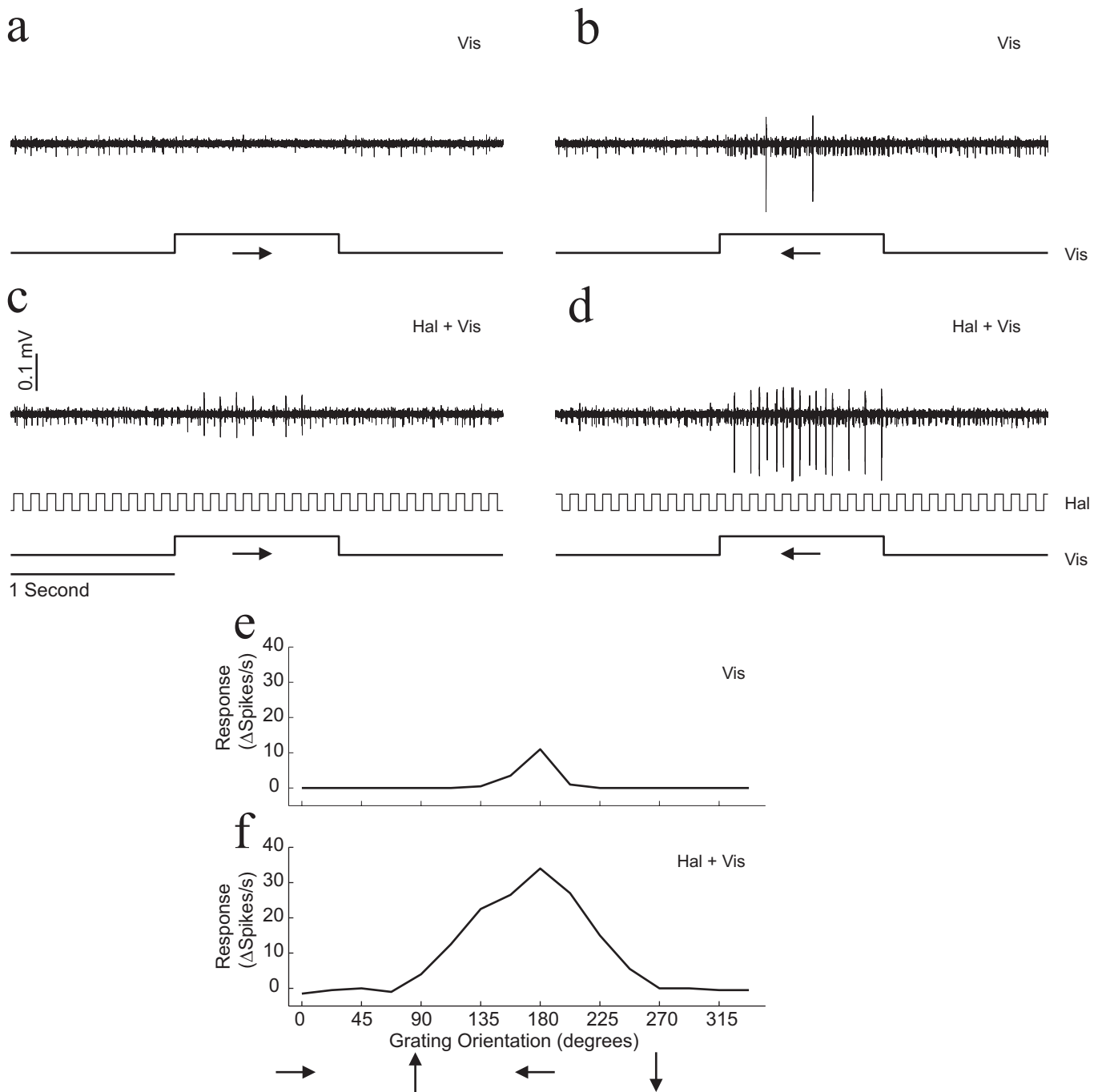
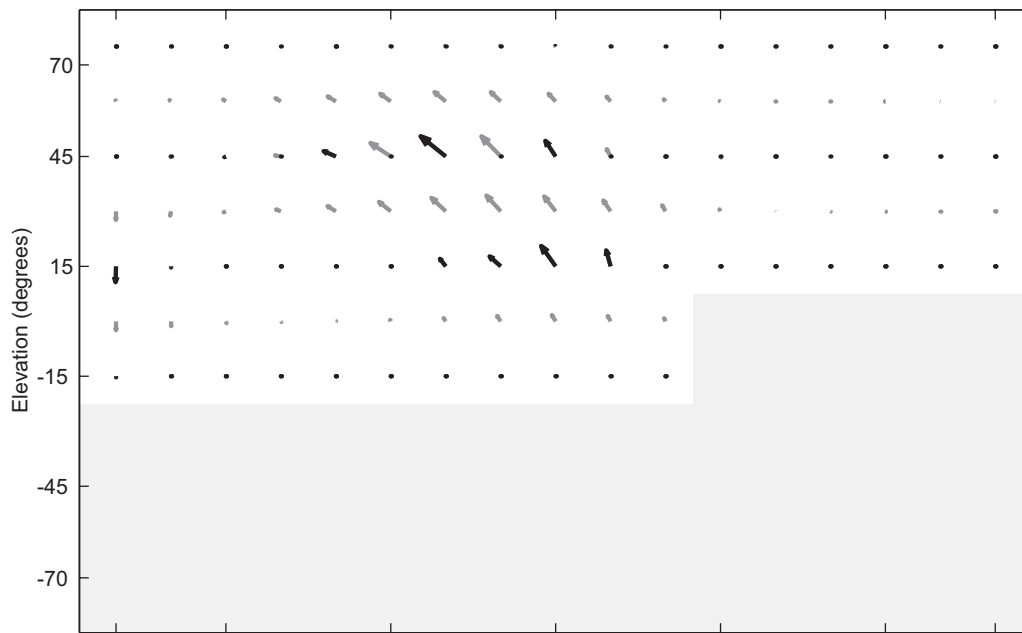
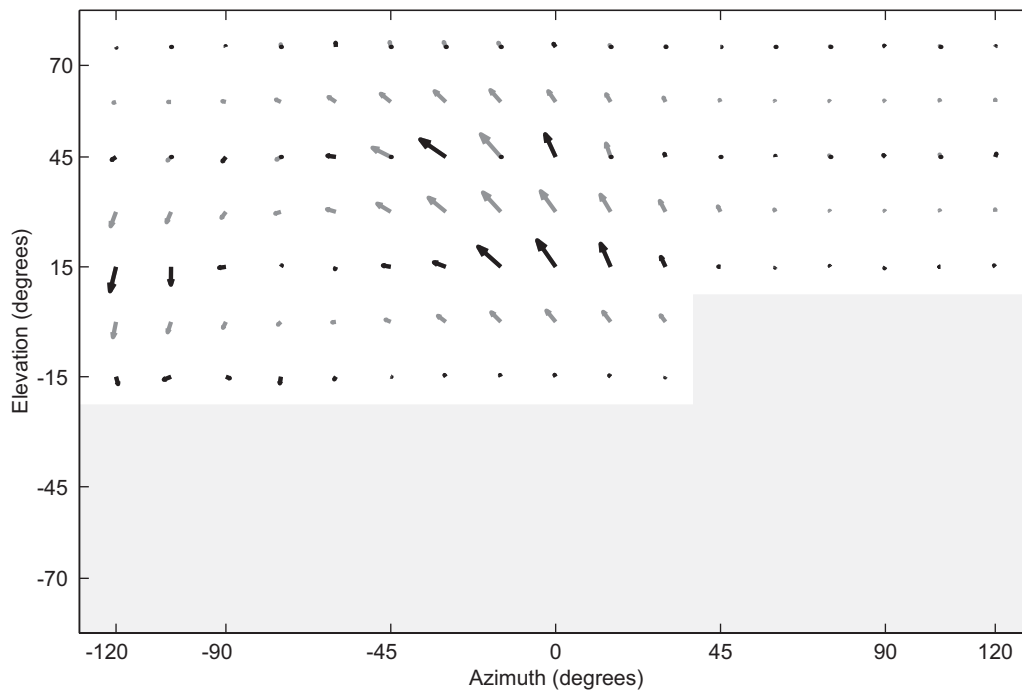


Figure 3.6 Spiking response of a type I NMN to haltere and visual stimuli. Response of the NMN to rightwards (a) and leftwards (b) visual motion; (c) and (d) are responses to rightwards and leftwards visual motion combined with 10 Hz squarewave right haltere stimulation. In panels a-d the traces at the bottom of the panels indicate the waveforms of the visual and haltere stimuli; Also shown are directional visual tuning curves resulting from the NMN's responses to 16 different directions of visual grating without (e, $n=2$ for each grating direction) and with (f, $n=2$, error bars = standard error) 10 Hz right haltere stimulation. All panels share common scale bars. The mis-match between the spike rate in the raw traces and the spike rates in the tuning curves is due to a larger spiking response occurring in the trial that is not shown in the raw traces.

a

Vis

b

Hal + Vis

Figure 3.7 Comparison of visual receptive field maps taken from a type I NMN with (b) and without (a) concurrent 10 Hz stimulation of the right haltere.

3.4.2 Intracellular recordings from Neck Motor Neurons

The results of the extracellular recordings show that the type II NMNs only spike in response to visual stimuli when the halteres are moved at the same time. To investigate the sub-threshold events underlying this gating, intracellular recordings were taken from 27 type II NMNs of one motor nerve, the Frontal Nerve (FN). As the recordings were taken from axons far from the dendrites all sub-threshold events observed were small but well above the noise level.

3.4.2.1 Responses to visual stimuli

Moving visual gratings in type II neurons' preferred direction produced small, sustained, sub-threshold depolarisations in the range 0.5-2 mV, as seen in the example in figure 3.9a. The sub-threshold response, defined as the change in mean membrane potential induced by the visual stimulus, was highly dependent on the direction of visual motion (figure 3.9a: response to motion in the preferred direction, figure 3.10a: response to motion in the opposite direction), resulting in single peaked tuning curves as seen in figure 3.11a. This directionality of the visual sub-threshold response was statistically significant for all type II units recorded (visual tuning curves subjected to a non-linear regression with cosines of amplitude $\neq 0$, $P < 0.05$ for all units, $P \ll 0.001$ for 18/27 units). In all but two of the units studied, the directional tuning seen was due to depolarisation during motion in the units' preferred direction (figure 3.9a) with no, or only subtle, hyperpolarisation in the units' anti-preferred direction (figure 3.10a). This vertical asymmetry of the directional tuning curve can be seen in figure 3.11a where the magnitude of change in membrane potential during motion in the NMNs preferred direction ($\sim +0.75\text{mV}$) is much larger than that during motion in the opposite direction ($\sim -0.25\text{mV}$).

3.4.2.2 Responses to 10.5 Hz haltere stimuli

Vertical movements of the haltere resulted in compound Excitatory Postsynaptic Potentials (EPSPs) and action potentials that were highly phase-locked to the haltere stimulus cycle. Before using the controlled haltere stimulus, each

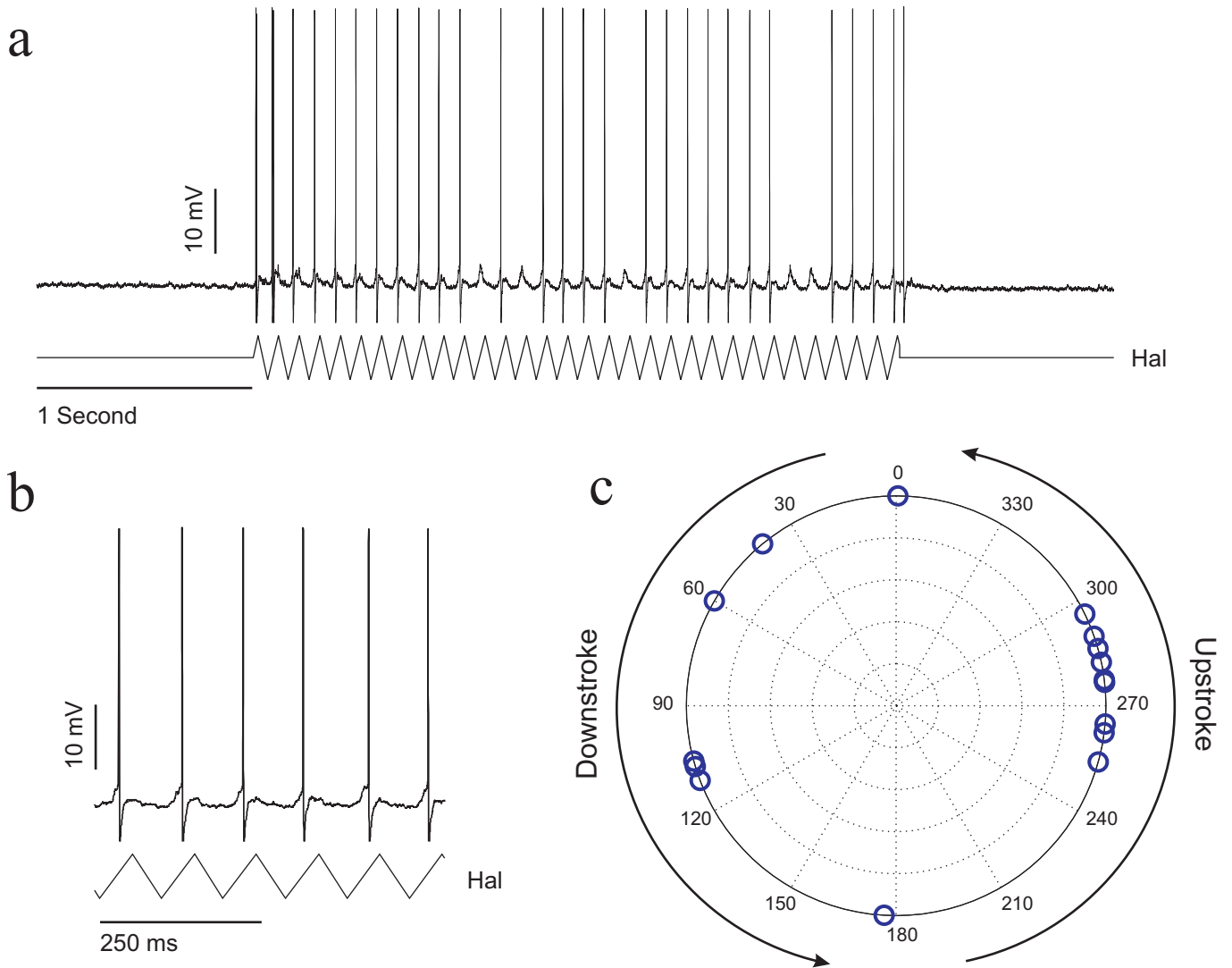


Figure 3.8 Phase locking of type II NMN responses to the haltere stimulus: (a) Intracellular recording from a type II NMN during 10.5 Hz triangular waveform vertical movements of the contralateral/preferred haltere. The trace at the bottom of the figure indicates the haltere stimulus waveform. (b) A segment of the response shown in (a) with a finer temporal resolution showing the phase locking of the NMN's spikes to the haltere stimulus. The trace at the bottom of the figure indicates the haltere stimulus waveform. (c) Plot of the spiking phases of different NMNs. The phase of the contralateral haltere stimulus where each NMN spiked most commonly is shown for those NMNs whose 'preferred haltere' was contralateral, (n=16). The distribution of spiking phases across the 16 NMNs is plotted in polar coordinates.

haltere was touched with a fine plastic tube. In all cases touching one haltere would produce a much larger spiking response than touching the other. The haltere that gave the strongest spiking response was defined as the NMNs 'preferred haltere'. The difference between the responses to movement of the two halteres was clear-cut and unambiguous in all cases. In the vast majority of the cases, only movement of the 'preferred haltere' would result in NMN spikes. The preferred haltere could be either ipsilateral or contralateral depending on the cell. Once the preferred haltere had been identified, all further experiments utilised the controlled haltere stimulus attached to the left haltere. Therefore, in some experiments the haltere stimulus was on the 'preferred haltere' and in others it was on the 'non-preferred haltere'.

As in the extracellular experiments, vertically oscillating the preferred haltere at 10.5 Hz resulted in spikes phase-locked to the stimulus waveform. An example of this can be seen in figure 3.8a and b, where all spikes occurred during the end of the haltere upswing within a 19 millisecond window of a 95 millisecond haltere stimulus cycle. For each type II NMN where the preferred haltere was contralateral and had been stimulated, the phase of the haltere stimulus where the cell was most likely to spike was found. These phases are plotted in figure 3.8c to see whether NMNs in the FN spike at the same phase of haltere movement. Those units that spike during the upstroke of the haltere stimulus can be seen to all fire at similar phases, between 250-300°, whereas those that fire during the down stroke do so at widely distributed phases (figure 3.8c). No relationship was found between the phase of haltere stimulation at which a NMN would fire and either the NMN's preferred haltere or its directional sensitivity to motion (data not shown).

If the amplitude of the haltere stimulus was reduced, the action potentials ceased and compound EPSPs could be seen, as in the first second and inset of figure 3.9b. These compound EPSPs were phase-locked to the same phase of the haltere stimulus as the spikes were, implying that the compound EPSPs are responsible for the phase-locked action potentials. Stimulating the 'non-preferred' haltere also resulted in phase-locked sub-threshold events that, for nine out of ten cells tested, did not result in NMN action potentials regardless of the haltere stimulus amplitude.

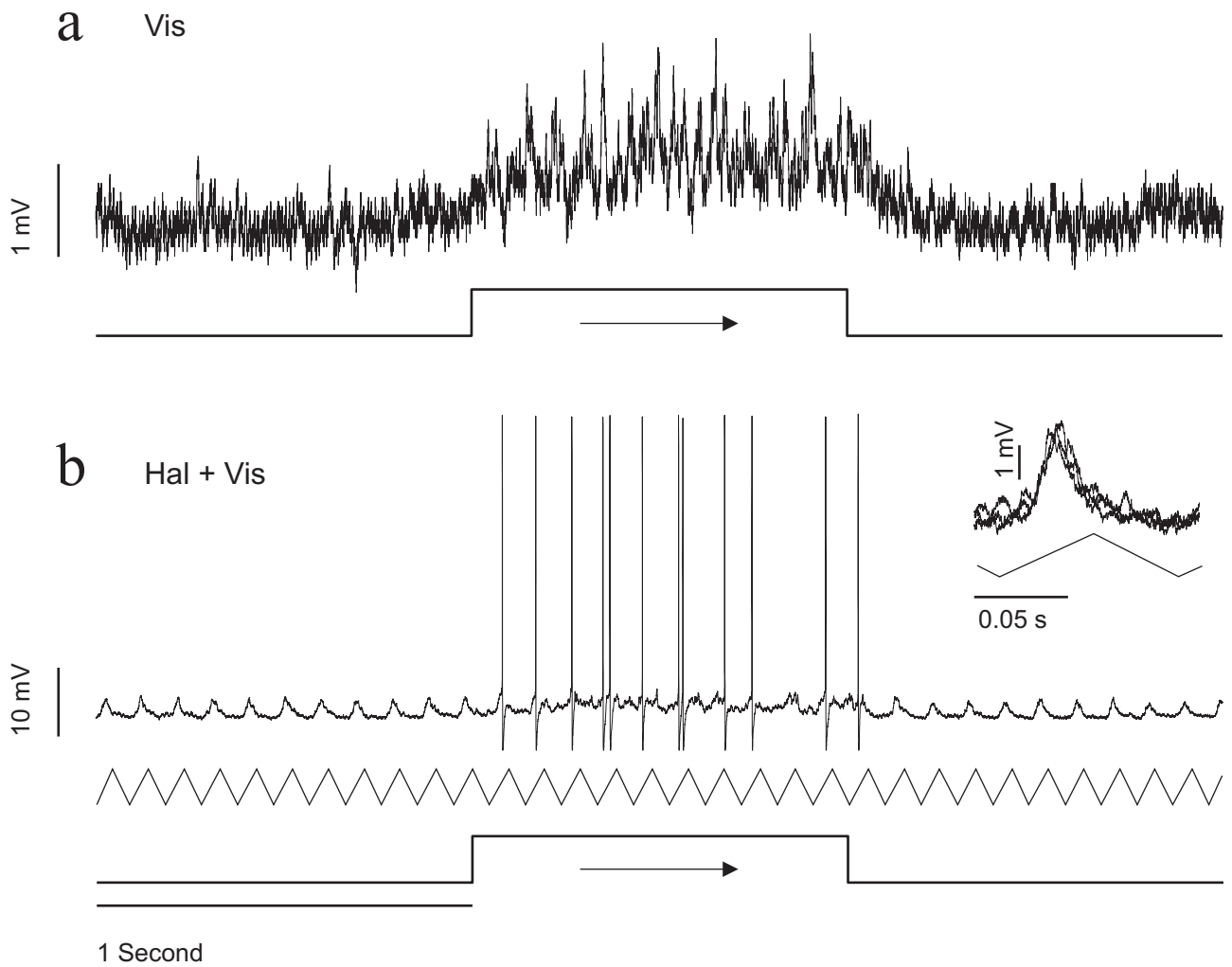


Figure 3.9 Response of a type II NMN to motion in the unit's preferred direction (rightwards) with (b) and without (a) simultaneous 10.5 Hz haltere stimulation of the 'preferred' (contralateral) haltere. Inset in (b) shows three examples of magnified compound EPSPs that were evoked by haltere stimulation. The bottom traces indicate the haltere and visual stimulus waveforms.

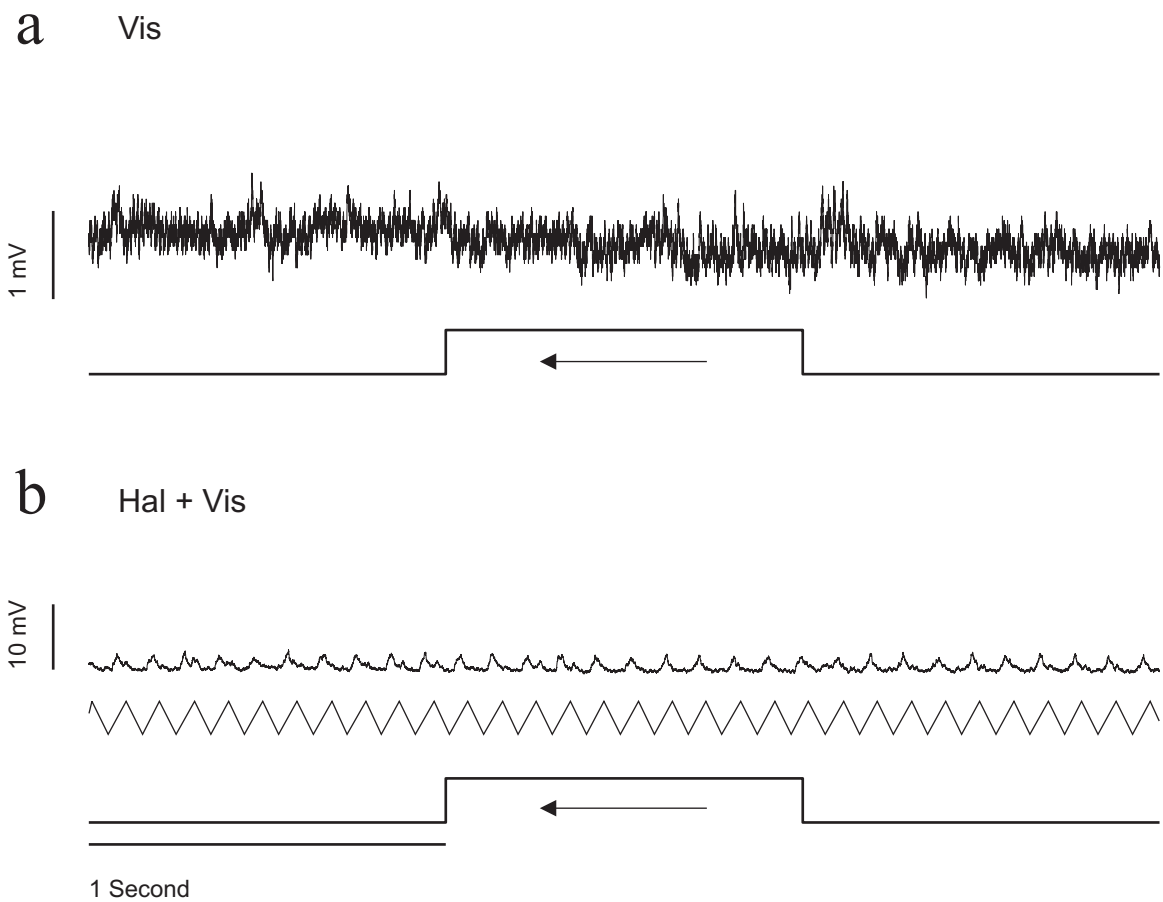


Figure 3.10 Response of the same type II NMN as in figure 3.9 to motion in the unit's anti-preferred direction (leftwards) with (b) and without (a) simultaneous 10.5 Hz haltere stimulation of the 'preferred' (contralateral) haltere. The bottom traces indicate the haltere and visual stimulus waveforms.

3.4.2.3 Responses to visual and 10.5 Hz haltere stimuli combined

As observed in the extracellular experiments, combining visual gratings moving in a NMN's preferred direction with haltere stimulation produced a higher spike rate than haltere stimulation alone. This effect enabled the visual inputs of type II units to influence the spiking output of the cell where they previously could not. When the visual stimulus is presented without any haltere stimulus, it produces only a small sub-threshold depolarisation (figure 3.9a). In figure 3.9b the haltere stimulus amplitude has been set to a level just below that required to produce spikes, so on its own the stimulus produces only phase locked compound EPSPs (figure 3.9b, 1st second). When the visual stimulus is presented in addition, the compound EPSPs are replaced with action potentials (figure 3.9b, 2nd second). Thus visual inputs only affect the cell's output if the haltere stimulus is also present. This effect is directional: if during haltere stimulation a visual stimulus moves opposite to the NMN's preferred direction none of the haltere induced EPSPs result in spikes (figure 3.10b).

One possible explanation for the visually induced increase in spike rate during haltere stimulation is simple summation of the two inputs. The visual depolarisation may be raising more haltere induced EPSPs above the threshold for spike generation. This hypothesis predicts that the direction of visual motion producing the largest depolarisation is the same as that resulting in the largest spike rate increase during haltere stimulation. To test this hypothesis, the directionality of the sub-threshold input and the spiking output were compared. The visual tuning curves obtained from spiking responses during simultaneous visual and haltere stimulation were plotted together with the visual tuning curves obtained from the same NMN's' membrane potential changes during just visual stimulation. The two tuning curves were very similar, as can be seen in the example in figure 3.11a. This correspondence was shown for all the recorded type II cells by plotting the peaks of the two tuning curves against each other (figure 3.11b). The preferred direction of the subthreshold visual input is highly correlated with the preferred direction of the spiking output seen during combined haltere-visual stimulation (ranked non-parametric circular correlation, $P \ll 0.01$ $n=14$ (Zar, 1996), critical values were only available to $P=0.01$), falling upon a straight line. This correlation is consistent with the hypothesis that the

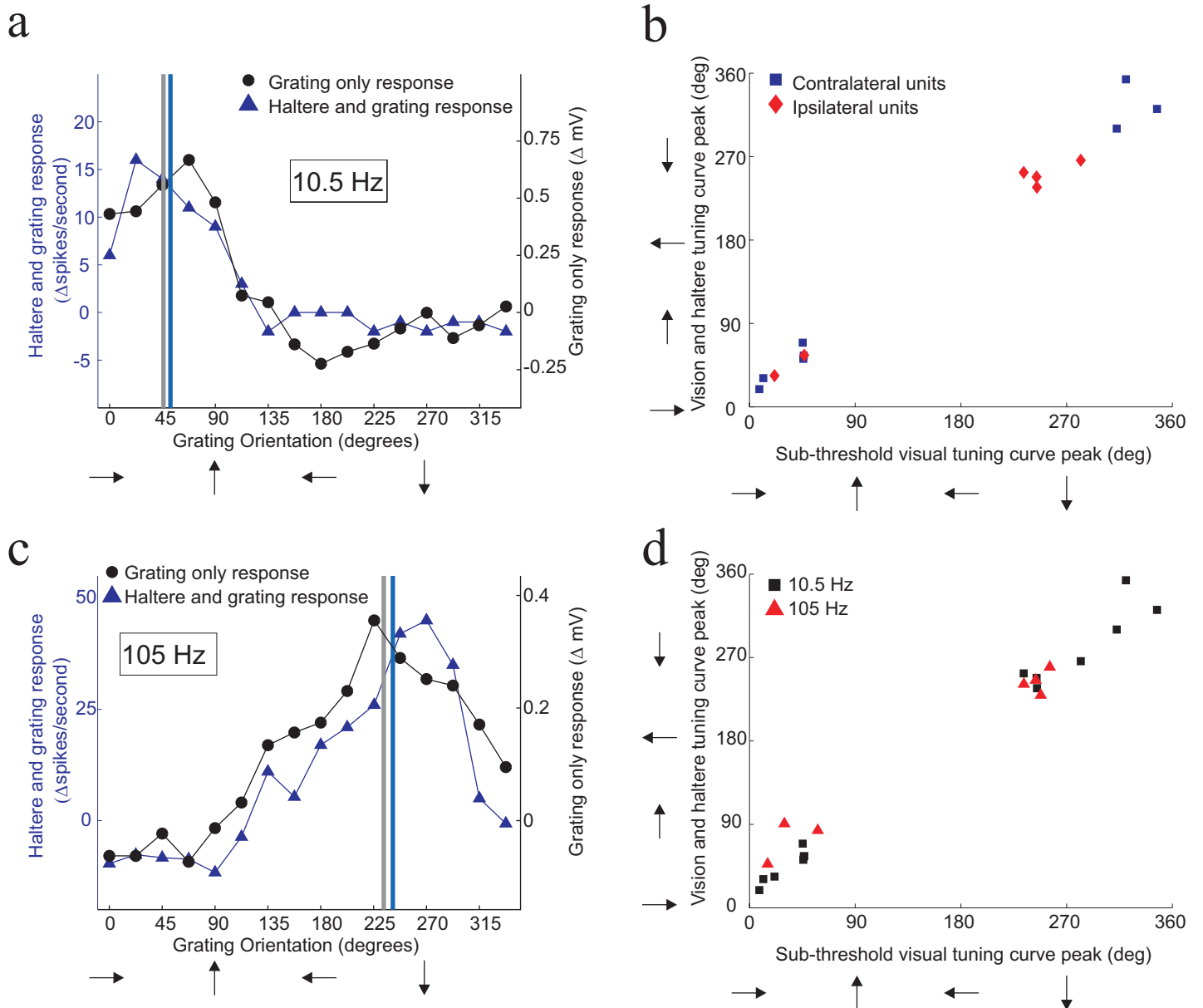


Figure 3.11 Correlation between the directional tuning of the subthreshold visual input and the directionality of the spiking output during combined haltere and visual stimulation:

(a) Example tuning curves obtained from one type II NMN. The tuning curve obtained from the sub-threshold responses to just visual stimuli (black circles, $n=1$) is plotted with the tuning curve obtained from the spiking responses to combined visual and 10.5 Hz haltere stimuli (blue triangles, $n=1$). Vertical lines indicate the preferred directions estimated from the tuning curves (grey = visual tuning curve, blue = combined stimulus tuning curve).

(b) Plot of the preferred directions (tuning curve peaks) obtained with visual stimuli against those obtained from the same NMNs with combined 10.5 Hz 'preferred haltere' and visual stimuli. Those NMNs with a contralateral preferred/stimulated haltere are plotted as blue squares ($N=8$), those NMNs with an ipsilateral preferred/stimulated haltere are plotted as red diamonds ($N=6$).

(c) Example tuning curves obtained from one type II NMN. The tuning curve obtained from the sub-threshold responses to just visual stimuli (black circles, $n=2$) is plotted with the tuning curve obtained from the spiking responses to combined visual and 105 Hz haltere stimuli (blue triangles, $n=3$). Vertical lines indicate the preferred directions estimated from the tuning curves (grey = visual tuning curve, blue = combined stimulus tuning curve).

(d) Plot of the preferred directions (tuning curve peaks) obtained with visual stimuli against those obtained with combined haltere and visual stimuli for all type II NMNs subjected to this stimulus paradigm. Those NMNs studied with a 10.5 Hz haltere stimulus are plotted as black squares ($N=14$), those NMNs studied with a 105 Hz haltere stimulus are plotted as red triangles ($N=7$).

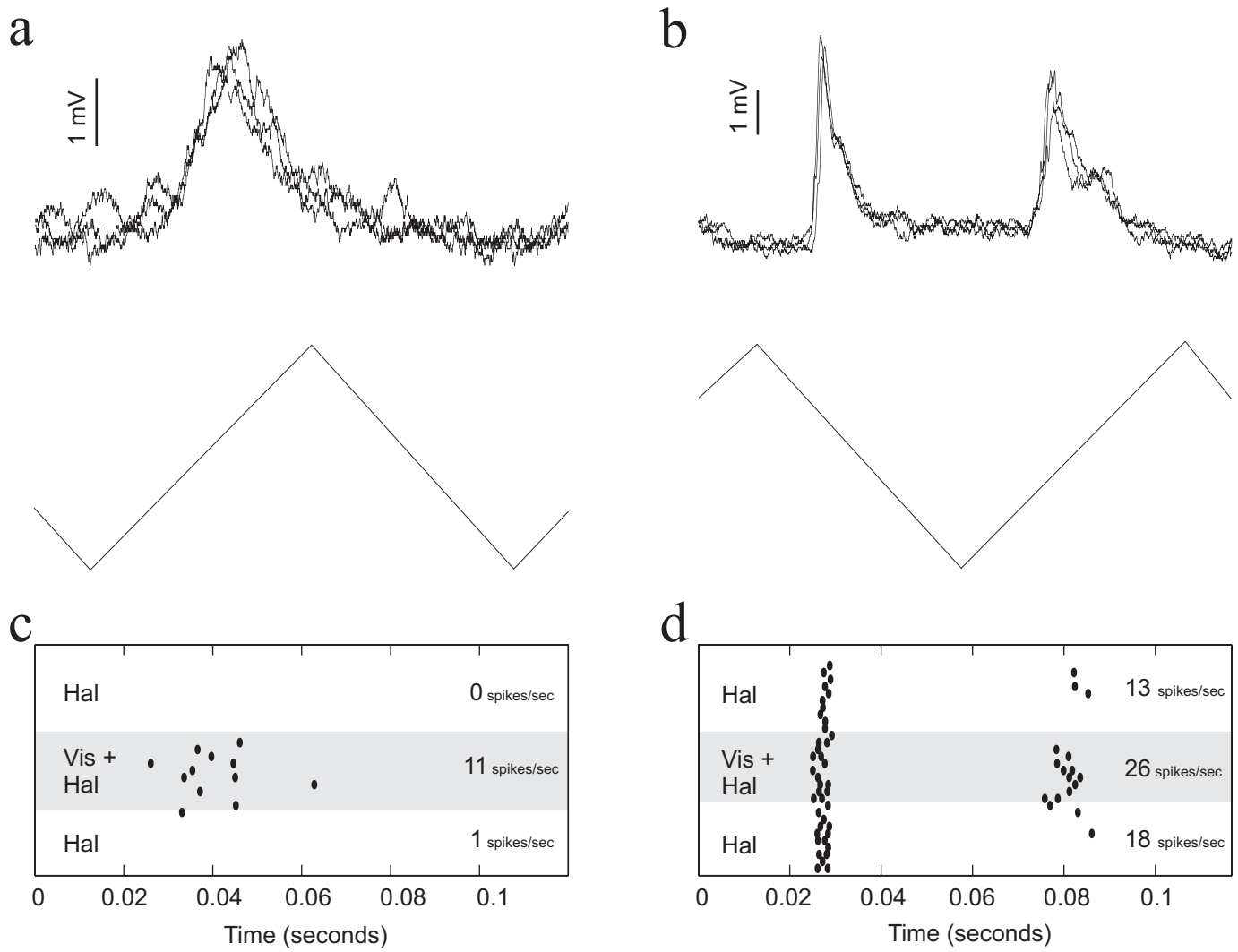


Figure 3.12 Temporal relationship between visually evoked spikes and haltere evoked compound EPSPs. Middle traces give the haltere stimulus waveforms. All panels share a common time axis.

(a) & (b) Show three overlaid examples of compound EPSPs evoked from two different type II NMNs by 10.5 Hz stimulation of the preferred haltere (contralateral in the case of (a), ipsilateral in the case of (b)).

(c) Shows a raster plot of the spikes evoked from the same cell as in (a), (d) shows the same thing for the cell in (b). The grey segment indicates the time period during which there was a 10.5 Hz haltere stimulus combined with visual motion in the cell's preferred direction (rightwards for (c), diagonally up and to the right for (d)). The white segments indicate the time periods before and after the visual stimulus (top and bottom respectively) where only the haltere stimulus was presented. The numbers on the raster plots give the spike frequency during each one-second segment of the stimulus.

sub-threshold visual input is responsible for the visual modulation of the spiking output seen during haltere stimulation.

The manner in which the spike rate increases when a moving grating is presented during haltere stimulation is dependent on the nature of the haltere-stimulus-induced compound EPSPs in a particular NMN. Some cells responded to vertical oscillation of a haltere with one compound EPSP per haltere stimulus cycle, as in figure 3.12a, whereas others would respond with two compound EPSPs each stimulus cycle, one on the haltere down stroke and one on the upstroke, as in figure 3.12b. In both cases, the extra action potentials induced by visual stimuli would occur at the same point in the haltere stimulus cycle as the compound EPSPs. In this manner visual stimuli could induce extra action potentials at one (3.12c) or two (3.12d) points in the haltere cycle depending on how many compound EPSPs the cell normally produced in response to haltere stimulation.

3.4.2.4 Responses to 105 Hz haltere stimuli and visual stimuli combined

All the experiments described so far have used a haltere stimulus that oscillated vertically at a frequency of 10.5 Hz, approximately ten times slower than the frequency at which female blowflies beat their halteres during flight (105-120 Hz Pringle (1948)). Experiments were performed with a haltere stimulus oscillating at a frequency of 105 Hz to see if the effects observed at lower frequencies are still present at the frequency range seen during fly flight. These experiments showed that all the effects seen with a 10.5 Hz haltere stimulus were also seen with a 105 Hz haltere stimulus.

As with 10.5 Hz haltere stimulation, 105 Hz haltere stimulation produced phase locked compound EPSPs and action potentials. Moving visual gratings could modulate the number of compound EPSPs that resulted in spikes, as seen in figure 3.13b. This visual modulation of haltere induced spiking output enabled the visual inputs to affect the spike rate of type II cells (figure 3.13b), something that they could not do without haltere stimulation (figure 3.13a). Visual modulation of the number of haltere-induced action potentials was dependent on the direction of the visual grating used (figure 3.13: response to preferred direction motion, figure 3.14: response to the opposite direction of motion, figure 3.11c: tuning curve). The peak of a NMNs sub-threshold directional visual tuning curve matched the peak of the same NMNs

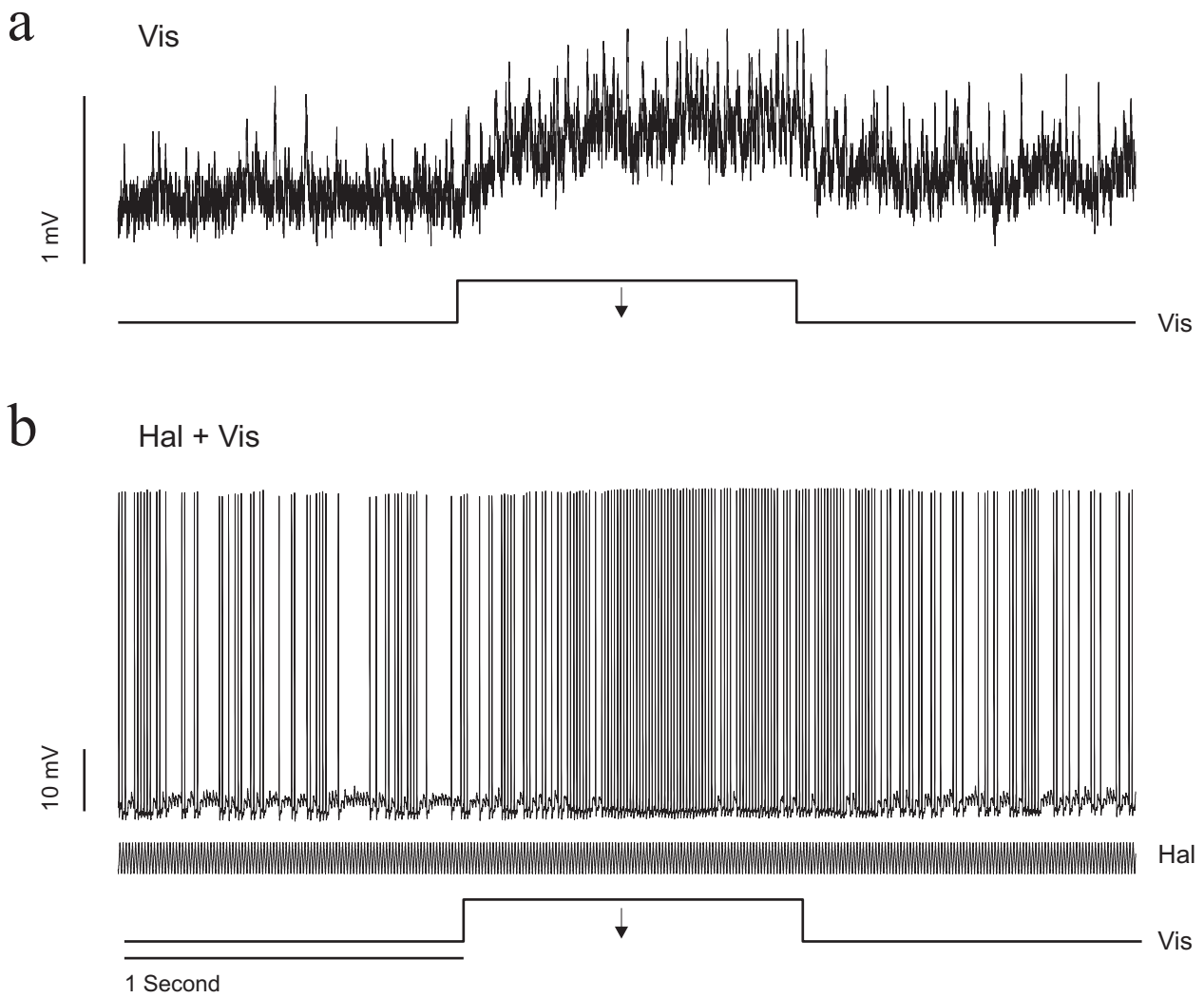


Figure 3.13 Response of a type II NMN to motion in the unit's preferred direction (downwards) with (b) and without (a) simultaneous 105Hz haltere stimulation. In (a) the bottom trace gives the period of the visual stimulus, in (b) the bottom two traces indicate the visual and haltere stimulus waveforms.

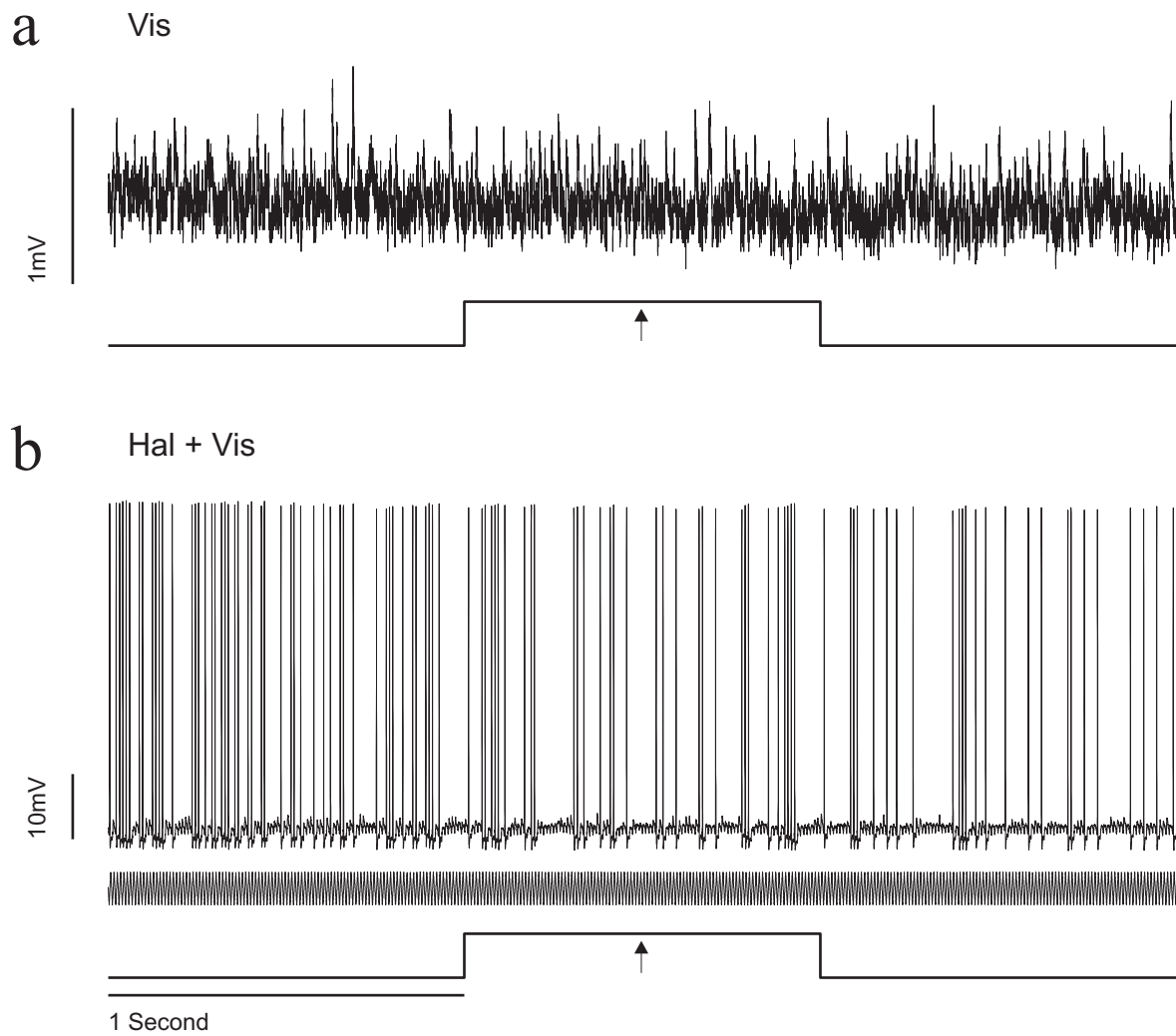


Figure 3.14 Response of the same type II NMN as in 3.13 to motion in the unit's anti-preferred direction (upwards) with (b) and without (a) simultaneous 105Hz haltere stimulation. In (a) the bottom trace gives the period of the visual stimulus, in (b) the bottom two traces indicate the visual and haltere stimulus waveforms

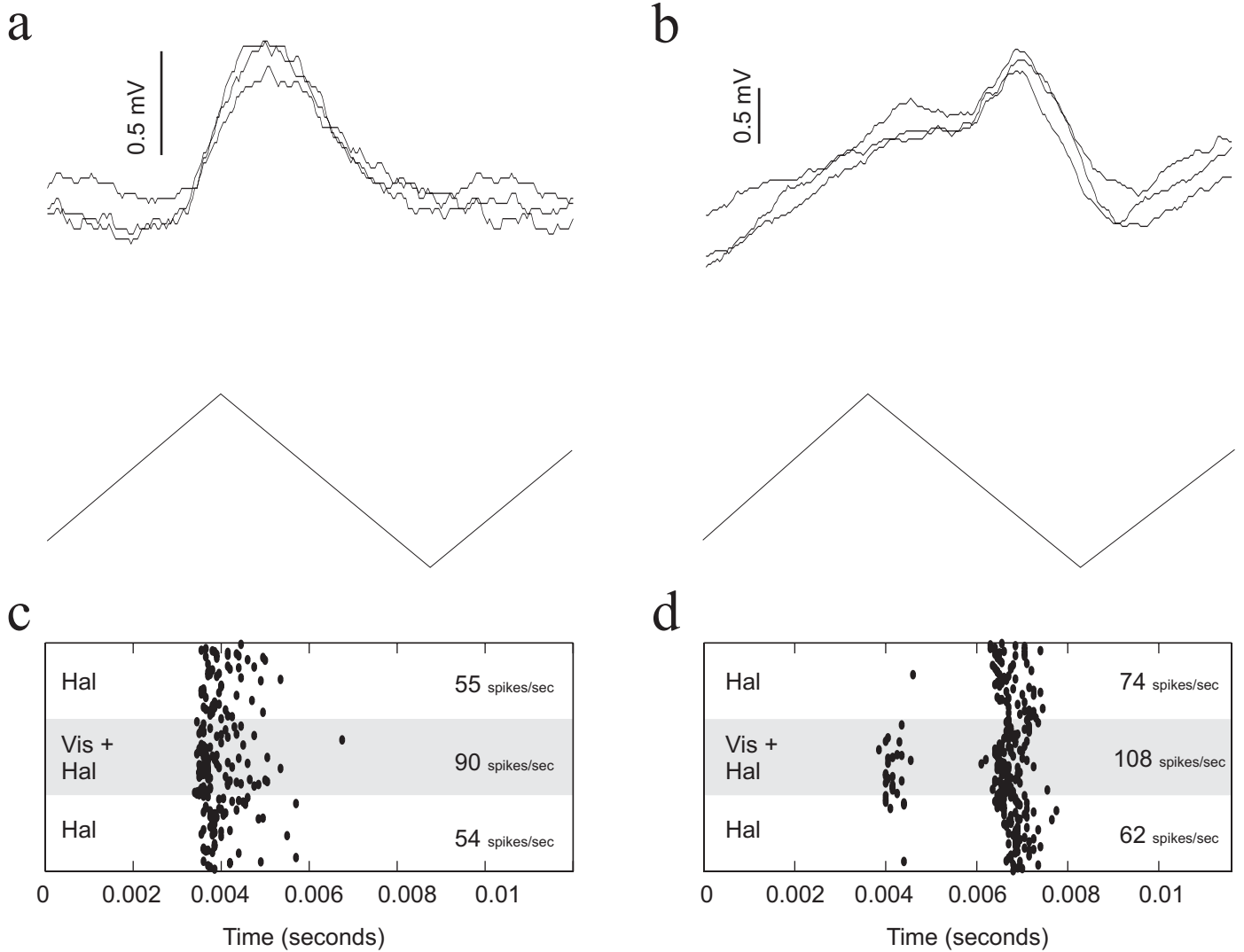


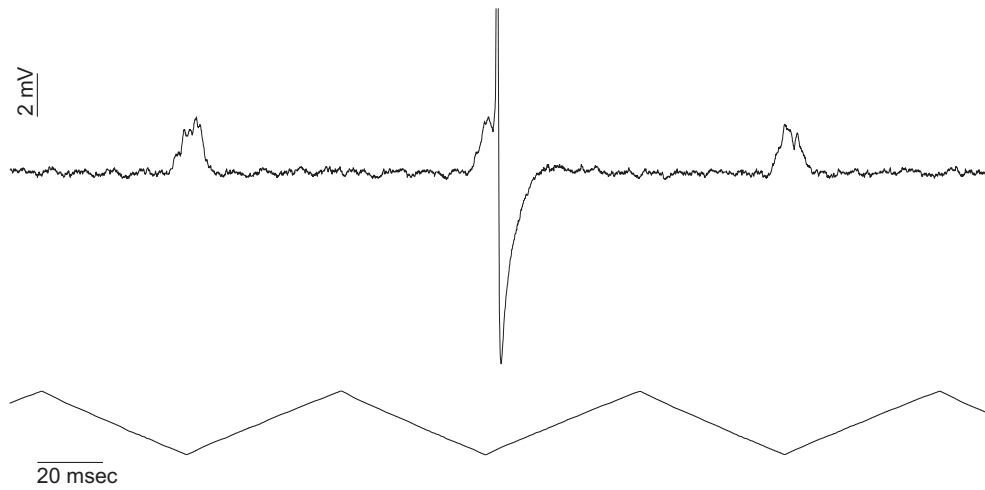
Figure 3.15 Temporal relationship between visually evoked spikes and 105 Hz haltere stimulus evoked compound EPSPs. Middle traces give the haltere stimulus waveforms. All panels share a common time axis. (a) and (b) show three overlaid examples of compound EPSPs evoked in two different type II NMNs by 105 Hz stimulation of the preferred haltere (ipsilateral for both cells). (c) and (d) show raster plots of the spikes evoked from the same cells as in (a) and (b) respectively. The grey segment indicates the time period during which there was a 105 Hz haltere stimulus combined with visual motion in the cell's preferred direction (downwards for both cells). The white segments indicate the time periods before and after the visual stimulus (top and bottom respectively) where only the haltere stimulus was presented. The numbers on the raster plots give the spike frequency during each one-second segment of the stimulus.

directional visual tuning curve derived from spike rate during simultaneous haltere and visual stimulation (figures 3.11c and 3.11d). As with the 10.5 Hz experiments, this correlation between the directional tuning of the visual input and that of the spiking output suggests that the sub-threshold visual input is responsible for the visual modulation of spike rate seen in the combined haltere and vision experiments.

As in the 10.5 Hz experiments the way in which spike rate increased when a visual stimulus was presented in addition to a haltere stimulus depended on the shape of the haltere induced compound EPSP. Figure 3.15a shows an example in which the haltere induced compound EPSP is one humped. In this case the extra spikes induced by adding a moving visual grating to the haltere stimulus occur at only one phase (figure 3.15c), that of the EPSP hump. In a different cell (figure 3.15b), the haltere induced compound EPSP is two-humped, and the extra spikes induced by a visual stimulus during haltere stimulation can occur at the phase of either compound EPSP 'hump' (figure 3.15d).

From the widths of the compound EPSPs obtained during 10.5 Hz haltere stimulation it is surprising that there are still haltere stimulus phase locked events occurring during 105 Hz haltere stimulation. The compound EPSPs resulting from 10.5 Hz haltere stimulation are wide enough that if they occurred at ten times the frequency they would overlap, smoothing out any phase locking of the response (figure 3.16a). However, if the haltere is oscillated at 105 Hz, phase-locked compound EPSPs are still seen (figure 3.16b). To maintain the phase-locked nature of the response, the shape of the compound EPSPs must sharpen at higher stimulation frequencies. Figure 3.17, taken from a different unit, shows that the compound EPSPs do sharpen when the haltere stimulus is moving at a faster rate. The NMN in figure 3.17 was not presented with an oscillating haltere stimulus, but with a 'ramp and hold' haltere stimulus. The haltere was held in a low position, and then moved upwards to a high position where it was held. Two ramp and hold haltere stimuli were used. In one the speed of movement in the ramp transition between low and high positions was set equal to the speed of movement during the 10.5 Hz oscillating stimulus. In the other ramp and hold stimulus the ramp portion's speed was set equal to that of the 105 Hz oscillating stimulus. The compound EPSP elicited during the fast ramp and hold stimulus (figure 3.17b and c, red) was much sharper than that elicited during the slow ramp and hold stimulus (figure 3.17a and c, blue). The

a



b

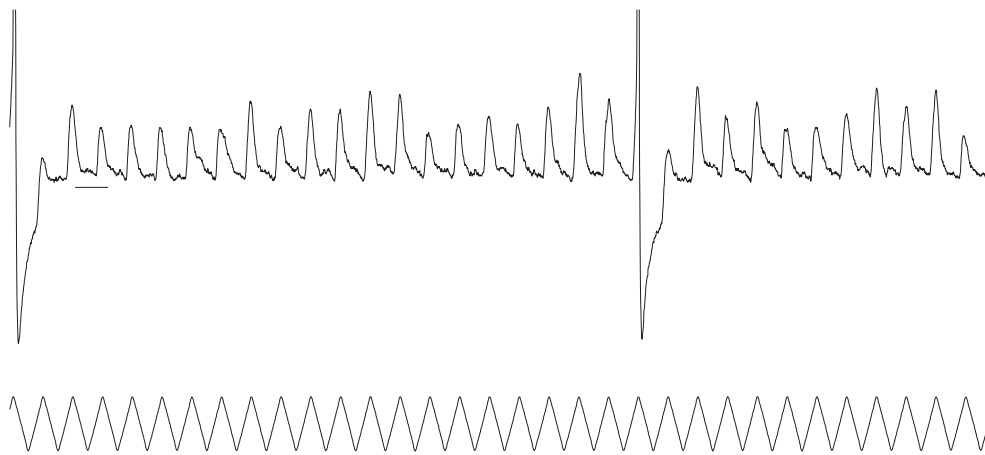


Figure 3.16 Compound EPSP response of a type II NMN to 10.5 (a) and 105 Hz (b) preferred haltere (ipsilateral) stimulation. In both figures the bottom trace gives the haltere stimulus waveform. The horizontal line in (b) indicates the cell's recorded resting membrane potential. Both panels share the same scale bars. The peaks of the action potentials are clipped to allow a high magnification view of the sub-threshold events.

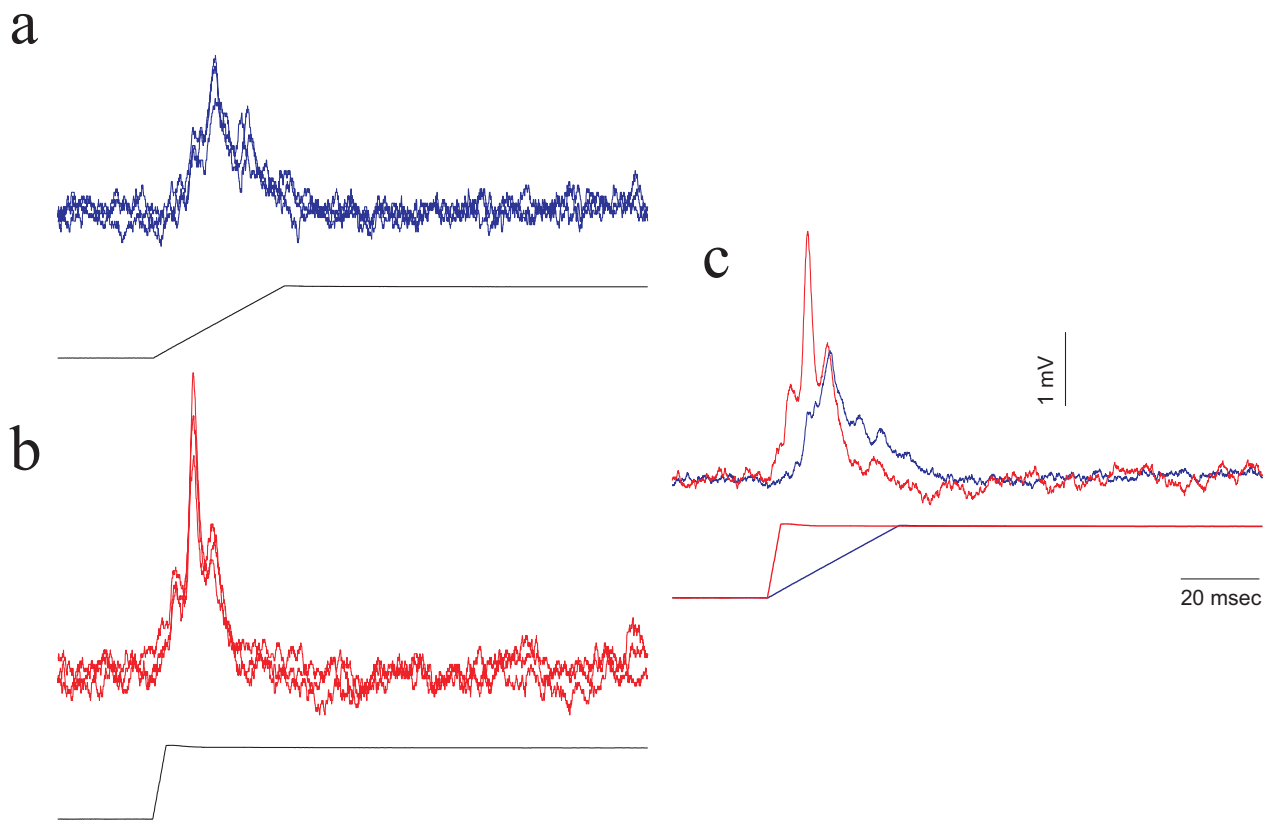


Figure 3.17 Sharpening of a type II NMN's haltere stimulus induced compound EPSPs with faster movement of the preferred haltere (contralateral) during ramp and hold stimuli. In all panels the bottom trace gives the haltere stimulus waveform:

(a) Compound EPSP response to a 'ramp and hold' stimulus applied to the contralateral haltere. The vertical upward 'ramp' portion of the stimulus was the same speed as that during the upwards component of the 10.5 Hz triangle waveform haltere stimulus used elsewhere in this study.

(b) Compound EPSP response to a 'ramp and hold' stimulus applied to the contralateral haltere. The vertical upward 'ramp' portion of the stimulus was the same speed as that during the upwards component of the 105 Hz triangle waveform haltere stimulus used elsewhere in this study.

(c) Average compound EPSP waveforms (n=8) in response to the fast (red) and slow (blue) ramp and hold haltere stimuli.

sharpening of the compound EPSP would be sufficient to allow distinguishable phase-locked responses during a 105 Hz haltere stimulus, as seen in figure 3.16b.

3.4.2.4 Responses of units that spike in response to vision alone

As in the extracellular experiments, type I NMNs fired action potentials in response to the visual stimulus alone (figure 3.18a). Intracellular recordings were made from 10 NMNs of this type. Like the type II NMNs, these cells had a ‘preferred haltere’, stimulation of which would induce phase locked action potentials (fig 3.18b, first second of response), this haltere could be either ipsilateral or contralateral depending on the NMN. As in the extracellular experiments, the presence of a haltere stimulus did not shift the peak of the directional visual tuning curve (figure 3.18c), but in some cases increased its amplitude. The haltere stimulation entrained the visually evoked spikes to make them phase-locked to the cycle of haltere movement. In figures 3.18a and b, an example of this entrainment can be seen: the visual stimulus on its own (figure 3.18a) induces action potentials, but when the haltere stimulus is applied, all visually induced action potentials occur within a 35 millisecond window of the 95 millisecond haltere stimulus cycle (figure 3.18b).

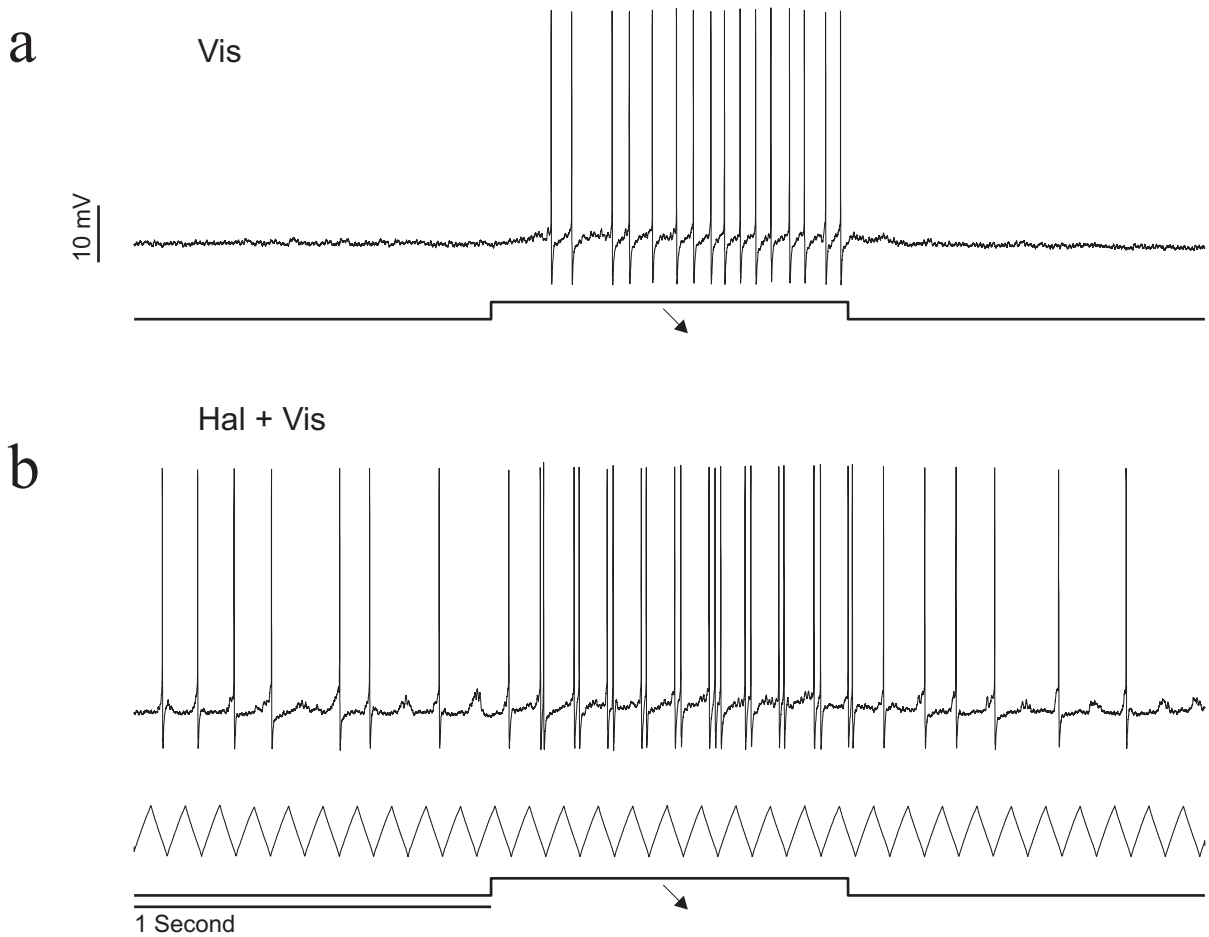
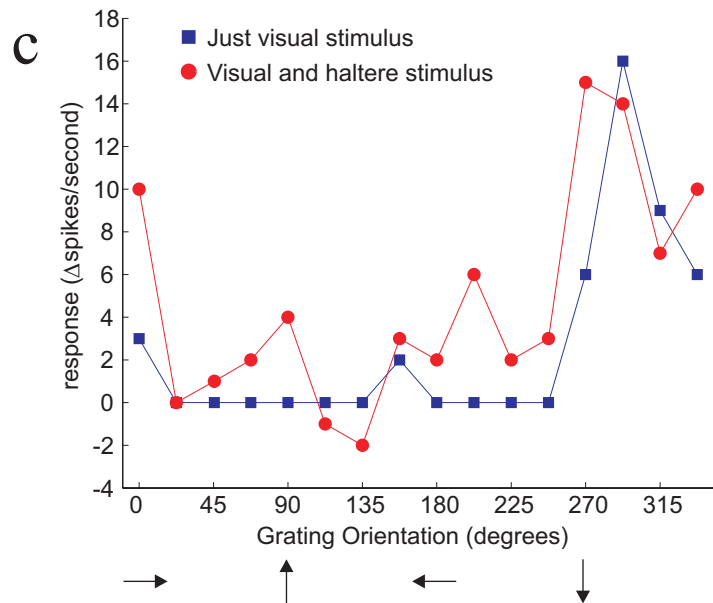


Figure 3.18 Entrainment of a type I NMN's visually induced spikes by a 10.5 Hz haltere stimulus:

(a) Response to a moving visual grating in the NMN's preferred direction (diagonally downwards/rightwards). Bottom trace gives the period of the visual stimulus.

(b) Response to combined visual stimulation in the NMN's preferred direction and 10.5 Hz haltere stimulation. Bottom two traces indicate the visual and haltere stimulus waveforms.

(c) The directional visual tuning curve of the type I NMN obtained during just visual (blue squares) and combined visual and haltere stimulation (red circles).



3.5 Discussion

The way in which fly Neck Motor Neurons (NMNs) integrate inputs from two different senses was studied. NMN responses to visual and haltere stimulation were compared, both individually and combined. It was found that some NMNs will only fire action potentials in response to visual inputs if there is concurrent haltere stimulation. Intracellular recordings suggest that this gating of visual input by haltere input is due to neural summation and the non-linearity of action potential generation.

3.5.1 Gating of visual responses by haltere input

The term *gating* is used in different ways by different authors. The term is either used to refer to a class of sub-threshold and synaptic mechanisms, such as presynaptic inhibition or postsynaptic shunting inhibition, that determine whether or not a synaptic input is effective (Katz, 2003) or as a phenomenological description of the way a neuron's spiking output behaves (Reichert, 1985; Reichert and Rowell, 1986). Here the term is used in the phenomenological sense of Reichert et al. (1985). Gating is defined here as one sensory input influencing the action potential output of a neuron only if a certain condition is met, such as the presence of a specific motor pattern or a different sensory input.

Motor pattern dependent gating of sensory inputs has been seen in various systems. Some cricket descending neurons respond to visual motion and artificial conspecific calling songs when the cricket is walking but not when it is standing (Staudacher and Schildberger, 1998; Staudacher, 2001). Some locust sensory descending neurons can only affect the spiking outputs of pre-motor interneurons when the flight central pattern generator is active (Reichert and Rowell, 1985; Reichert, 1985). Rare examples of the gating of one sensory input by another are also known, but are less well characterised. One example is seen in the fly contralateral giant mimetic descending neuron where wind stimuli alone will not induce action potentials but combined wind and visual stimuli can (Milde and Strausfeld, 1990).

The experiments in this study are the first to ever present NMNs with combined haltere and visual stimuli. They are also the first set of experiments to ever present NMNs with controlled haltere stimuli. The data show that for type II NMNs the visual stimuli used were unable to alter the spiking output of the neurons unless a haltere was simultaneously stimulated. In other words, the effect of visual input on the output of these NMNs is permissively gated by the haltere input. Conversely, the results can be equally well thought of as an enhancement of the NMN response to haltere movement by visual inputs.

Due to only a sub-population of NMNs spiking in response to visual stimuli, only a few of the NMNs were previously known to receive visual input (Milde et al., 1987). Here it has been shown that all NMNs of the FN recorded from have visual inputs. This provides an ideal opportunity for further studies to treat the NMNs as a model system for investigating the nature and mechanism of one sensory input gating another sensory input's effect in a comparatively simple nervous system where the sensory inputs have been well characterised.

3.5.2 Sub-threshold response properties

This study is the first time NMN sub-threshold events have been analysed. Those few intracellular NMN recordings that have been published were only analysed for spiking activity (Milde et al., 1987). What can be inferred from the NMN subthreshold responses?

The depolarisation seen during visual stimulation is accompanied by an increase in variance of the membrane potential (see figure 3.9a). This increase in variance implies that the depolarisation is due to the addition of an excitatory synaptic input as opposed to the removal of a tonic inhibitory input. To accurately test this hypothesis would require injecting current into the NMNs. A train of brief current pulses could be injected and the resulting voltage changes observed before and during visual stimuli. If the voltage change resulting from a given amplitude of current pulse reduces during visual stimuli then, by ohms law, the membrane resistance has also reduced, implying that a synaptic input is present. The most likely source of the visual input to Frontal Nerve NMNs is from the descending neurons, which convey

visual information from the TCs to the NMNs (Gronenberg and Strausfeld, 1990; Strausfeld and Gronenberg, 1990; Gronenberg et al., 1995).

The EPSPs seen during haltere stimulation occurred at the same phase of the haltere cycle as the action potentials. Therefore, it seems highly likely that those EPSPs that crossed threshold were responsible for the action potentials. It is interesting that large sub-threshold events such as the haltere induced EPSPs can be observed in the axon, far from the dendrites. It has been shown that invertebrate neurons often have long space constants (Rall, 1981) and recordings from other insect neuron axons have shown sizable postsynaptic potentials (Milde and Strausfeld, 1990). Therefore, it is not too surprising that sub-threshold events were observed so far down the axon in this study. Although it seems highly unlikely, the possibility that the haltere-induced EPSPs were due to a pre-synaptic input cannot be completely excluded. However, no anatomy is known that could support the hypothesis that the haltere induced EPSPs are of pre-synaptic origin.

The spiking behaviour of the NMNs was the same in both the intracellular and extracellular experiments. This strongly suggests that the results seen in the intracellular recordings were not due to any experimental artefact such as the intracellular electrode making the cell more 'leaky'.

3.5.3 Functional sensory gating through a simple mechanism

The extracellular results presented in this study show that, for type II NMNs, visual inputs only affect the motor neuron output if the halteres are moving at the same time. This is a gating of visual information's effect on NMN outputs by haltere inputs. The gating seen at the level of the NMNs correlates well with behavioural observations that flies will not make gaze-stabilising head movements when their halteres are removed (Sandeman, 1980). What is the mechanism underlying this gating? It has been suggested that visual information is relayed to the neck muscles indirectly, passing through the halteres via haltere control muscles (Chan et al., 1998). This hypothesis could explain the extracellular results observed here, however it cannot explain the visually induced sub-threshold input that was seen in all NMNs recorded from intracellularly.

The most likely mechanism to explain the gating seen here is neural summation of inputs combined with the non-linearity of action potential generation. The sub-threshold visual inputs to type II NMNs had the same directional tuning as the NMNs spiking output, as seen when haltere and visual stimuli were combined. This similarity between the visual input and spiking output suggests that the sub-threshold visual inputs were responsible for the visual modulation of the spiking haltere response. It is proposed that the visually induced depolarisation results in more of the haltere induced compound EPSPs becoming suprathreshold, increasing the spike rate. In this way the haltere input to a NMN enables the sub-threshold visual input to affect the neurons spiking output and hence the activity of the neck muscles. Similar gating mechanisms resulting from neural summation are seen in both the locust (Reichert and Rowell, 1985; Reichert, 1985) and crab (Silvey and Sandeman, 1976). Evidence for summation underlying the NMN gating of visual information also comes from one recording from a NMN in another study where it was shown that this neuron did not spike in response to visual stimuli unless current was simultaneously injected into the cell (Gronenberg et al., 1995). If simple neural summation is the mechanism underlying the gating of visual responses, then other mechanosensory NMN inputs (Milde et al., 1987) may also allow visual inputs to affect the NMNs spiking output.

3.5.4 Behavioural correlates of electrophysiological results

Behavioural studies have shown that blowflies only make gaze stabilising head movements when they are flying or walking, not when immobile (Hengstenberg et al., 1986). The differences in gaze-stabilising head movements during different behavioural states have been attributed to motor pattern dependent gating (Hengstenberg, 1993). However, given the results of this study, it seems possible that the reason no visually induced head movements are seen in immobile flies is that the halteres do not beat when a fly is immobile, as they do when the fly is flying or walking. If the halteres are not beating then type II NMNs will not spike in response to their visual input and therefore will not drive the neck muscles. Many type I NMNs will also reduce their sensitivity to visual stimuli when the halteres are not

moving (figure 3.6), further reducing the visual drive to the neck muscles. Thus, the reafferent haltere input to the NMNs may be acting as an indirect monitor of the current motor state, gating the visual responses appropriately according to whether the fly is walking/flying or immobile. Further support for this hypothesis comes from a behavioural study showing that if the halteres are removed, flies no longer make gaze-stabilising head movements (Sandeman, 1980).

If, as suggested above, the reafferent haltere sensory inputs to NMNs are acting as an indirect motor-pattern-dependent gating signal, the question arises as to why the motor signal that drives the halteres is not used as the motor pattern dependent gating signal instead. The output of the halteres not only correlates with the current motor pattern, its main role is to provide information about the angular velocity of the fly during flight (Pringle, 1948; Nalbach, 1993). It is known from behavioural studies that the haltere inputs to the neck motor system are providing information about the fly's current angular velocity (Hengstenberg, 1988). If NMNs received no haltere input and the motor signal that drives the halteres was used to gate the NMNs directly, the NMNs would not receive any angular velocity information. It seems likely that the halteres are providing NMNs with information about both the current motor pattern and the current angular velocity being experienced. In this study, the halteres were oscillated in a vertical plane in an attempt to simulate the beating activity seen when there are no imposed rotations (angular velocity = 0) upon the fly. However due to limitations of the haltere stimulus used, it was not possible to ensure that inputs that are usually active during rotations of the fly were not stimulated.

Does the gating seen in the NMNs confer any behavioural advantage? The main reason for gaze-stabilising head/eye movements is to reduce the motion blur induced by whole body movements (Land, 1999). When the fly's halteres are not moving the fly is at rest, therefore it is unlikely that there will be any whole-body movements to induce motion blur. In this case it is probably advantageous for the fly not move its head because any noise in the gaze-stabilisation system would induce more motion blur than that the fly would experience if it just kept its head immobile. In addition, because type II NMNs have low spontaneous rates and large extracellular spike waveforms, they are therefore more likely to innervate fast, metabolically expensive muscles (Henneman, 1965). Not utilising these muscles when the fly is

immobile will therefore save energy, giving another advantage to the gating of the type II NMNs seen here.

3.5.5 Visually induced action potentials are phase locked to the haltere beating phase

The only way visual stimuli could induce action potentials in type II NMNs was for the visual stimulus to be co-presented with haltere stimulation. In this case, any extra action potentials induced by the visual stimulus were tightly phase locked to the haltere beating cycle. This phase locking was even seen at a haltere stimulation frequency of 105 Hz, within the range of normal haltere beating frequencies for female blowflies (Pringle, 1948). In the flying fly, the halteres beat at the same frequency but anti-phase to the wings. Presumably this means that, during flight, any visually induced action potentials in the type II NMNs will be phase-locked to the wing beat cycle. In the following section, three questions are discussed: Is this phase-locking reflected in the fly's head movements? Is it of functional significance, or is the phase locking just a consequence of the haltere input coming from an oscillating system? What is the nature of the haltere induced EPSPs?

3.5.5.1 Is the Neck Motor Neuron phase-locked activity reflected in head movements?

If the responses of neck muscles are slow enough they will low-pass filter the NMN activity, removing the phase-locked signal structure. The type II NMNs were those with low spontaneous rates and large extracellular action potential waveforms, these attributes are usually associated with motor neurons that innervate fast muscle fibres (Henneman, 1965). If the type II NMNs do innervate fast muscles, those muscles might be fast enough to follow the phase-locked NMN spiking activity. In simultaneous recordings of locust fast neck motor neurons and head torque, it was possible to correlate single neck motor neuron spikes with individual head twitches (Kien, 1977). Furthermore, the force output of a fly flight steering muscle is known not to reach full tetanus at spike rates up to 150 Hz (Heide, 1983; Tu and Dickinson,

1994). So it is conceivable that neck muscle outputs may follow their phase-locked inputs, this issue requires behavioural experiments to be answered conclusively.

The other requirement for the phase-locked activity seen in NMNs to be reflected in head movements is that the phase of firing is not randomly distributed across the NMN population. If all the NMNs fire at the same point in the haltere cycle, the neck muscles will receive synchronous inputs and head movements will be phase-locked. If each NMN spikes at a different point in the haltere cycle, there will be no synchronous activity across the NMN or neck muscle population and head movements will be smooth. Figure 3.8c shows that the distribution of phases across the NMN population lies between these two extremes. Those NMNs that fire during the haltere upstroke do so at very similar phases of the haltere cycle whereas those NMNs that fire during the haltere down stroke fire at very different phases (fig 3.8c). Thus, from the available data, it is uncertain whether head movements are phase-locked to the haltere beating cycle. Again, behavioural experiments are required to resolve this issue.

3.5.5.2 Is the Neck Motor Neuron phase-locked activity of functional significance?

Gating of sensory inputs in a manner that is phase locked to a motor rhythm has been observed in several systems. In the locust, sensory signals conveyed by descending neurons cause pre-motor interneurons to spike only at certain phases of the flight rhythm (Reichert and Rowell, 1985; Reichert, 1985). In *Xenopus* embryos, skin stimulation produces sensory interneuron action potentials only during phases in the swim cycle where activity in the interneuron's motor neuron targets would result in swimming away from the stimulus (Sillar and Roberts, 1988). During flight, fly steering muscles spike during turns elicited by visual stimuli, and do so in a manner phase-locked to the wing beat cycle (Heide, 1983). In all these examples, the phase-locked nature of the sensory gating makes functional sense because the output system is a rhythmic motor system and thus its reaction depends on the phase of the input. Our current knowledge of the neck motor system suggests that it is not a rhythmic motor system and that head movements are occurring on a slower time scale than the wing beat cycle. In this case, it is difficult to imagine what functional use the haltere cycle phase-locked gating of visual inputs has. It may be that the phase-locked nature

of the gating has no functional importance and is just a consequence of the haltere system's outputs being highly rhythmic. On the other hand, small pitch oscillations of the fly head at the wing-beat frequency have been observed in free flight (van Hateren and Schilstra, 1999). It may be advantageous to make head movements at a certain phase of these head oscillations in order to minimise motion blur. In this case, the phase-locking of visually induced NMN spikes would have a functional role. Again, further behavioural experiments are necessary to determine whether the phase-locking of NMN visually-induced spikes has any functional significance.

3.5.5.3 Nature of the haltere cycle phase-locked EPSPs

The NMNs display compound EPSPs whose timing is tightly locked to the phase of haltere oscillation. It is highly likely that it is the timing of these compound EPSPs that results in the phase-locked nature of NMN action potentials. Comparing intracellular results from 10.5 and 105 Hz haltere stimulation (figures 3.16 and 3.17) shows that compound EPSPs were considerably sharpened when the haltere was moved at a high velocity, accounting for the fact that phase-locked activity remains even at high stimulation frequencies. A limitation of this study is that the intracellular recordings were taken from the NMN axons, which makes it difficult to ascertain the exact nature of the compound EPSPs. To determine the mechanism underlying the sharpening of EPSPs at fast speeds of haltere movement would require intracellular recordings from NMN dendrites.

There are several non-exclusive explanations that could account for the sharpening of the compound EPSP at higher speeds of haltere movement. The sharpening could simply be due to the barrage of haltere inputs arriving closer together due to the same haltere movement occurring in a shorter period of time. The sharpening of the EPSP may also reflect boosting of the haltere input by non-linear dendritic processes (Laurent et al., 1993) or the addition of an electrical haltere input on top of the normal haltere induced compound EPSP, as is seen in one of the blowfly flight motor neurons (Fayyazuddin and Dickinson, 1996).

3.5.5.4 Predictions for behaviour

The results obtained here suggest the following model of visually induced head movements. When the fly is flying straight, the sensory inputs from its beating halteres result in phase locked spikes in the NMNs. For each beat of the halteres, any given NMN has a chance to fire a spike. In the absence of any other sensory inputs, the ratio of NMN spikes to number of haltere beats will remain approximately equal for equivalent NMNs on either side of the body. The neck muscles on either side of the fly will therefore exert equivalent force, maintaining a fixed head position. If the fly then rotates, the resulting optic flow will excite some NMNs more than others, depending on the NMNs' preferred directions of motion. As a consequence NMNs on one side of the body will fire more spikes over a given number of haltere beats than the equivalent NMNs on the other side of the body. The neck muscles on different sides of the body will therefore generate unmatched forces, and the fly's head will move with the direction of visual motion (Gilbert et al., 1995), maintaining a fixed gaze.

The results presented here predict that if the halteres of a fly in tethered flight were prevented from moving, the amplitude of visually induced head movements would significantly decrease. If the halteres were prevented from moving then the visual inputs to type II NMNs would not result in action potential outputs, and type I NMNs would respond to visual stimuli with fewer spikes. In this case, the neck muscles would receive significantly reduced visual drive, and the visually induced head movements would therefore decrease in amplitude.

In conclusion, it has been found that type II NMN visual inputs can only affect the spiking output of the NMNs if the halteres are simultaneously moving. This gating of visual information by haltere inputs correlates well with behavioural results. Evidence from intracellular recordings suggests that this gating is the result of subthreshold visual inputs summing with haltere compound EPSPs resulting in more of the EPSPs becoming suprathreshold and thus raising the NMN's spike rate. In such a manner, a simple neuronal mechanism may be able to explain apparently complex behavioural features such as the context dependent effect of a visual stimulus.

4. Discussion

The work presented in this dissertation investigates how outputs of the fly's visual system are utilised by the neck motor system. Of particular interest is the relationship between the way in which information is extracted by the visual system and the way in which it is used by the motor system.

4.1 Visual and motor coordinate systems

The experiments presented in chapter two showed that individual Neck Motor Neurons (NMNs) have similar visual receptive fields, and thus similar preferred axes of self-rotation, to those of Tangential Cells (TCs). In other words, the visual system and neck motor system use the same coordinate system to process rotational optic flow. This alignment between sensory and motor systems considerably simplifies the sensory motor transformation and hence the neural circuitry required.

The alignment between TCs and NMNs explains a previously puzzling feature of the TC coordinate system. The axes of rotational optic flow to which TCs respond are not equally distributed across the population. An equal distribution would be expected if the TC coordinate system was optimised to reduce redundancy in its encoding of visual inputs. From the results presented in chapter two, however, we see that the non-equal spacing of TC axes results from an alignment with the motor system. Thus, the visual system is not simply optimised to efficiently encode information, but it is also adapted to make it easier for a motor system to extract this information. This principle is further illustrated by the matching between compound eye geometry and NMN receptive field structure; two points at opposite ends of the visuo-motor circuit.

The visual system TCs extract optic flow information in a manner already aligned with the requirements of the motor system. Thus, a significant portion of the visuo-motor transformation is already occurring at the TCs. Much is already known about the TCs. Therefore, a significant amount is already known about the visuo-motor transformation.

4.1.1 Choice of coordinate systems

As discussed in chapter one, two general strategies have been observed in sensory-motor systems. The first has been described in systems where sensory information is encoded over a population of neurons. It has been suggested that in these systems, the transformation from sensory to motor coordinates occurs via an intermediate orthogonal coordinate system (Masino and Knudsen, 1990). In simple reflex arcs however, the sensory apparatus is often pre-aligned with the requirements of the motor system. This alignment removes the requirement for a coordinate based transformation. The results presented in chapter two of this dissertation show that the TC-NMN sensory-motor circuit adopts a similar strategy of pre-aligning its sensory coordinates with the requirements of the motor system. The TC population however is not part of a simple reflex arc; it encodes sensory information over a population of neurons and sends outputs to multiple motor systems. Therefore, the strategy of sensory-motor alignment is not used exclusively by simple reflex arcs.

What then determines whether a sensory-motor circuit uses the strategy of sensory-motor alignment or the strategy of a sensory-motor transformation via an orthogonal coordinate system? An intermediate orthogonal coordinate system is convenient for transforming between different non-orthogonal coordinate systems. Therefore, an orthogonal intermediate would be advantageous in a situation where sensory inputs with different coordinate systems needed to be combined or outputs needed to be made to motor systems with different coordinate systems. However, the use of an orthogonal coordinate system between sensory and motor systems necessitates an extra layer in the sensory-motor circuit. The strategy of having non-aligned coordinate systems, and using an orthogonal intermediate to translate between the two, allows for more flexibility in the choice of coordinate systems. Yet, this flexibility comes at the cost of extra processing. In contrast, a strategy of aligning the sensory and motor coordinate systems allows for a simple circuit. It thus seems likely that, if possible, sensory-motor circuits will use the strategy of alignment. Still, if it is not possible to align the sensory and motor systems an orthogonal intermediate may be used.

In what situations is it not possible to align the sensory and motor coordinate systems, necessitating the use of an orthogonal intermediate? The sensory or motor coordinate systems may be constrained by the physical structure of the sense organ or

the pulling planes of the muscles. If such constraints result in a misalignment between sensory and motor coordinate systems, then an orthogonal intermediate may be required. Often the frame of reference of a sensory system will move with respect to the motor system or that of another sensory system. For example, in animals with eyes that are not fixed to the head, the retina can move with respect to the neck motor system. In such a system it is impossible to pre-align the sensory and motor coordinates as the relationship between the two is continually changing. Thus, an orthogonal intermediate coordinate system may be required between the sensory and motor system to facilitate the constantly changing visuo-motor transform.

In summary, it is suggested that sensory-motor circuits will align their sensory and motor coordinate systems whenever possible. This strategy simplifies the neural processing required. In many situations, however, such an alignment is not possible and an intermediate orthogonal coordinate system is used. This intermediate facilitates the transformation from sensory to motor coordinates. To test this hypothesis would require a comparative study where the coordinate transform strategies used in different sensory-motor circuits were correlated with the constraints operating upon the circuit's sensory and motor coordinate systems.

4.2 A qualitative model of the visual contribution to gaze-stabilisation

Taking the results of chapters two and three together with the literature, a general picture can be painted of how TCs contribute to the gaze-stabilisation system. Each TC integrates local motion information (e.g. Hausen (1984) and Egelhaaf & Borst (1993)) in such a way as to tune itself to the optic flow resulting from self-rotation about a specific axis (Krapp, 2000). The axis of self-rotation detected by each TC is roughly aligned with the requirements of a certain sub-set of NMNs (chapter two). NMNs probably receive inputs from those TCs with preferred axes of rotation appropriate to that required by the NMN (section 2.4.3). NMNs also integrate such TC inputs from either side of the brain, thus extending their receptive field and increasing the reliability with which they can estimate the axis of self-rotation. The spiking response of NMNs to their visual input is either low or non-existent unless the halteres are simultaneously beating (chapter three). In other words,

the overall gain of the neck motor system to TC inputs is low unless the fly is walking or flying, behaviours where the halteres beat.

If the halteres are beating then each NMN and its symmetrically opposite ‘twin’ on the other side of the fly will have an equal probability of firing at a particular point in the haltere cycle (chapter three). The ratio of spikes to haltere cycles will therefore be approximately equal between each NMN and its twin. If however, rotational optic flow is detected about one of the NMNs’ preferred axes, then the NMN will be more likely to fire during each haltere cycle. The resulting difference in the spike rate between the NMN and its twin will translate into a difference in muscle tension in equivalent muscles on either side of the fly. This difference in muscle tension will produce a head movement that follows the direction of visual motion (Gilbert et al., 1995), keeping the fly’s direction of gaze constant.

4.3 Suggested further experiments

The results of this dissertation have presented the opportunity for a variety of further studies. The general structure of the neck motor coordinate system has been described here. However, this description was based on extracellular recordings from unidentified cells. Performing intracellular recordings would enable the preferred self-rotation axes to be obtained for identified NMNs in the same way they were for identified TCs (Krapp, 2000; Karmeier et al., 2003, 2005). Such data would allow a more rigorous comparison of the visual and neck motor coordinate systems. The general pattern of TC-NMN connectivity was inferred from NMN receptive field structures. To confirm these inferences would require paired TC and NMN intracellular recordings.

Here the TC coordinate system has been compared to the coordinate system described by the NMN visual responses. It is important to compare these results to the coordinate system described by the actual neck muscle pulling planes. The neck muscle pulling planes have so far only been estimated from anatomy (Strausfeld et al., 1987). Further experiments are necessary to quantify the pulling planes.

Is the entire gaze stabilisation circuit aligned across all sensory and motor systems? To answer this question requires a comparison of this dissertation’s results to the coordinate systems of other motor and sensory systems in the fly. The

coordinate system used by the halteres to detect self-rotations has already been described by Nalbach (1994) and bears a striking similarity to that used by the NMNs.

The haltere stimulus used in chapter three approximately simulated the haltere movements seen during straight flight. The main role of the halteres, however, is to detect self-rotation (Pringle, 1948; Nalbach, 1993). If a more controlled haltere stimulus could be developed, it would be very interesting to investigate how NMNs integrate the haltere and visual responses to self-rotations. Finally, behavioural experiments could determine whether the haltere cycle phase-locked activity in NMNs translates into phase locked head movements or whether the phase-locking is smoothed out by the low-pass filter properties of neck muscles.

4.4 Conclusions

Over the past four decades the visual responses of TCs have been extensively studied. However, it is only by considering the properties of a motor system that we have started to understand certain aspects of TC function. There was an apparent discrepancy between the fact that TCs will respond to visual stimuli when the fly is not moving and the fact that flies will not make visually guided head movements under the same conditions (Hengstenberg, 1991; Hengstenberg, 1993). These two facts are linked by the observation that, in many cases, TC inputs only get through to the neck muscles if the halteres are moving concurrently, as they do in walking or flight. The unequally spaced coordinate system of the TC population was also puzzling, until the motor coordinate system was considered as well; revealing an alignment between the two systems. Thus, it is important to study sensory systems in the context of the motor systems that receive their output.

5. Bibliography

- Barlow HB (1961) Possible principles underlying the transmission of sensory messages. In: *Sensory Communication* (Rosenblith WA, ed), pp 217-234. Cambridge, MA: MIT Press.
- Borst A, Haag J (2002) Neural networks in the cockpit of the fly. *J Comp Physiol A Neuroethol Sens Neural Behav Physiol* 188:419-437.
- Buchner E (1976) Elementary Movement Detectors in an Insect Visual-System. *Biological Cybernetics* 24:85-101.
- Buschges A, Wolf H (1999) Phase-dependent presynaptic modulation of mechanosensory signals in the locust flight system. *J Neurophysiol* 81:959-962.
- Chan WP, Prete F, Dickinson MH (1998) Visual input to the efferent control system of a fly's "gyroscope". *Science* 280:289-292.
- Dahmen H, Franz M, Krapp H (2001) Extracting Egomotion from Optic Flow: Limits of Accuracy and Neural Matched Filters. In: *Motion Vision - Computational, Neural, and Ecological Constraints* (Zanker JZ, J., ed). Berlin: Springer Verlag.
- Eccles JC, Fatt P, Koketsu K (1954) Cholinergic and inhibitory synapses in a pathway from motor-axon collaterals to motoneurons. *J Physiol* 126:524-562.
- Egelhaaf M, Borst A (1993) Movement detection in arthropods. In: *Visual Motion and Its Role in the Stabilization of Gaze* (Miles FW, J., ed): Elsevier.
- Egelhaaf M, Kern R, Krapp HG, Kretzberg J, Kurtz R, Warzecha AK (2002) Neural encoding of behaviourally relevant visual-motion information in the fly. *Trends Neurosci* 25:96-102.
- Fayyazuddin A, Dickinson MH (1996) Haltere afferents provide direct, electrotonic input to a steering motor neuron in the blowfly, *Calliphora*. *J Neurosci* 16:5225-5232.
- Fernandez C, Goldberg JM (1971) Physiology of peripheral neurons innervating semicircular canals of the squirrel monkey. II. Response to sinusoidal stimulation and dynamics of peripheral vestibular system. *J Neurophysiol* 34:661-675.

- Franceschini N (1975) Sampling of the visual environment by the compound eye of the fly: fundamentals and applications. In: Photoreceptor Optics (Snyder AW, Menzel R, eds), pp 98-125. New York: Springer.
- Franz MO, Krapp HG (2000) Wide-field, motion-sensitive neurons and matched filters for optic flow fields. *Biol Cybern* 83:185-197.
- Frost BJ, Wylie DR (2000) A common frame of reference for the analysis of optic flow and vestibular information. *Int Rev Neurobiol* 44:121-140.
- Geiger G, Nassel DR (1981) Visual orientation behaviour of flies after selective laser beam ablation of interneurons. *Nature* 293:398-399.
- Gilbert C, Gronenberg W, Strausfeld NJ (1995) Oculomotor control in calliphorid flies: head movements during activation and inhibition of neck motor neurons corroborate neuroanatomical predictions. *J Comp Neurol* 361:285-297.
- Graf W, Simpson JJ, Leonard CS (1988) Spatial organization of visual messages of the rabbit's cerebellar flocculus. II. Complex and simple spike responses of Purkinje cells. *J Neurophysiol* 60:2091-2121.
- Gronenberg W, Strausfeld NJ (1990) Descending neurons supplying the neck and flight motor of Diptera: physiological and anatomical characteristics. *J Comp Neurol* 302:973-991.
- Gronenberg W, Milde JJ, Strausfeld NJ (1995) Oculomotor control in calliphorid flies: organization of descending neurons to neck motor neurons responding to visual stimuli. *J Comp Neurol* 361:267-284.
- Haag J, Borst A (2004) Neural mechanism underlying complex receptive field properties of motion-sensitive interneurons. *Nat Neurosci* 7:628-634.
- Hausen K (1982) Motion sensitive interneurons in the optomotor system of the fly. I. The horizontal cells: structure and signals. *Biol Cybern* 45:143-156.
- Hausen K (1984) The lobula-complex of the fly: structure, function and significance in visual behaviour. In: Photoreception and vision in invertebrates (Ali MA, ed), pp 523-559: Plenum Publishing Corporation.
- Hausen K, Wehrhahn C (1983) Microsurgical Lesion of Horizontal Cells Changes Optomotor Yaw Responses in the Blowfly *Calliphora-Erythrocephala*. *Proceedings of the Royal Society of London Series B-Biological Sciences* 219:211-216.
- Heide G (1983) Neural mechanisms of flight control in Diptera. In: Biona-report 2 (Nachtigall W, ed), pp 35-52. Stuttgart, New York: Akad. Wiss. Mainz.

- Hengstenberg B (1991) Gaze control in the blowfly *Calliphora*: a multisensory, two-stage integration process. seminars in THE NEUROSCIENCES 3:19-29.
- Hengstenberg R (1988) Mechanosensory Control of Compensatory Head Roll During Flight in the Blowfly *Calliphora-Erythrocephala* Meig. Journal of Comparative Physiology a-Sensory Neural and Behavioral Physiology 163:151-165.
- Hengstenberg R (1993) Multisensory control in insect oculomotor systems. In: Visual Motion and its Role in the Stabilization of Gaze (Miles FW, J., ed): Elsevier Science Publishers.
- Hengstenberg R, Sandeman DC, Hengstenberg B (1986) Compensatory Head Roll in the Blowfly *Calliphora* During Flight. Proceedings of the Royal Society of London Series B-Biological Sciences 227:455-482.
- Henneman ES, G. Carpenter, DO. (1965) Functional Significance of Cell Size in Spinal Motoneurons. J Neurophysiol 28:560–580.
- Jacobs GA, Theunissen FE (2000) Extraction of sensory parameters from a neural map by primary sensory interneurons. J Neurosci 20:2934-2943.
- Jay MF, Sparks DL (1984) Auditory receptive fields in primate superior colliculus shift with changes in eye position. Nature 309:345-347.
- Jones GM, Milsum JH (1970) Characteristics of neural transmission from the semicircular canal to the vestibular nuclei of cats. J Physiol 209:295-316.
- Karmeier K, Krapp HG, Egelhaaf M (2003) Robustness of the tuning of fly visual interneurons to rotatory optic flow. J Neurophysiol 90:1626-1634.
- Karmeier K, Krapp HG, Egelhaaf M (2005) Population coding of self-motion: applying bayesian analysis to a population of visual interneurons in the fly. J Neurophysiol 94:2182-2194.
- Katz PS (2003) Synaptic gating: the potential to open closed doors. Curr Biol 13:R554-556.
- Kern R, van Hateren JH, Michaelis C, Lindemann JP, Egelhaaf M (2005) Function of a fly motion-sensitive neuron matches eye movements during free flight. PLoS Biol 3:e171.
- Kien J (1977) Comparison of Sensory Input with Motor Output in Locust Optomotor System. Journal of Comparative Physiology 113:161-179.
- Kirkpatrick S, Gelatt CD, Vecchi MP (1983) Optimization by Simulated Annealing. Science 220:671-680.

- Koenderink Jv, AJ. (1987) Facts on optic flow. *Biol Cybern* 56:247-254.
- Krapp HG (1995) Repräsentation von Eigenbewegungen der Schmeißfliege *Calliphora erythrocephala* in VS-Neuronen des dritten visuellen Neuropils. In: Fakultät für Biologie. Tübingen: University of Tübingen.
- Krapp HG (2000) Neuronal matched filters for optic flow processing in flying insects. *Int Rev Neurobiol* 44:93-120.
- Krapp HG, Hengstenberg R (1996) Estimation of self-motion by optic flow processing in single visual interneurons. *Nature* 384:463-466.
- Krapp HG, Hengstenberg R (1997) A fast stimulus procedure to determine local receptive field properties of motion-sensitive visual interneurons. *Vision Res* 37:225-234.
- Krapp HG, Hengstenberg B, Hengstenberg R (1998) Dendritic structure and receptive-field organization of optic flow processing interneurons in the fly. *J Neurophysiol* 79:1902-1917.
- Krapp HG, Hengstenberg R, Egelhaaf M (2001) Binocular contributions to optic flow processing in the fly visual system. *J Neurophysiol* 85:724-734.
- Kurtz R, Warzecha AK, Egelhaaf M (2001) Transfer of visual motion information via graded synapses operates linearly in the natural activity range. *J Neurosci* 21:6957-6966.
- Land MF (1999) Motion and vision: why animals move their eyes. *J Comp Physiol [A]* 185:341-352.
- Laurent G, Seymour-Laurent KJ, Johnson K (1993) Dendritic excitability and a voltage-gated calcium current in locust nonspiking local interneurons. *J Neurophysiol* 69:1484-1498.
- Lewis JE, Kristan WB, Jr. (1998) A neuronal network for computing population vectors in the leech. *Nature* 391:76-79.
- Lindemann JP, Kern R, Michaelis C, Meyer P, van Hateren JH, Egelhaaf M (2003) FliMax, a novel stimulus device for panoramic and highspeed presentation of behaviourally generated optic flow. *Vision Res* 43:779-791.
- Lloyd D (1943) Conduction and synaptic transmission of the reflex response to stretch in spinal cats. *Journal of Neurophysiology* 6:317-326.
- Masino T, Knudsen EI (1990) Horizontal and vertical components of head movement are controlled by distinct neural circuits in the barn owl. *Nature* 345:434-437.

- Masino T, Knudsen EI (1993) Orienting head movements resulting from electrical microstimulation of the brainstem tegmentum in the barn owl. *J Neurosci* 13:351-370.
- Meredith MA, Stein BE (1983) Interactions among converging sensory inputs in the superior colliculus. *Science* 221:389-391.
- Milde JJ, Strausfeld NJ (1990) Cluster organization and response characteristics of the giant fiber pathway of the blowfly *Calliphora erythrocephala*. *J Comp Neurol* 294:59-75.
- Milde JJ, Seyan HS, Strausfeld NJ (1987) The Neck Motor System of the Fly *Calliphora-Erythrocephala* .2. Sensory Organization. *Journal of Comparative Physiology a-Sensory Neural and Behavioral Physiology* 160:225-238.
- Nalbach G (1993) The Halteres of the Blowfly *Calliphora* .1. Kinematics and Dynamics. *Journal of Comparative Physiology a-Sensory Neural and Behavioral Physiology* 173:293-300.
- Nalbach G (1994) Extremely non-orthogonal axes in a sense organ for rotation: behavioural analysis of the dipteran haltere system. *Neuroscience* 61:149-163.
- Nalbach G, Hengstenberg R (1994) The Halteres of the Blowfly *Calliphora* .2. 3-Dimensional Organization of Compensatory Reactions to Real and Simulated Rotations. *Journal of Comparative Physiology a-Sensory Neural and Behavioral Physiology* 175:695-708.
- Newland PL (1999) Processing of gustatory information by spiking local interneurons in the locust. *J Neurophysiol* 82:3149-3159.
- Oyster CW (1968) The analysis of image motion by the rabbit retina. *J Physiol* 199:613-635.
- Oyster CW, Barlow HB (1967) Direction-selective units in rabbit retina: distribution of preferred directions. *Science* 155:841-842.
- Pellionisz A, Llinas R (1980) Tensorial approach to the geometry of brain function: cerebellar coordination via a metric tensor. *Neuroscience* 5:1125-1138.
- Petrowitz R, Dahmen H, Egelhaaf M, Krapp HG (2000) Arrangement of optical axes and spatial resolution in the compound eye of the female blowfly *Calliphora*. *J Comp Physiol [A]* 186:737-746.
- Poulet JF, Hedwig B (2002) A corollary discharge maintains auditory sensitivity during sound production. *Nature* 418:872-876.

- Pringle JWS (1948) The Gyroscopic Mechanism of the Halteres of Diptera. *Philos Trans R Soc Lond B Biol Sci* 233:347-385.
- Rall W (1981) Functional aspects of neuronal geometry. In: *Neurones without impulses* (Roberts AB, BMH, ed). Cambridge, U.K: Cambridge University Press.
- Reichardt W (1961) Autocorrelation, a principle for the evaluation of sensory information in the central nervous system. In: *Sensory Communication* (Rosenblith WA, ed), pp 303-317. Cambridge, MA: MIT Press.
- Reichert H, Rowell CH (1985) Integration of nonphaselocked exteroceptive information in the control of rhythmic flight in the locust. *J Neurophysiol* 53:1201-1218.
- Reichert H, Rowell CHF (1986) Neuronal Circuits Controlling Flight in the Locust - How Sensory Information Is Processed for Motor Control. *Trends in Neurosciences* 9:281-283.
- Reichert HR, CHF. Griss, C. (1985) Course correction circuitry translates feature detection into behavioural action in locusts. *Nature* 315:142-144.
- Rowell CHF, Reichert H (1986) Three descending interneurons reporting deviation from course in the locust. *Journal of Comparative Physiology A: Sensory, Neural, and Behavioral Physiology (Historical Archive)* 158:775-794.
- Sandeman DC (1980) Angular-Acceleration, Compensatory Head Movements and the Halteres of Flies (*Lucilia-Serricata*). *Journal of Comparative Physiology* 136:361-367.
- Sandeman DC, Markl H (1980) Head Movements in Flies (*Calliphora*) Produced by Deflection of the Halteres. *Journal of Experimental Biology* 85:43-60.
- Sandwell DT (1987) Biharmonic Spline Interpolation of Geos-3 and Seasat Altimeter Data. *Geophysical Research Letters* 14:139-142.
- Schilstra C, Hateren JH (1999) Blowfly flight and optic flow. I. Thorax kinematics and flight dynamics. *J Exp Biol* 202 (Pt 11):1481-1490.
- Sherman A, Dickinson MH (2003) A comparison of visual and haltere-mediated equilibrium reflexes in the fruit fly *Drosophila melanogaster*. *J Exp Biol* 206:295-302.
- Sillar KT, Roberts A (1988) A neuronal mechanism for sensory gating during locomotion in a vertebrate. *Nature* 331:262-265.

- Silvey GE, Sandeman DC (1976) Integration between Statocyst Sensory Neurons and Oculomotor Neurons in Crab *Scylla-Serrata* .4. Integration Phase Lags and Conjugate Eye-Movements. *Journal of Comparative Physiology* 108:67-73.
- Simpson JI, Leonard CS, Soodak RE (1988) The accessory optic system of rabbit. II. Spatial organization of direction selectivity. *J Neurophysiol* 60:2055-2072.
- Skavenski AA, Robinson DA (1973) Role of abducens neurons in vestibuloocular reflex. *J Neurophysiol* 36:724-738.
- Soechting JF, Flanders M (1992) Moving in three-dimensional space: frames of reference, vectors, and coordinate systems. *Annu Rev Neurosci* 15:167-191.
- Staudacher E, Schildberger K (1998) Gating of sensory responses of descending brain neurones during walking in crickets. *Journal of Experimental Biology* 201:559-572.
- Staudacher EM (2001) Sensory responses of descending brain neurons in the walking cricket, *Gryllus bimaculatus*. *J Comp Physiol [A]* 187:1-17.
- Strausfeld NJ (1976) *Atlas of an Insect Brain*. Berlin: Springer-Verlag.
- Strausfeld NJ, Seyan HS (1985) Convergence of Visual, Haltere, and Prosternal Inputs at Neck Motor Neurons of *Calliphora-Erythrocephala*. *Cell and Tissue Research* 240:601-615.
- Strausfeld NJ, Gronenberg W (1990) Descending neurons supplying the neck and flight motor of Diptera: organization and neuroanatomical relationships with visual pathways. *J Comp Neurol* 302:954-972.
- Strausfeld NJ, Seyan HS, Milde JJ (1987) The Neck Motor System of the Fly *Calliphora-Erythrocephala* .1. Muscles and Motor Neurons. *Journal of Comparative Physiology a-Sensory Neural and Behavioral Physiology* 160:205-224.
- Tu M, Dickinson M (1994) Modulation of Negative Work Output from a Steering Muscle of the Blowfly *Calliphora Vicina*. *J Exp Biol* 192:207-224.
- van Hateren JH, Schilstra C (1999) Blowfly flight and optic flow II. Head movements during flight. *Journal of Experimental Biology* 202:1491-1500.
- Warzecha AK, Kurtz R, Egelhaaf M (2003) Synaptic transfer of dynamic motion information between identified neurons in the visual system of the blowfly. *Neuroscience* 119:1103-1112.
- Widrow GH, M.E. (1960) Adaptive switching circuits. In: *Institute of radio engineers, Western Electronic show & convention*, pp 96-104.

- Wiersma C (1966) Integration in the visual pathway of crustacea. In: Nervous and hormonal mechanisms of integration, pp 151-177: Cambridge University Press.
- Wolf H, Burrows M (1995) Proprioceptive sensory neurons of a locust leg receive rhythmic presynaptic inhibition during walking. *J Neurosci* 15:5623-5636.
- Wylie DR, Frost BJ (1993) Responses of pigeon vestibulocerebellar neurons to optokinetic stimulation. II. The 3-dimensional reference frame of rotation neurons in the flocculus. *J Neurophysiol* 70:2647-2659.
- Wylie DR, Bischof WF, Frost BJ (1998) Common reference frame for neural coding of translational and rotational optic flow. *Nature* 392:278-282.
- Zar JH (1996) *Biostatistical Analysis*, 3rd Edition: Prentice Hall.